Niche Occupation in Biological Species Competition

Adriaan Janse van Vuuren

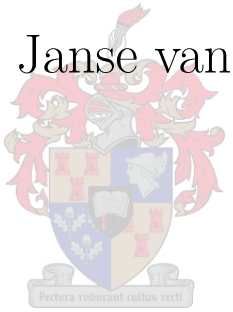

Thesis presented in partial fulfilment of the requirements for the degree
Master of Science
in the inter-departmental programme of Operational Analysis
at the University of Stellenbosch, South Africa

Supervisor: Prof JH van Vuuren

March 2008

Declaration

I, the undersigned, hereby declare that the work contained in this thesis is my own original work and that I have not previously in its entirety or in part submitted it at any university for a degree.

Signature: _____ Date: _____

Abstract

The primary question considered in this study is whether a small population of a biological species introduced into a resource-heterogeneous environment, where it competes for these resources with an already established native species, will be able to invade successfully. A two-component autonomous system of reaction-diffusion equations with spatially inhomogeneous Lotka-Volterra competitive reaction terms and diffusion coefficients is derived as the governing equations of the competitive scenario. The model parameters for which the introduced species is able to invade describe the realized niche of that species.

A linear stability analysis is performed for the model in the case where the resource heterogeneity is represented by, and the diffusion coefficients are, two-toned functions. In the case where the native species is not directly affected by the resource heterogeneity, necessary and sufficient conditions for successful invasion are derived. In the case where the native species is directly affected by the resource heterogeneity only sufficient conditions for successful invasion are derived.

The reaction-diffusion equations employed in the model are deterministic. However, in reality biological species are subject to stochastic population perturbations. It is argued that the ability of the invading species to recover from a population perturbation is correlated with the persistence of the species in the niche that it occupies. Hence, invasion time is used as a relative measure to quantify the rate at which a species' population distribution recovers from perturbation.

Moreover, finite difference and spectral difference methods are employed to solve the model scenarios numerically and to corroborate the results of the linear stability analysis.

Finally, a case study is performed. The model is instantiated with parameters that represent two different cultivars of barley in a hypothetical environment characterized by spatially varying water availability and the sufficient conditions for successful invasion are verified for this hypothetical scenario.

Opsomming

Die primêre vraagstuk wat in hierdie verhandeling beskou word, is of ‘n klein bevolking van ‘n biologiese spesie wat in ‘n hulpbron-heterogene omgewing losgelaat word, waar dit met ‘n reeds gevestigde spesie om hulpbronne moet meeding, suksesvol sal kan vestig. ‘n Twee-komponent outonome sisteem reaksie-diffusie vergelykings met ruimtelik nie-homogene Lotka-Volterra mededingingsreaksieterme en diffusie-koëffisiënte word as model vir hierdie situasie afgelei. Die modelparameters waarvoor die ingevoerde spesie in staat is om suksesvol te vestig, beskryf die gerealiseerde nis van hierdie spesie.

‘n Lineêre stabiliteitsanalise word op die model uitgevoer in die geval waar die hulpbron-heterogeniteit en die diffusie-koëffisiënte stuksgewys konstante periodiese funksies is. In die geval waar die reeds-gevestigde spesie nie direk geaffekteer word deur die hulpbron heterogeniteit nie, word nodige en voldoende voorwaardes vir suksesvolle vestiging afgelei. In die geval waar die reeds-gevestigde spesie wel direk deur die hulpbron heterogeniteit geaffekteer word, word slegs voldoende voorwaardes vir suksesvolle vestiging afgelei.

Die reaksie-duffusie vergelykings wat in die model voorkom, is deterministies. Tog is biologiese spesies in werklikheid onderhewig aan stogastiese steurings. Daar word geargumenteer dat die vermoë van die ingevoerde spesie om ná ‘n bevolkingsteuring te herstel, gekorreleer is met die oorlewing van die spesie in die nis wat dit beset. Gevolglik word vestigingstyd as ‘n relatiewe maatstaf gebruik om die koers te kwantifiseer waarteen ‘n spesie se bevolkingsverdeling ná steurings herstel.

Verder word eindige verskil- en spektraal-verskilmetodes gebruik om die model numeries op te los en om die resultate van die stabiliteitsanalise te staaf.

Laastens word ‘n gevallestudie uitgevoer. Die modelparameters word opgestel sodat die model twee verskillende gars kultivars in ‘n hipotetiese omgewing voorstel wat deur wisselende water beskikbaarheid gekenmerk word. Die voldoende voorwaardes vir suksesvolle vestiging word vir hierdie hipotetiese geval bevestig.

Acknowledgements

Guidance and support from many people helped to shape this thesis. The author hereby wishes to express his gratitude towards

- professor Jan van Vuuren for his unwavering commitment and excellent guidance,
- doctor Elmari Roos for her guidance on the subject of Floquet theory,
- Francois Potgieter of the South African Barley Breeding Institute for taking the time to talk with me,
- doctor Milton Maritz for his advice on the subject of numerical methods,
- my family for their unconditional love,
- Cornell Pretorius for guidance with structuring my thoughts,
- my friends for the support and stability they gave me,
- the Department of Applied Mathematics.

This thesis is based upon work supported by the South African National Research Foundation (NRF) under grant number GUN 2066456. Any opinions, findings and conclusions or recommendations expressed in this thesis are those of the author and do not necessarily reflect the views of the NRF. Financial assistance contributing towards this research project was also granted by the Post-graduate Bursary Office of Stellenbosch University.

Table of Contents

List of Figures

List of Tables

List of Reserved Symbols and Notation

$\binom{n}{k}$	the binomial coefficient denoting the number of ways to choose a k-element, unordered subset from an n-element, unordered set.
$\mathbb{C}$	the set of complex numbers.
$C(\mathbb{F}_1, \mathbb{F}_2)$	the set of continuous functions from a field $\mathbb{F}_1$ to a field $\mathbb{F}_2$.
$C^k(\mathbb{F}_1, \mathbb{F}_2)$	the set of functions, from a field $\mathbb{F}_1$ to a field $\mathbb{F}_2$, with k continuous derivatives.
$\det(\mathbf{M})$	the determinant of a matrix $\mathbf{M}$.
e	the natural constant defined by $\lim_{n\to\infty} \left(1 + \frac{1}{n}\right)^n \approx 2.718\,281$.
e^x	the real exponential function.
$e^{\mathbf{X}}$	the matrix exponential.
$E(X)$	the expected value of a random variate X.
∞	infinity.
$\inf_x f(x)$	the infimum of a function f over a set of values that x may assume.
$L^2(\mathbb{F})$	the set of square-integrable functions from the field $\mathbb{F}$ to the field $\mathbb{F}$.
$M_n(\mathbb{F})$	the set of $n \times n$ matrices with elements in a field $\mathbb{F}$.
$\mathbb{N}$	the set of non-negative integers.
$\mathbb{N}^+$	the set of positive integers.
$o(g(x))$	a function $f(x)$ for which $f(x)/g(x) \to 0$ as $x \to \infty$.
$O(g(x))$	a function $f(x)$ for which there exist constants $x_0 > 0$ and $C > 0$ where $\lvert f(x)\rvert \leq Cg(x)$ for all $x \geq x_0$.
$P(E)$	the probability that an event E occurs.
∂R	the boundary of a spatial region R.
$\mathbb{R}$	the set of real numbers.
$\mathbb{R}^+$	the set of positive real numbers.
$\operatorname{sgn}(p)$	the sign of a permutation p.
$f(n) \sim g(n)$	binary relation indicating that $\lim_{n\to\infty} f(n)/g(n) = 1$.
$PC(\mathbb{F}_1, \mathbb{F}_2)$	the set of piecewise continuous functions from a field $\mathbb{F}_1$ to a field $\mathbb{F}_2$.
$\sup_x f(x)$	the supremum of a function f over a set of values that x may assume.
t	a (non-negative) real number denoting a point in time.
$\operatorname{tr}(\mathbf{M})$	the trace of a matrix $\mathbf{M}$.
$var(X)$	the variance of a random variable X.

$W_{\mathbf{X}}(x)$	the Wronskian of a matrix function $\mathbf{X}(x)$.
x	a real number denoting a point on a spatial axis.
$\mathbf{X}$	a matrix of constants.
$\mathbf{X}(x)$	a matrix of functions of x.
$\underline{x}$	a vector of constants.
$\underline{X}(x)$	a vector of functions of x.
$\mathbb{Z}$	the set of integers.

Chapter 1

Introduction

Population modelling and population projection have been important parts of demography and ecology since the pioneering contribution of John Graunt [32]. It was, however, the seminal work of Alfred J. Lotka (1880–1949) and Vito Volterra (1860–1940) in the 1920s and 1930s that provided the framework for competition studies in ecology.

1.1 Background

During the 1920's the Italian biologist Umberto D'Ancona studied various interacting fish species. In particular, during the course of his research, he considered the percentages of predator fish, such as sharks, of total catches brought into the ports of Trieste, Venice, and Fiume on the upper Adriatic coast in the years spanning the first World War. D'Ancona was puzzled by the large increase in the percentage of predator fish during the war years, and could not explain why greatly reduced levels of fishing would benefit the predator fish more than their prey [16]. D'Ancona turned to his friend and colleague Vito Volterra in the hope that he would find answers with the aid of mathematics.

The research of Volterra resulted in the continuous time coupled system of ordinary differential equations, now known as the Lotka-Volterra predator-prey model, of the form

$$\left.\begin{aligned} \frac{\mathrm{d}w_1}{\mathrm{d}t}(t) &= aw_1(t) - dw_1(t)w_2(t), \\ \frac{\mathrm{d}w_2}{\mathrm{d}t}(t) &= -cw_2(t) - bw_1(t)w_2(t), \end{aligned}\right\} \tag{1.1}$$

together with suitable initial conditions. Here a, b, c, and d are positive constants; a representing the birthrate of the prey at low population density, whose population density at time $t \geq 0$ is denoted by $w_1(t)$, c representing the death rate proportion due to overcrowding of the predators, whose population density at time $t \geq 0$ is denoted by $w_2(t)$, d represents the death rate proportion of the prey as a result of the predators preying on them, and b the birth rate proportion of the predators sustained by the prey population. At about the same time (1925) the American mathematician Alfred J. Lotka formulated a similar growth law for interacting biological populations [55].

A numerical solution to the Lotka-Volterra system is plotted in Figure 1.1. The curve with smaller amplitude is that of the predator population density. It is apparent that

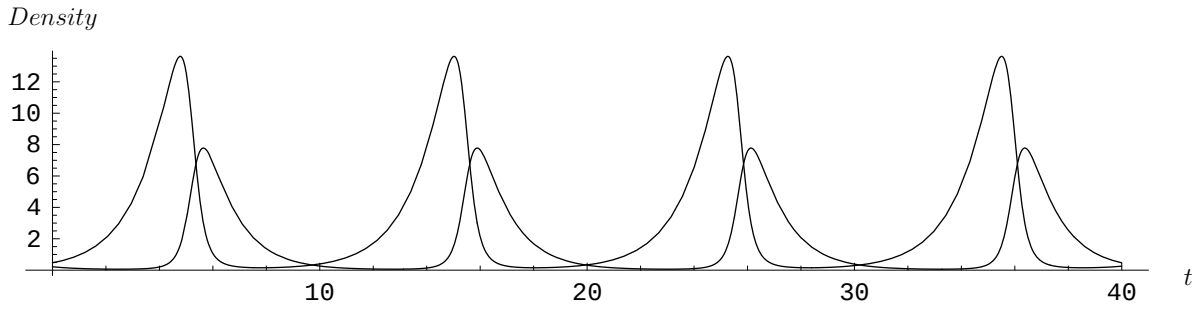

Figure 1.1: A numerical solution to the Lotka-Volterra system (1.1) for coefficients $a = 0.8$, $b = 0.3$, $c = 0.9$, and $d = 0.5$, and initial populations $w_1(0) = 0.5$ and $w_2(0) = 0.2$.

an increase of the population density of the predator population lags behind that of the prey population. Heuristically, an increase in the prey population encourages growth in the predator population. More predators, however, consume more prey, the population of which hence declines. With less food available the predator population starts to decline, and the cycle begins again. The pattern in the data observed by D'Ancona could thus be explained by arguing that the data reflects the predator population in the phase after the prey population had started to decline because of an increase in the predator population.

In 1931 Volterra generalized the system of coupled differential equations to the form

$$\frac{\mathrm{d}w_i}{\mathrm{d}t}(t) = w_i(t)\left(b_i - \sum_{j=1}^{n} a_{ij}w_j\right), \quad i = 1, \ldots, n, \tag{1.2}$$

where the a_{ij} are now positive or negative, which, together with suitable initial conditions, model the interaction of n species [89]. These models are sometimes called phenomenological models because their coefficients have little direct relation to the underlying biology or the resources competed for [9, pp. 51]. In the case of two species with the coefficients a_{11}, a_{12}, a_{21}, and a_{22} positive the model is of species competing for shared resources. In the case that $a_{11}, a_{22} = 1$ the parameters b_1 and b_2 may be interpreted as environmental carrying capacities. This is because, according to (1.2), when $w_i(t) > b_i$ the population density decreases. Thus the population cannot grow denser than b_i.

The simplistic Lotka-Volterra models have formed the cornerstone of mathematical population modelling, being the point of departure for more sophisticated models. Among the most influential concepts in community ecology are the theory of ecological niche occupation and the associated theory of competitive exclusion. These derive in large part from the mathematical approaches of Lotka and Volterra. Gause's *principle of competitive exclusion* [31, pp. 113], in short, states that if two species are able to coexist, there must be some difference between them in terms of their resource use. A *fundamental niche* are those resources that allow a species to exist, and a *realized niche* those resources that allow a species to coexist in the presence of interacting species [9, pp. 53].

The Lotka-Volterra models assume that the biological populations' densities are constant over the habitat where they occur. However, natural biological populations tend not to be homogeneously distributed over the whole of the habitat. Varying population densities should influence members of the population accordingly. The simplicity of the Lotka-Volterra models of biological interactions also allows for parallels to be drawn with

chemical systems, where reactions are assumed to take place as per the law of mass action. That is, the greater the density of chemical reactants the greater the number of collisions between molecules and hence the greater the number of reactions. The physical system described by the Lotka-Volterra models is analoguous to a well-stirred, or homogenous, chemical system, where the chemical densities are constant throughout the solution. However, there exist among unstirred chemical systems dramatic examples of spatial variation of chemical concentrations that result from the random movement of the chemical molecules. A well known collection of such reactions, known as the Belousov-Zhabotinskii reactions [61], exhibit a visually impressive spatial pattern of colours, according to varying chemical concentrations, in the forms of spirals and concentric circles.

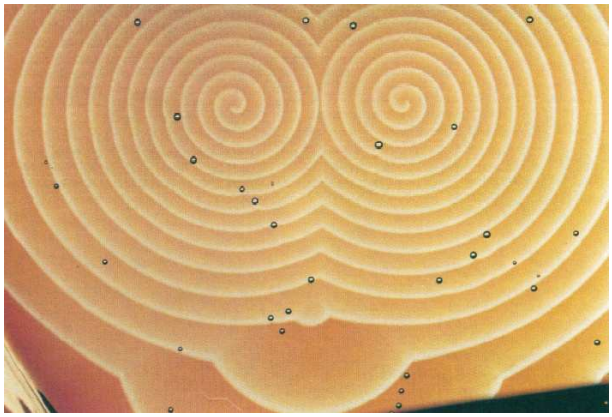

Figure 1.2: Spiral waves formed in a thin layer of Belousov-Zhabotinskii reaction mixture. Each spiral rotates with the same period (30 s) and has the same frequency [43].

The first major advances in incorporating spatially heterogeneous population densities in a model came in 1937 from population genetics, and, in particular, from the work of J.B.S. Haldane (1892–1964) and R.A. Fisher (1890–1962). Fisher recognized the similarities between the spreading of heat in a plate and the dispersion of biological species members. The former had already been described by A. Fick (1829–1901) in 1855, who had adopted the mathematical equation of heat conduction derived earlier by J.B. Fourier (1768–1830). Fisher incorporated spatial variation of densities in population dynamic models by using the concept of diffusion [26]. Fisher modelled the spatial spread of an advantageous gene through a population by means of an equation of the form

$$\frac{\partial p}{\partial t}(x,t) = \frac{\partial^2 p}{\partial x^2}(x,t) + s\,p(x,t)(1-p(x,t)), \tag{1.3}$$

where $p(x,t)$ is the concentration of an advantageous gene, and s a measure of intensity of selection.

Incorporating spatially varying population densities in a model means that there is a region being modelled. As is the case in the real biological, or genetic, situation the behaviour of the population at the boundaries of this region influences the population being modelled. Thus the complete description of a model requires a description of what happens at the boundaries of the region where the population is modelled. Two physically plausible possibilities are that the movement of the members of the population across the boundary is regulated, which is known as Neumann boundary conditions, or that the population's density at the boundary is regulated, which is known as Dirichlet boundary conditions.

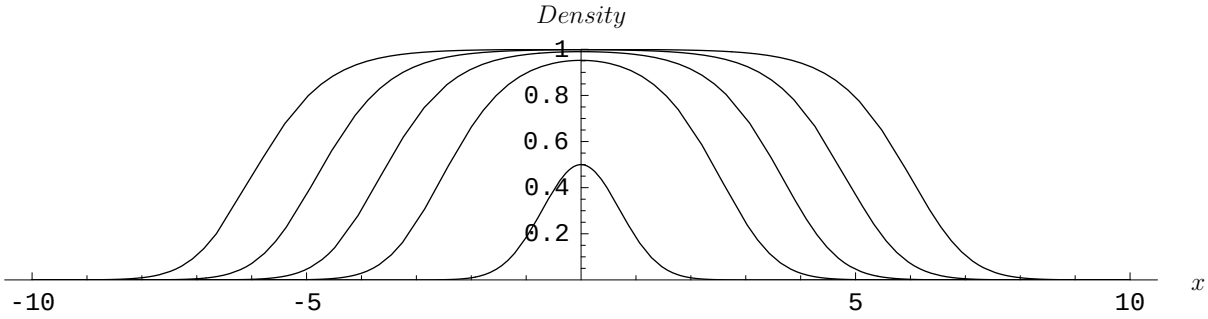

Figure 1.3: Solutions to Fisher's equation, with zero-Dirichlet boundary conditions at infinity, when the advantageous gene is initially introduced at $x = 0$. The successively widening curves represent solutions at times $t = 0.1$, $t = 4$, $t = 6$, $t = 8$, and $t = 10$, respectively.

Figure 1.3 shows a solution to Fisher's equation (1.3) with zero-Dirichlet boundary conditions at infinity, where each successively wider curve represents a snapshot in time, as time progresses, of the density distribution of the spreading gene. As time progresses the region where the the gene has reached, given by the x-axis under the curve where the curve is not zero, expands like a travelling wave; the density of the gene is highest in the region where it has had most time to increase.

1.2 Informal Problem Description

Fisher's model reduces to a single reaction-diffusion equation, where the term *reaction-diffusion* refers to the dual nature of the equations; the reaction part being that of a Lotka-Volterra model, and the diffusion part the elements describing the spatial distribution of the population. A system of equations coupled in their reaction parts representing population densities follows naturally from the Lotka-Volterra models. Moreover, extending Fisher's model, which takes into account spatial variation in population density, to a model that takes into account spatial variation of the habitat too seems useful. Armed with such a model, an interesting question in terms of biological niche occupation theory is whether a species will be able to coexist in a given heterogeneous environment in the presence of a given competitor. The sufficiency part of the question reduces to whether a species is able to invade an already occupied habitat. Since, if the species can invade, it will also survive in that habitat, assuming there is no temporal variation in the habitat.

The aim of this study is to describe in a sufficiency sense the realized niche of a species in a heterogeneous environment (although the heterogeneity of the environment will, in a sense, be minimal). Of further interest is how marginal an invasion is. Specifically, if an invading population takes a long time to reach a population equilibrium and the average population density remains low, the population could well be susceptible to stochastic perturbation, which is only accounted for, on average, in the deterministic model.

Thus the first problem considered in this thesis is whether a given species is able to invade a given environment where another species is already established modelled by a coupled system of equations similar in form to (1.3). If it is able to invade, the next problem considered is quantifying how well it does invade.

1.3 Thesis Objectives

The following objectives are pursued in this thesis.

Objective I: To derive from first principles a continuous reaction-diffusion model governing the spatial distribution and population dynamics, on the average, of two competing biological species.

Objective II: To derive the same model as in Objective I, but without appealing to the principle of Fickian diffusion, by making explicit the assumptions on the nature of the redistribution process of the biological population.

Objective III: To place the work in this thesis in context by conducting a concise survey of literature on analyses and biological applications of reaction-diffusion models.

Objective IV: To review efficient numerical schemes for finding approximate solutions to the reaction-diffusion model derived in Objectives I and II for two sets of different boundary conditions.

(a) The first numerical method will be used to solve the model with zero flux (Neumann) boundary conditions on a finite habitat.

(b) The second numerical method will be used to solve the model on a periodic, infinite habitat.

Objective V: To compute numerical solutions, using the numerical schemes reviewed in fulfilment of objective IV, of instances of the coupled system of reaction-diffusion equations (together with suitable initial and boundary conditions) modelling competition between two biological species and to present these solutions graphically.

Objective VI: To perform a linear stability analysis of the invasion capability of a species introduced into a heterogeneous habitat where another species is already established.

Objective VII: To define a meaningful measure of how marginal an invasion of a habitat containing an already established species is.

Objective VIII: To present a case study where the analyses performed in fulfilment of Objectives V and VI are applied to real data.

1.4 Layout of Thesis

A continuous model of two-species biological competition in one dimension with spatially varying population densities and varying habitat is derived in Chapter 2, first by appealing to the principle of Fickian diffusion and then by making explicit the assumptions on the redistribution of the biological populations. This is done in fulfilment of Objectives I and II of the previous section. Thereafter the model is extended to three spatial dimensions.

Chapter 3 contains a concise survey of literature pertaining to models that describe populations by means of a coupled system of reaction-diffusion equations, in fulfilment of

Objective III. In addition to providing background, this chapter will place the problem considered in this thesis within a broader mathematical context.

In fulfilment of Objective IV two numerical methods capable of finding approximate solutions to the reaction-diffusion model derived in Chapter 2 are reviewed in Chapter 4. The first method employs finite differences to solve the model on a bounded domain with zero flux (Neumann) boundary conditions. The second method employs Fourier spectral methods to solve the model on a periodic (infinite) domain. The convergence and stability of both methods are discussed. The methods are then applied in the form of numerical examples to problems typical of those encountered later in the thesis.

In Chapter 5 the stability of a small initial population invading a heterogeneous habitat is analysed where another species is already established. This is done in fulfilment of Objective V. The model is first nondimensionalized and then linearised about the zero invading population equilibrium. Floquet theory is employed in the analysis of the linearised model. Hereafter a measure of how marginal the invasion is, which will be referred to as *invasion* time, is established. The numerical methods reviewed in Chapter 4 are used to implement this measure numerically, in fulfilment of Objective VI

A case study on two cultivars of malt barley is presented in Chapter 6 in fulfilment of Objective VII. The analysis of Chapter 5 is applied to the data. A sensitivity analysis is performed in terms of both the invasion time and the stability analysis of the model parameters that could not be obtained empirically.

Chapter 7 contains a summary of the results in this thesis and ideas with respect to future work.

Finally, Appendix A contains classical results used mainly during derivation of the model in Chapter 2, whilst Appendix B contains results on ordinary differential equations used mainly in the analysis of Chapter 5 (among these are results of the Floquet theory).

Chapter 2

Biological Diffusion

In this chapter a mathematical model of the spatial diffusion of coexisting biological species is derived. In the first section the model is derived using the empirical principle of Fickian diffusion. Furthermore, the rationale of treating the mean distribution of a biological population as continuous and of approximating the actual redistribution process by means of a diffusion process is considered and motivated. In the following section the same model is derived from explicit assumptions on the nature of the redistribution process, but without appealing to the principle of Fickian diffusion. In the next section the model is extended to three dimensional space. Finally, the specific problem considered in the remainder of the thesis is formulated formally in terms of the mathematical model.

2.1 Classical Derivation of Model

The movement or transportation of matter particles suspended in a gas or liquid tends to progress in the direction of lower concentration. This is the observation formalized in Fick's first law [24], which, together with the principle of mass conservation [54], leads to a time-dependent differential equation approximating the diffusion of matter. In this section a mathematical model of the spatial diffusion of members of a biological species, comprising an equation of the same form, is derived, considered and motivated, using Fick's law as a point of departure.

2.1.1 Fickian Diffusion

Consider n populations of particles in three dimensional space, equipped with the Cartesian co-ordinate system, but consider only their movement relative to the x-axis. Denote by $\rho_i(x,t)$ the density of particles of type i at position $x \in \mathbb{R}$ and time $t \geq 0$, which is assumed to be a function continuously differentiable in t and twice continuously differentiable in x, and by $J_i(x,t)$ the rate at which the particles of type i diffuse per unit surface area at position x and time t in the increasing direction of the x-axis (see Figure 2.1). Let $\underline{\rho}(x,t) = [\rho_1(x,t), \ldots, \rho_n(x,t)]^T$ and $\underline{J}(x,t) = [J_1(x,t), \ldots, J_n(x,t)]^T$. Then Fick's first law may be expressed mathematically as

$$\underline{J}(x,t) = -\mathbf{D}(x,t)\frac{\partial \underline{\rho}}{\partial x}(x,t), \tag{2.1}$$

where $\mathbf{D}(x,t)$ is a continuous positive diagonal matrix, known as the diffusion matrix, in which the i-th entry on the diagonal is a function of proportionality measuring how readily the particles of type i flow in a direction down the concentration gradient at position x and time t. Hence $\underline{J}(x,t)$ is continuous. When dealing with matter particle concentrations a diagonal diffusion matrix may appear counter-intuitive. However, when dealing with biological species it has often been assumed that populations are not subject to cross-diffusion (see for example [61]). Some motivation with respect to the validity of this assumption is presented in §2.1.2 and §2.1.3 for the case where a region is sparsely populated and the movements of a species member are thus independent of individuals of other species.

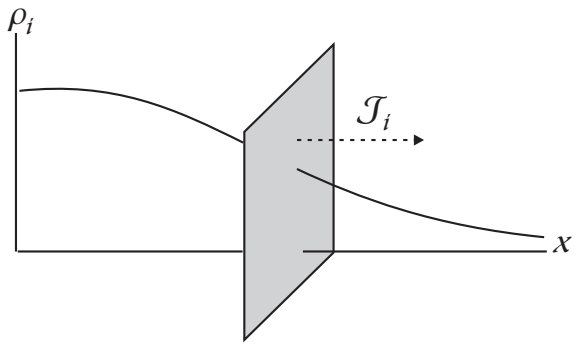

Figure 2.1: The rate at which particles diffuse per unit surface area.

By the principle of mass conservation the rate of change of the concentration of particles of type i in an arbitrary interval $I = (a,b) \subseteq \mathbb{R}$ equals the rate at which particles of type i flow across the boundary of I into I, together with the rate at which particles of type i are created in I. The concentration of particles flowing into I per unit time is $\underline{J}(a,t) - \underline{J}(b,t)$, which, by the fundamental theorem of the calculus (See Theorem A.1), is equivalent to

$$-\int_a^b \frac{\partial \underline{J}}{\partial x}(x,t)\,\mathrm{d}x. \tag{2.2}$$

Let $G_i(x,t,\underline{\rho}(x,t))$ denote the concentration of particles of type i created per unit time at position $x \in \mathbb{R}$ at time $t \geq 0$, and $\underline{G}(x,t,\underline{\rho}(x,t)) = [G_1(x,t,\underline{\rho}(x,t)),\ldots,G_n(x,t,\underline{\rho}(x,t))]^T$. Now, using (2.2), the equivalence emanating from the principle of mass conservation may be expressed as

$$\frac{\mathrm{d}}{\mathrm{d}t}\int_a^b \underline{\rho}(x,t)\,\mathrm{d}x = -\int_a^b \frac{\partial \underline{J}}{\partial x}(x,t)\,\mathrm{d}x + \int_a^b \underline{G}(x,t,\underline{\rho}(x,t))\,\mathrm{d}x,$$

which may, in turn, be written as

$$\int_a^b \left(\frac{\partial \underline{\rho}}{\partial t}(x,t) + \frac{\partial \underline{J}}{\partial x}(x,t) - \underline{G}(x,t,\underline{\rho}(x,t))\right)\mathrm{d}x = 0. \tag{2.3}$$

If, in some arbitrary region within I, the above integrand were not identically zero, that is, if for some i,

$$\frac{\partial \rho_i}{\partial t}(x,t) + \frac{\partial J_i}{\partial x}(x,t) - G_i(x,t,\underline{\rho}(x,t)) > 0,$$

then for some $x \in I$ there would exist an open interval $I_1 = (x - \delta, x + \delta) \subset I$ for which

$$\int_{I_1} \left(\frac{\partial \rho_i}{\partial t}(x,t) + \frac{\partial J_i}{\partial x}(x,t) - G_i(x,t,\underline{\rho}(x,t)) \right) \mathrm{d}x > 0, \tag{2.4}$$

because $\underline{J}$ is a continuous vector function. But (2.4) contradicts (2.3). A similar argument may be used to show that

$$\frac{\partial \underline{\rho}}{\partial t}(x,t) + \frac{\partial \underline{J}}{\partial x}(x,t) - \underline{G}(x,t,\underline{\rho}(x,t)) \not< 0$$

on I. Thus (2.3) implies that

$$\frac{\partial \underline{\rho}}{\partial t}(x,t) + \frac{\partial \underline{J}}{\partial x}(x,t) - \underline{G}(x,t,\underline{\rho}(x,t)) = 0 \tag{2.5}$$

on I. By Fick's law this is equivalent to

$$\frac{\partial \underline{\rho}}{\partial t}(x,t) = \frac{\partial}{\partial x} \left(\mathbf{D}(x,t) \frac{\partial \underline{\rho}}{\partial x}(x,t) \right) + \underline{G}(x,t,\underline{\rho}(x,t)). \tag{2.6}$$

In the special case where $\mathbf{D}$ is independent of position, (2.6) reduces to

$$\frac{\partial \underline{\rho}}{\partial t}(x,t) = \mathbf{D} \, \frac{\partial^2 \underline{\rho}}{\partial x^2}(x,t) + \underline{G}(x,t,\underline{\rho}(x,t)), \tag{2.7}$$

which is known as the diffusion equation. Here $\mathbf{D}$ is a measure of how quickly or easily the particle density of a specific material tends to smooth out or diffuse.

In addition to (2.6) or (2.7) derived above, which governs the diffusion of a set of materials, the description of a specific system will also include boundary conditions that are to be satisfied by a solution to the equation. From physical considerations such boundary conditions would typically include a description of the initial state or distribution of the materials, that is a particle distribution specification of the form

$$\underline{\rho}(x,0) = \underline{f}(x). \tag{2.8}$$

If the domain considered is infinite the populations are still assumed finite from which it follows that $\underline{\rho}(-\infty,t) = \underline{\rho}(+\infty,t) = 0$. If the domain considered is a region of finite physical proportions, the behaviour of particles at the boundary of the region should also be described. A physically plausible possibility is that the particle density on the boundary is regulated, which corresponds to Dirichlet boundary conditions of the form

$$\underline{\rho}(x,t) = \underline{\theta}(x,t), \quad x \in \partial I, \quad t \geq 0. \tag{2.9}$$

Another possibility is that the flow of particles across the boundary of the region is regulated, which corresponds to Neumann boundary conditions of the form

$$\frac{\partial \underline{\rho}}{\partial t}(x,t) = \underline{\theta}(x,t), \quad x \in \partial I, \quad t \geq 0. \tag{2.10}$$

2.1.2 Fixed Step Random Walk Motivation of Continuity

A biological population consists of individuals that are discrete entities. Yet, in the diffusion equation (2.6) the population density is treated as a continuous quantity. In this section the rationale of treating the mean distribution of a large discrete population over a long time period as a continuous quantity is considered and motivated.

In the absence of reactions (*i.e.* the creation and demise of individuals of a species) the migration process is one merely of redistribution. Furthermore, since no reactions occur, the population may as well be treated as that of a single species in view of the diagonal structure of $\mathbf{D}(x,t)$. Therefore, consider a single population in three dimensional space, equipped with the Cartesian coordinate system, but again consider only their movement relative to the x-axis. The direction of movement in the decreasing direction of the x-axis will be referred to as *left* and movement in the increasing direction as *right*. Let the time line be divided into intervals of length τ and assume that each individual of the population steps a distance λ with equal probability to the left or to the right, during each time interval, independent of its position or movement of the rest of the population.

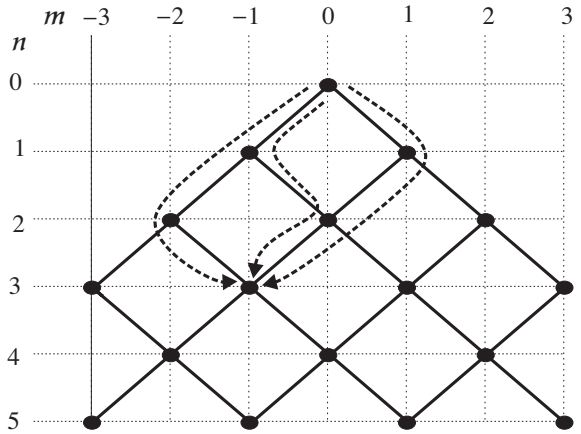

Figure 2.2: The three step paths consisting of a steps to the right and b steps to the left such that $m = a + b = -1$.

Let $X_\tau(t)$ denote the position of an individual at time t that was released on the plane $x = 0$ at $t = 0$, and let $p_n(m)$ be the (discrete) probability mass function of its position, where $n = \lfloor t/\tau \rfloor$ and m is the distance of the individual from the origin, measured in steps of length τ, in the direction of the positive x-axis. If the path followed by the individual was a steps to the right and b steps to the left (in any order) then $n = a+b$ and $m = a-b$, or, solving for a and b,

$$a = \frac{n+m}{2} \quad \text{and} \quad b = \frac{n-m}{2}.$$

Moreover, $m = a - b = a - n + a = 2a - n$. Therefore

$$m \in \Omega_n := \{-n, -n+2, \ldots, n-2, n\}.$$

The number of distinct paths that the individuals may have followed, each consisting of n steps, is 2^n, since each step taken by the individual could have been either to the right or to the left. The number of distinct paths, each comprising a right and b left steps, corresponds with the number of ways of choosing a subset of a time intervals from $a + b$ time intervals during which the right steps occur (see Figure 2.2). There are

$$\binom{a+b}{a} = \frac{(a+b)!}{a![(a+b)-a]!} = \frac{n!}{a!\,b!} = \frac{n!}{\left(\frac{n+m}{2}\right)!\left(\frac{n-m}{2}\right)!}$$

such selections and hence paths. Therefore

$$p_n(m) = 2^{-n}\frac{n!}{\left(\frac{n+m}{2}\right)!\left(\frac{n-m}{2}\right)!} = \frac{2^{-n}n!}{n!\ (n-a)!} =: p(n,a). \tag{2.11}$$

Here $p(n,a)$ is the probability mass function of the binomial distribution over the probability space $\Omega_a = \{0,1,\ldots,n\}$ with probability of success during the i-th trial being $\frac{1}{2}$. Hence, by (2.11) and the one-to-one correspondence $a \mapsto (2a-n)$, $p_n(m)$ is a binomial distribution over the subset $\lambda \cdot \Omega_n$ of the the real line.

To show that $p_n(m)$ approaches a normal distribution as $n \to \infty$, the central limit theorem is invoked. If Y_i is a random variable taking the value 1 if the individual steps to the right during time interval i and -1 if to the left, then

$$X_\tau(t) = \lambda\left(Y_1 + \ldots + Y_{\lfloor t/\tau \rfloor}\right). \tag{2.12}$$

From (2.12), and since $\mathrm{Var}(Y_i) = 1$ for every i,

$$\mathrm{Var}\left(X_\tau(t)\right) = \lambda^2 \mathrm{Var}\left(\sum_{i=1}^{\lfloor t/\tau \rfloor} Y_i\right) = \lambda^2 \left\lfloor t/\tau \right\rfloor.$$

Therefore, $X_\tau(t)$ may be normalized as

$$\eta_\tau(t) = \frac{\lambda\left(\sum_{i=1}^{\lfloor t/\tau \rfloor} Y_i\right)}{\sqrt{\lambda^2 \left\lfloor t/\tau \right\rfloor}} = \frac{\left(\sum_{i=1}^{\lfloor t/\tau \rfloor} Y_i\right)}{\sqrt{\left\lfloor t/\tau \right\rfloor}}.$$

Now $\{\lambda Y_i\}_{i=1}^{\lfloor t/\tau \rfloor}$ is a sequence of identically independently distributed random variables with mean 0 and variance λ^2. Hence it follows by the central limit theorem (see Theorem A.12), in the limit as $\tau \to 0$, that $\eta_\tau(t)$ is a random variable with the standard normal distribution (*i.e.* with mean 0 and variance 1). If λ varies with τ in such a way that

$$\lim_{\tau \to 0} \lambda^2 \left\lfloor t/\tau \right\rfloor = \lim_{\tau \to 0} \frac{\lambda^2}{\tau}\, t \tag{2.13}$$

exists, then, since $X_\tau(t) = \eta_\tau(t)\sqrt{\lambda^2 \left\lfloor t/\tau \right\rfloor}$ for every τ, it follows that $X(t) := \lim_{\tau \to 0} X_\tau(t)$ has a normal distribution with mean $\mu = 0$ and variance σ^2 equal to the limit in (2.13). That is, the probability density function of $X(t)$ is

$$\varphi_t(x) = \frac{1}{2\sqrt{(\pi D t)}}\, e^{-\left(x^2/4Dt\right)}, \tag{2.14}$$

where

$$D = \lim_{\tau \to 0} \frac{\lambda^2}{2\tau}.$$

Note that the function $\varphi(x,t) := \varphi_t(x)$ is continuous for $t > 0$.

If the population consists of k individuals released at $x = 0$, whose positions are given by k random variables that are independently identically distributed like $X(t)$, then the portion of the population at time t between two planes, parallel to the yz-plane, cutting the x-axis at a and x respectively, is that portion of k observations of $X(t)$ that are in

the interval (a, x). Let $Z_i = 1$ if on the i-th observation $X(t) \in (a, x)$ and zero otherwise then the expected value of Z_i is $\int_a^x \varphi(\xi, t)\,\mathrm{d}\xi$. The portion of the k observations of $X(t)$ that are in the interval (a, x) is the average of Z_i for $i \in (1, 2, \ldots, k)$. Thus, by the strong law of large numbers (see Theorem A.9), this portion is

$$\int_a^x \varphi(\xi, t)\,\mathrm{d}\xi \tag{2.15}$$

with probability 1 in the limit as $k \to \infty$. Thus, for large k, the portion of individuals in the interval (a, x) is

$$k \int_a^x \varphi(\xi, t)\,\mathrm{d}\xi. \tag{2.16}$$

Because the integral of the concentration of the population over the interval $[a, x]$ also gives the portion of the population in the interval, the derivative with respect to x of (2.16) is, by the fundamental theorem of the calculus (see Appendix A.1), the concentration of the population at position x at time t. Thus, if $\rho(x, t)$ is the concentration of the species at position x at time t, then $\rho(x, t) = k\varphi(x, t)$. By (2.14) $\varphi(x, t)$ is smooth in x and continuous in t, and hence $\rho(x, t)$ is a smooth (in x) and continuous (in t) approximation of the concentration of the biological species.

2.1.3 Random Walk Motivation of the Diffusion Process

In the previous section the general practice of approximating the mean distribution of a large population by a continuous function was justified by means of the central limit theorem. In this section the practice of approximating the actual redistribution process of a population by a diffusion process is justified by means of Taylor's theorem.

In a simplistic idealised situation the small-time movements of an individual of a biological species, say the displacement of a fish darting in one direction before darting in the next direction in a sparsely occupied area of open ocean, may be considered random and independent of the other individuals of the population. If γ is the length of a time interval of roughly the magnitude of time spanned by such a movement, and is very small compared to the time span over which the population is observed, then in a time interval of length γ the position of each individual, again considered only relative to the x-axis, will increase by Δ, where Δ is a continuous random variable which is symmetric about zero, with a probability density function ϕ. Thus

$$\int_{-\infty}^{+\infty} \phi(\Delta)\,\mathrm{d}\Delta = 1. \tag{2.17}$$

If $\rho(x, t)$ is the density of the population at position $x \in \mathbb{R}$ at time $t \geq 0$, the expected number of individuals per unit volume at position x at time $t + \gamma$ is the integral, over all possible values of Δ, of the portion of the individuals per unit volume at $x + \Delta$ that are expected to be displaced by an amount of exactly $-\Delta$. This gives the relationship

$$\rho(x, t + \gamma) = \int_{\mathbb{R}} \rho(x + \Delta, t)\phi(\Delta)\,\mathrm{d}\Delta. \tag{2.18}$$

Now, in the limit as $\gamma \to 0$,

$$\rho(x, t + \gamma) = \rho(x, t) + \gamma \frac{\partial \rho}{\partial t}(x, t).$$

Further, a Taylor expansion of $\rho(x+\Delta,t)$ about the point x yields

$$\rho(x+\Delta,t)=\rho(x,t)+\Delta\frac{\partial\rho}{\partial x}(x,t)+\frac{\Delta^2}{2!}\frac{\partial^2\rho}{\partial x^2}(x,t)+\dots \tag{2.19}$$

(see Theorem A.4). If the expansion (2.19) is substituted into (2.18), then the first term becomes

$$\rho(x,t)\int_{\mathbb{R}}\phi(\Delta)\,\mathrm{d}\Delta=\rho(x,t)$$

by virtue of (2.17). Furthermore,

$$\frac{\partial\rho}{\partial x}(x,t)\int_{\mathbb{R}}(\Delta\,\phi(\Delta))\;\mathrm{d}\Delta=0,$$

because $\Delta\,\phi(\Delta)$ is an odd function by the symmetry of ϕ. All the terms involving odd order partial derivatives similarly vanish. Because ϕ only differs from zero for small magnitudes of Δ, the fourth and larger order partial derivative terms are very small relative to the second order partial derivative term. Thus fourth and higher degree partial derivative terms may be disregarded as $\Delta\to 0$.

Thus, putting

$$D=\lim_{\gamma\to 0}\frac{1}{2\gamma}\int_{\mathbb{R}}((\Delta)^2\;\phi(\Delta))\,\mathrm{d}\Delta,$$

equation (2.18) reduces to the diffusion equation

$$\frac{\partial\rho}{\partial t}(x,t)=D\,\nabla^2\rho(x,t) \tag{2.20}$$

encountered in §2.1.1, which was derived there from the principle of Fickian diffusion, in the case where no new individuals are created as a result of the reaction term in (2.7).

2.2 An Alternative Derivation of the Model

In this section a number of postulates on the nature of a population's distribution and how the distribution evolves over time are introduced. The number of postulates are small in the sense that the model situation is still quite general. A rigorous argument shows that these postulates lead to a reaction-diffusion model for the time-evolution of the populations of coexisting species. This development closely follows [25].

2.2.1 Basic Assumptions

The two most basic assumptions are that a population's spatial distribution may be approximated by a smooth density function and that the time evolution of these functions proceed deterministically. Both of these assumptions are most reasonable when the population is large. In the first case since observation of a large population over a large spatial scale resembles that of a smeared out substance. In the second case the behaviour of an individual may only credibly be described as having a probability distribution, and hence the behaviour of the whole population will be more accurately predictable when the population is large.

Assumption 1 *To each species i there corresponds a density function $\rho_i(x,t)$ so that the number of individuals of that species located in the interval $a < x < b$ at time t is approximately $\int_a^b \rho_i(x,t)\,\mathrm{d}x$. These density functions ρ_i are twice continuously differentiable in x, and once in t.* ■

Assumption 2 *The time evolution of the functions ρ_i proceeds by a deterministic process, in the sense that if any initial distribution in the form of bounded functions $\rho_i^0(x) \in C^2$ is given at any time t_0, then there is a uniquely determined set of density functions $\rho_i(x,t)$ defined for $t \geq t_0$ with $\rho_i(x,t_0) = \rho_i^0(x)$.* ■

The remaining assumptions elaborate on the deterministic process from which the spatial density function evolves. A *migration rule* and a *reaction rule* are introduced. The migration rule is more conveniently described under the condition that no species interactions take place. Since under the migration rule no individuals are created or annihilated, the population is merely redistributed. The reaction rule describes how individuals appear and disappear in the presence of the migration rule.

2.2.2 The Redistribution Process

For the present development the habitat is taken to be the entire real line. A sampling function $g_i(x,t,y,s)$ is introduced. This function may be interpreted as the probability distribution of the position of an individual at time t that was located at position y at time s, for $t > s$. Since the redistribution process is deterministic the distribution at time t is independent of the time s chosen. Once the dynamics of the model population are shown to be governed by a partial differential equation it follows that boundaries have only local effect.

Assumption 3 *There is a non-negative function $g_i(x,t,y,s)$, for any $t > s$, such that the density $\rho_i(x,t)$ satisfies*

$$\rho_i(x,t) = \int_{-\infty}^{\infty} g_i(x,t,y,s)\rho_i(y,s)\,\mathrm{d}y$$

for every $x \in \mathbb{R}$. ■

Thus the deterministic redistribution process is linear. Moreover, since Assumption 3 implies that

$$\int_{-\infty}^{\infty} g_i(x,t,y,s)\,\mathrm{d}y < \infty,$$

it follows, if $\rho_i^{(1)}$ and $\rho_i^{(2)}$ are any two density functions, that

$$\left|\rho_i^{(1)}(x,t) - \rho_i^{(2)}(x,t)\right| \leq \sup_y \left|\rho_i^{(1)}(y,s) - \rho_i^{(2)}(y,s)\right| \int_{-\infty}^{\infty} g_i(x,t,y,s)\,\mathrm{d}y$$

and hence $\rho_i(x,t)$ depends continuously on $\rho_i(\cdot,s)$. That is, given any $\epsilon > 0$, there exists a $\delta(\epsilon,x,t,s)$, for all $x \in \mathbb{R}$ and $t > s$, such that, if $\rho_i^{(1)}$ and $\rho_i^{(2)}$ satisfy

$$\sup_y \left|\rho_i^{(1)}(y,s) - \rho_i^{(2)}(y,s)\right| < \delta(\epsilon,x,t,s),$$

then

$$\left|\rho_i^{(1)}(x,t) - \rho_i^{(2)}(x,t)\right| < \epsilon.$$

For a finite population the population size is to remain constant, leading to the following assumption.

Assumption 4

$$\int_{-\infty}^{\infty} g_i(x,t,y,s)\,\mathrm{d}x = 1$$

for $t > s$. ■

The next assumption is that the probability of an individual moving a finite distance during a time interval $[s,t]$ of length $h = t-s$ approaches zero as $h \to 0$. This assumption is weaker than assuming that an individual can travel only at finite speed. However, assuming that an individual moves at a finite speed would be too strong an assumption considered in conjunction with Assumption 1.

Assumption 5

$$\lim_{t\to s} \frac{1}{t-s} \int\limits_{|x-y|>a} g_i(x,t,y,s)\,\mathrm{d}x = 0$$

for every $a > 0$. ■

The following theorem shows that under Assumptions 1–5 the function ρ_i is governed by a parabolic partial differential equation.

Theorem 2.1 *To each single-species evolution process subject to Assumptions 1–5 there correspond functions $D(x,t) \geq 0$ and $C(x,t)$ such that the density function ρ_i for the process satisfies*

$$\frac{\partial \rho_i}{\partial t}(x,t) = \frac{\partial}{\partial x}\left(D(x,t)\frac{\partial \rho_i}{\partial x}(x,t) + C(x,t)\rho_i(x,t)\right). \tag{2.21}$$

Proof. Let (a,b) be some sub-interval of $\mathbb{R}$ and let

$$N(t) = \int_a^b \rho_i(x,t)\,\mathrm{d}x$$

be the approximate number of individuals in the interval at time t. Rather than work with the probability distribution of the position of an individual at time t define the redistribution kernel to be

$$k_i(\xi,y,t,h) \equiv g_i(y+\xi, t+h, y, t)$$

for $h > 0$. The redistribution kernel may be interpreted as the probability that an individual will move a distance ξ in a time interval of length h. Now

$$\rho_i(x,t+h) = \int_{-\infty}^{\infty} k_i(\xi, x-\xi, t, h)\rho_i(x-\xi,t)\,\mathrm{d}\xi.$$

Since by Assumption 4 and (2.2.2)

$$N(t) = \int_a^b \left[\int_{-\infty}^{\infty} k_i(\xi, x, t, h)\, \mathrm{d}\xi \right] \rho_i(x,t)\, \mathrm{d}x,$$

it follows that

$$\frac{1}{h}\left(N(t+h) - N(t)\right) = \frac{1}{h}\int_a^b \int_{-\infty}^{\infty} [k_i(\xi, x-\xi, t, h)\rho_i(x-\xi, t) - k_i(\xi, x, t, h)\rho_i(x,t)]\, \mathrm{d}\xi \mathrm{d}x.$$

When

$$D_\epsilon(t,h) = \frac{1}{h}\int_a^b \int_{|\xi|<\epsilon} [k_i(\xi, x-\xi, t, h)\rho_i(x-\xi, t) - k_i(\xi, x, t, h)\rho_i(x,t)]\, \mathrm{d}\xi \mathrm{d}x,$$

and $R_\epsilon(t,h) = \frac{1}{h}\left(N(t+h) - N(t)\right) - D_\epsilon(t,h)$, it follows by Assumption 5, since the population is finite, that for each $\epsilon > 0$,

$$\lim_{h\to 0} R_\epsilon(t,h) = 0.$$

Since $\frac{\partial \rho_i}{\partial t}(x,t)$ is continuous, it holds that

$$\lim_{h\to 0}\left(D_\epsilon + R_\epsilon\right) = \lim_{h\to 0}\frac{1}{h}\left(N(t+h) - N(t)\right) = \int_a^b \frac{\partial \rho_i}{\partial t}(x,t)\, \mathrm{d}x,$$

and hence

$$\lim_{h\to 0} D_\epsilon(t,h) = \int_a^b \frac{\partial \rho_i}{\partial t}(x,t)\, \mathrm{d}x. \tag{2.22}$$

The function D_ϵ may be written differently by interchanging the variables of integration to obtain

$$D_\epsilon(t,h) = \frac{1}{h}\int_{-\epsilon}^{\epsilon}\int_a^b k_i(\xi, x-\xi, t, h)\rho_i(x-\xi, t))\mathrm{d}x\mathrm{d}\xi - \frac{1}{h}\int_{-\epsilon}^{\epsilon}\int_a^b k_i(\xi, x, t, h)\rho_i(x,t))\, \mathrm{d}x\mathrm{d}\xi.$$

By substituting the variable z for $x - \xi$ the function D_ϵ may be written as

$$\begin{aligned} D_\epsilon(t,h) &= \frac{1}{h}\int_{-\epsilon}^{\epsilon}\int_{a-\xi}^{a} k_i(\xi, z, t, h)\rho_i(z,t))\mathrm{d}z\mathrm{d}\xi - \frac{1}{h}\int_{-\epsilon}^{\epsilon}\int_{b-\xi}^{b} k_i(\xi, z, t, h)\rho_i(z,t))\, \mathrm{d}z\mathrm{d}\xi \\ &= H(a,t,h) - H(b,t,h), \end{aligned}$$

where

$$\begin{aligned} H(x,t,h) &= \frac{1}{h}\int_{-\epsilon}^{\epsilon}\int_{x-\xi}^{x} k_i(\xi, z, t, h)\rho_i(z,t)\, \mathrm{d}z\mathrm{d}\xi \\ &= \frac{1}{h}\int_{-\epsilon}^{\epsilon}\int_0^{\xi} k_i(\xi, x-s, t, h)\rho_i(x-s,t)\, \mathrm{d}s\mathrm{d}\xi. \end{aligned}$$

Let $\delta_x = \frac{\partial \rho_i}{\partial x}(\hat{x}(s), t) - \frac{\partial \rho_i}{\partial x}(x,t)$ and expand $\rho_i(x-s,t)$ as a Taylor series about x to get

$$H(x,t,h) = \frac{1}{h}\int_{-\epsilon}^{\epsilon}\int_0^{\xi} k_i(\xi, x-s, t, h)\left[\rho_i(x,t) - s\left(\frac{\partial \rho_i}{\partial x}(x,t) + \delta_x\right)\right]\mathrm{d}s\mathrm{d}\xi,$$

where $\hat{x}(s)$ is some value between x and $x-s$. Since $\rho_i(x,t)$ and $\frac{\partial \rho_i}{\partial x}(x,t)$ are independent of the variables of integration it follows that

$$H(x,t,h) = A(x,t,h)\rho_i(x,t) - B(x,t,h)\frac{\partial \rho_i}{\partial x}(x,t) + Q(x,t,h).$$

Next $A(x,t,h)$, $B(x,t,h)$, and $Q(x,t,h)$ are shown to exist in the limit as $h \to 0$ and that $Q(x,t,h)$ is zero in this limit. Consider $\rho_i(x,t) = 0$ for x in a neighbourhood of a at time t and $\rho_i(x,t) = \rho_i^{(c)} = c$ for x in a neighbourhood of b, where c is constant. Then

$$D_\epsilon(t,h) = -H(b,t,h) = -A(b,t,h)\rho_i^{(c)}.$$

Hence, by (2.22),

$$C(x,t) = -\lim_{h\to 0} A(b,t,h)$$

exists. Next, consider $\rho_i(x,t)$ still zero for x in a neighbourhood of a, but $\rho_i(x,t)$ linear in a neighbourhood of b. Now

$$D_\epsilon(t,h) = -A(b,t,h)\rho_i(x,t) - B(x,t,h)\frac{\partial \rho_i}{\partial x}(x,t),$$

hence

$$-D(x,t) = -\lim_{h\to 0} B(b,t,h)$$

exists. Furthermore,

$$|Q(x,t,h)| \le \frac{1}{h}\int_{-\epsilon}^{\epsilon}\int_0^{\xi} sk(\xi, x-s, t, t+h)\,|\delta_x|\,\mathrm{d}s\mathrm{d}\xi \le \sup_{|s|<\epsilon}|\delta_x|\,B(x,t,h).$$

Hence

$$\lim_{h\to 0}|Q(x,t,h)| \;\le\; \lim_{h\to 0}\sup_{|s|<\epsilon}|\delta_x|\,B(x,t,h).$$

By the continuity of $\frac{\partial \rho_i}{\partial x}(x,t)$,

$$\sup_{|s|<\epsilon}|\delta_x| \to 0$$

as $h \to 0$, and so $|Q(x,t,h)| \to 0$ as $h \to 0$. Hence

$$H(x,t) = \lim_{h\to 0} H(x,t,h) = -C(x,t)\rho_i(x,t) - D(x,t)\frac{\partial \rho_i}{\partial x}(x,t),$$

and thus, from (2.22), it follows that

$$\int_a^b \frac{\partial \rho_i}{\partial t}(x,t)\,\mathrm{d}x = \lim_{h\to 0}\frac{N(t+h)-N(t)}{h} = H(a,t) - H(b,t). \tag{2.23}$$

Since the left hand side of (2.23) may be differentiated with respect to b, so too may the right hand side of the equation. Hence it follows that

$$\frac{\partial \rho_i}{\partial t}(x,t) = \frac{\partial}{\partial x}\left(D(x,t)\frac{\partial \rho_i}{\partial x}(x,t) + C(x,t)\rho_i(x,t)\right),$$

thereby concluding the proof. ■

2.2.3 The Reaction Process

The next step is to extend the model equations (2.21) to include the creation and annihilation of individuals of the population. Let $\underline{\rho}(x,t) = (\rho_1(x,t), \ldots, \rho_n(x,t))$ denote the vector of densities of the n species that make up the population, and let $\underline{k}(x,t) = (k_1(x,t), \ldots, k_n(x,t))$ be the vector of redistribution kernels. Furthermore, denote by $\underline{v}(x,t,h)$ the vector density at time $t+h$ of new individuals which have appeared during the time interval $(t, t+h)$. Accordingly the model is now

$$\rho_i(x, t+h) = \int_{-\infty}^{\infty} k_i(x-y, y, t, h)\rho_i(y,t)\,\mathrm{d}y + v_i(x,t,h).$$

However, this does not yet explain how the individuals make their appearance.

Assumption 6 *The function $\underline{v}(x,t,h)$ depends on the entire function $\underline{\rho}(\cdot,t)$. Symbolize this by writing*

$$\underline{v}(x,t,h) = h\underline{F}(x,t,h,\underline{\rho}(\cdot,t)). \qquad \blacksquare$$

The next assumption centres on the dependence of $\underline{F}$ upon $\underline{\rho}$. The vector $\underline{v}$ at a point x should not depend strongly on the value of $\underline{\rho}$ at distant points. To affect this, introduce a weight function $\kappa(\xi, h)$, which may be interpreted as a measure of the relative influence exerted by the value of $\underline{\rho}(x+\xi, t)$ on the value of $\underline{v}(x,t,h)$. To be only minimally restrictive, it is assumed that

$$\kappa \geq 0 \quad \text{and that} \quad \int_{-\infty}^{\infty} \kappa(\xi, h)\,\mathrm{d}\xi < C \tag{2.24}$$

independently of h, for some constant C. In order that κ reflect the local dependence property it is required that

$$\lim_{h\to 0} \int_{\infty}^{\infty} \xi^2 \kappa(\xi, h)\,\mathrm{d}\xi = 0. \tag{2.25}$$

The assumption is now as follows.

Assumption 7 *For each (x,t,h), $\underline{F}$ is a uniformly continuous functional, for all $h > 0$, on the space of functions $\underline{f}$ for which the integral $\int_{-\infty}^{\infty} \kappa(x-y,h)\left|\underline{f}(y,t)\right|\mathrm{d}y$ exists.* $\blacksquare$

That is, for every (x,t) and $\epsilon > 0$, there exists a $\delta(x,t,\epsilon)$ such that, if $\underline{\rho}^{(1)}$ and $\underline{\rho}^{(2)}$ are two density functions such that

$$\int_{-\infty}^{\infty} \kappa(x-y,h)\left|\underline{\rho}^{(1)}(y,t) - \underline{\rho}^{(1)}(y,t)\right|\mathrm{d}y < \delta(x,t,\epsilon),$$

then

$$\left|\underline{F}(x,t,h,\underline{\rho}^{(1)}(\cdot,t)) - \underline{F}(x,t,h,\underline{\rho}^{(2)}(\cdot,t))\right| < \epsilon$$

for all $h > 0$. The following intermediate lemma is required.

Lemma 2.1 *Let $\underline{\rho}^{(1)}(x,t)$ and $\underline{\rho}^{(2)}(x,t)$ be functions twice differentiable in x with $\underline{\rho}^{(1)}(x_0,t) = \underline{\rho}^{(2)}(x_0,t)$ for some $x_0 \in \mathbb{R}$. If κ is a weight function for which (2.24) and (2.25) hold, and Assumption 7 holds, then*

$$\lim_{h\to 0}\left|\underline{F}(x_0,t,h,\underline{\rho}^{(1)}(\cdot,t)) - \underline{F}(x_0,t,h,\underline{\rho}^{(2)}(\cdot,t))\right| = 0.$$

Proof. The result follows by the continuity property, Assumption 7, if

$$\lim_{h\to 0}\left|\int_{\infty}^{\infty}\kappa(x-y,h)\left[\rho_i^{(1)}(y)-\rho_i^{(2)}(y)\right]\mathrm{d}y\right|=0,$$

for each i. By a Taylor series expansion (see Theorem A.4) about x_0,

$$\rho_i^{(1)}(y)-\rho_i^{(2)}(y)=(y-x_0)\left[\frac{\partial\rho_i^{(1)}(x_0)}{\partial x}-\frac{\partial\rho_i^{(2)}(x_0)}{\partial x}\right]+\frac{1}{2}(y-x_0)^2\left[\frac{\partial^2\rho_i^{(1)}(\hat{x})}{\partial x^2}-\frac{\partial^2\rho_i^{(2)}(\hat{x})}{\partial x^2}\right],$$

for each i, where $\hat{x}$ is between x_0 and y. Thus

$$\left|\int_{\infty}^{\infty}\kappa(x-y,h)\left[\rho_i^{(1)}(y)-\rho_i^{(2)}(y)\right]\mathrm{d}y\right|\le C_1\int_{\infty}^{\infty}|\xi|\,\kappa(\xi,h)\mathrm{d}\xi+C_2\int_{\infty}^{\infty}(\xi)^2\,\kappa(\xi,h)\mathrm{d}\xi.$$

By the Swartz inequality (see Theorem A.13), and (2.24) and (2.25),

$$\int_{\infty}^{\infty}|\xi|\,\kappa(\xi,h)\,\mathrm{d}\xi\le\left(\int_{-\infty}^{\infty}\kappa(\xi,h)\,\mathrm{d}\xi\right)^{\frac{1}{2}}\left(\int_{-\infty}^{\infty}\xi^2\kappa(\xi,h)\,\mathrm{d}\xi\right)^{\frac{1}{2}}\to 0$$

as $h\to 0$. Also, by (2.25),

$$\int_{\infty}^{\infty}\xi^2\kappa(\xi,h)\,\mathrm{d}\xi\to 0$$

as $h\to 0$, thereby concluding the proof. ■

The main result of this section now follows from Assumptions 1–7 and Lemma 2.1.

Theorem 2.2 *To each evolution process satisfying Assumptions 1–7 with density vector function for the process* $\underline{\rho}(x,t)$ *such that, for every* i,

$$\rho_i(x,t+h)=\int_{-\infty}^{\infty}k_i(x-y,y,t,h)\rho_i(y,t)\mathrm{d}y+v_i(x,t,h),$$

there correspond functions $D_i(x,t)\ge 0$, $C_i(x,t)$, *and* $G_i(x,t,\underline{\rho}(x,t))$ *such that the density function satisfies*

$$\frac{\partial\rho_i}{\partial t}(x,t)=\frac{\partial}{\partial x}\left(D_i(x,t)\frac{\partial\rho_i}{\partial x}(x,t)+C_i(x,t)\rho_i(x,t)\right)+G_i(x,t,\underline{\rho}(x,t)).\tag{2.26}$$

Proof.
For each (x_0,t_0),

$$\frac{\partial\rho_i}{\partial t}(x_0,t_0)=\lim_{h\to 0}\frac{1}{h}\left(\rho_i(x_0,t_0+h)-\rho_i(x_0,t_h)\right).\tag{2.27}$$

Since the left hand side of (2.27) exists, the limit on the right hand side also exists. However,

$$\begin{aligned}\lim_{h\to 0}\frac{1}{h}\left(\rho_i(x_0,t_0+h)-\rho_i(x_0,t_h)\right) &= \lim_{h\to 0}\frac{1}{h}\left(\int_{-\infty}^{\infty}k_i(x-y,y,t,h)\rho_i(y,t)\mathrm{d}y-\rho_i(x_0,t_0)\right)\\ &\quad+\lim_{h\to 0}F_i(x_0,t_0,h,\underline{\rho}(\cdot,t_0))\end{aligned}\tag{2.28}$$

and hence

$$F_i(x_0, t_0, 0, \underline{\rho}(\cdot, t_0)) = \lim_{h \to 0} F_i(x_0, t_0, h, \underline{\rho}(\cdot, t_0))$$

exists. Lemma 2.1 implies that this limit depends only on the value $\rho(x_0, t_0)$. Thus G_i may be defined as

$$G_i(x, t, \underline{\rho}(x, t)) = F_i(x, t, 0, \underline{\rho}(\cdot, t_0)).$$

The result now follows on the basis of the proof of Theorem 2.1 and from (2.28). ■

The form of (2.26) is more general than (2.6). In particular, (2.6) follows from setting $C(x, t) \equiv 0$ in (2.26). The $\frac{\partial}{\partial x}(C_i(x, t)\rho_i(x, t))$ term in (2.26) accounts for convection; the bias of the biological population to move in some direction. A convection term is absent from (2.6) because the population flux is assumed to depend only on the gradient of the population density function. In the chapters that follow $C(x, t)$ will be zero.

2.3 The Model Extended to Three Dimensions

The derivation of the model presented in §2.1.1 in one spatial dimension can easily be extended to three dimensions. The chief difference is that the divergence theorem is used instead of the fundamental theorem of the calculus.

Again denote by $\rho_i(\underline{r}, t)$ the density of particles of type i at position $\underline{r} \in \mathbb{R}^3$ and time $t \geq 0$. The function $\rho_i(\underline{r}, t)$ is assumed to be continuously differentiable in t and twice continuously differentiable in $\underline{r}$. Further denote by $\underline{J}_i(\underline{r}, t)$ the row vector of rates at which the particles of type i diffuse per unit surface area at position $\underline{r}$ and time t in the x-, y- and z-directions of a Cartesian reference frame in $\mathbb{R}^3$. Let $\underline{\rho}(\underline{r}, t) = [\rho_1(\underline{r}, t), \ldots, \rho_n(\underline{r}, t)]^T$ and $\mathbf{J}(\underline{r}, t) = [\underline{J}_1(\underline{r}, t), \ldots, \underline{J}_n(\underline{r}, t)]^T$. The vector form of Fick's law may now be expressed as

$$\mathbf{J}(\underline{r}, t) = -\mathbf{D}(\underline{r}, t)\nabla\underline{\rho}(\underline{r}, t), \tag{2.29}$$

where $\mathbf{D}(\underline{r}, t)$ is again assumed to be a continuous positive diagonal matrix, and hence it follows that $\mathbf{J}(\underline{r}, t)$ is continuous.

Let R be a closed, connected subset of $\mathbb{R}^3$ with a smooth boundary ∂R and $\underline{n}(\underline{r})$ the outward unit normal to the closed surface ∂R, then the concentration of particles flowing into R per unit time is

$$-\iint_{\partial R} \mathbf{J}(\underline{r}, t) \cdot \underline{n}(\underline{r}) \, \mathrm{d}(\partial R),$$

which, by the divergence theorem (See Theorem A.2), is equivalent to

$$-\iiint_R \nabla \cdot \mathbf{J}(\underline{r}, t) \, \mathrm{d}\underline{r}.$$

Let $G_i(\underline{r}, t, \underline{\rho})$ denote the concentration of particles of type i created per unit time at position $\underline{r} \in \mathbb{R}^3$ at time $t \geq 0$, and $\underline{G}(\underline{r}, t, \underline{\rho}) = \left[G_1(\underline{r}, t, \underline{\rho}), \ldots, G_n(\underline{r}, t, \underline{\rho})\right]^T$, then the principle of mass conservation may be expressed as

$$\frac{\mathrm{d}}{\mathrm{d}t} \iiint_R \underline{\rho}(\underline{r}, t) \, \mathrm{d}\underline{r} = -\iiint_R \nabla \cdot \mathbf{J}(\underline{r}, t) \, \mathrm{d}\underline{r} + \iiint_R \underline{G}(\underline{r}, t, \underline{\rho}) \, \mathrm{d}\underline{r},$$

from which follows that

$$\frac{\partial \underline{\rho}}{\partial t}(\underline{r},t) + \nabla \cdot \mathbf{J}(\underline{r},t) - \underline{G}(\underline{r},t,\underline{\rho}) = 0. \tag{2.30}$$

By Fick's Law (2.29) this is equivalent to

$$\frac{\partial \underline{\rho}}{\partial t}(\underline{r},t) = \nabla \cdot \big(\mathbf{D}(\underline{r},t)\nabla \underline{\rho}(\underline{r},t)\big) + \underline{G}(\underline{r},t,\underline{\rho}). \tag{2.31}$$

Once again, in the special case where $\mathbf{D}$ is independent of position, (2.31) reduces to

$$\frac{\partial \underline{\rho}}{\partial t}(\underline{r},t) = \mathbf{D}\,\nabla^2 \underline{\rho}(\underline{r},t) + \underline{G}(\underline{r},t,\underline{\rho}). \tag{2.32}$$

A complete description of a specific system once again also includes boundary conditions. Typically boundary conditions include a description of the initial state of the particle populations in the form

$$\underline{\rho}(\underline{r},0) = \underline{f}(\underline{r}). \tag{2.33}$$

If the domain considered is a region of finite physical proportions the behaviour of particles at the boundary of the region should also be described. A physically plausible possibility is once again that the particle density on the boundary is regulated, which corresponds to Dirichlet boundary conditions of the form

$$\underline{\rho}(\underline{r},t) = \underline{\theta}(\underline{r},t), \quad \underline{r} \in \partial R, \quad t \geq 0. \tag{2.34}$$

Another possibility is that the flow of particles across the boundary of the region is regulated, which corresponds to Neumann boundary conditions of the form

$$\underline{n}(\underline{r}) \cdot \nabla \underline{\rho}(\underline{r},t) = \underline{\theta}(\underline{r},t), \quad \underline{r} \in \partial R, \quad t \geq 0. \tag{2.35}$$

2.4 Formal Problem Description

As stated in the informal problem description in §1.2 the aim in this thesis is to describe mathematically the realized niche, in a sufficiency sense, of a species in competition with another species in a heterogeneous environment. The description of the niche is in terms of the parameters describing the biological species competition model (2.6) as well as the structure of the habitat. Recalling (2.6) these parameters are the diffusion matrix $\mathbf{D}(x)$ and the parameters in the function $\underline{G}(x,t,\underline{\rho}(x,t))$, where $G_i(x,t,\underline{\rho}(x,t)) = r_i\rho_i(1 - \rho_i/k_i(x) - \beta_{ji}\rho_j/k_i(x))$ for $i,j = 1,2$ and $i \neq j$. $\underline{G}$ is a minor generalization of the Lotka-Volterra model introduced in Chapter 1 in the sense that the carrying capacities now depend on spatial position. The competition coefficients, however, remain constant.

Parameter ranges for which the invading species successfully invades represent the sufficient conditions under which a species will survive. It is the primary aim of this study to develop a method to determine such parameter ranges. A secondary aim is to attribute a measure of dominance of the invading species within the niche that it occupies.

2.5 Chapter Summary

A mathematical model of coexisting biological species was derived by two methods in this chapter. The first appealed to the principle of Fickian diffusion (§2.1.1), whilst the second was based on some assumptions on the nature of the redistribution and reaction processes (§2.2).

The mathematical model approximates a discrete population by a smooth density function which introduces the vanishingly small possibility of individuals of the population moving at infinite speed. Moreover, the redistribution process is approximated by a diffusion process which highlights the fact that the population dynamics are governed by local events. Both approximations were motivated by means of a central limit theorem (§A.3) and Taylor's theorem (§A.2). After the mathematical model was extended to three spatial dimensions (§2.3), the problem to be considered in the remainder of the thesis was formulated formally in terms of the mathematical model derived in this chapter (§2.4).

Chapter 3

Concise Literature Review

This chapter contains a survey of literature pertaining to models that describe populations by means of a coupled system of reaction-diffusion equations, in fulfilment of Objective III in § 1.3. In addition to providing background, this chapter therefore serves to place the problems considered in this thesis within a broader mathematical context.

3.1 Population Dynamics

The investigation in this thesis is in essence about the growth and decline of biological populations. The model in Chapter 2 is derived from oversimplified assumptions. However, in defence of simple, abstract models Pielou [68, 1969] writes, "Obviously one must study the behaviour of simple models before modifying and complicating the first, simplest assumptions, and the simple models provide a basis for elaboration."

3.1.1 The Pure Birth Process

The most basic of all biological models is perhaps the pure birth process, which is defined by the assumptions that the organisms are immortal and reproduce at the same rate for every individual. Furthermore, it is assumed that the individuals have no effect on one another. Let $n(t)$ denote the size of the population at time t and let r denote the rate at which the population increases. It follows that

$$\frac{\mathrm{d}n}{\mathrm{d}t}(t) = r\, n(t),$$

and hence, if the initial population size at time $t = 0$ were n_0, that $n(t) = n_0 e^{rt}$. Despite their extreme simplicity, these assumptions may hold approximately and over a short time interval for the growth of a population of single-celled organisms. However, the process described is deterministic. It assumes not that an organism *may* reproduce but that, in fact, it *does* reproduce.

Yule [92, 1924] assumed that there is a certain probability that a given individual will reproduce within a given time interval. The process he proposed is described by the differential difference equation

$$\frac{\mathrm{d}p_n}{\mathrm{d}t}(t) = r\, np_n(t) + r(n-1)p_{n-1}(t), \tag{3.1}$$

where $p_n(t)$ is the probability that a population is of size n at time t. The general solution to (3.1) is

$$p_n(t) = \binom{n-1}{n_0-1} e^{-rn_0t}(1-e^{-rt})^{n-n_0}. \tag{3.2}$$

It follows that the probability distribution of n depends only on rt. From (3.2) it follows that the expected population size at time t is n_0e^{rt}, which is equal to that predicted with certainty for the deterministic process. The variance of n is $n_0e^{rt}(e^{rt}-1)$. The variance increases with t, which amounts to saying that, even if the assumptions are true, the farther into the future a prediction refers to, the less precise that prediction will be.

3.1.2 Logistic Growth

It is assumed in the pure birth process that the rate of reproduction of an organism remains constant and is independent of the size of the population. However, in reality a population in a restricted environment must eventually be limited by a shortage of resources. To remedy this situation the pure birth process may be adapted by assuming that population growth depends on population size. The simplest dependence assumption is that the growth rate depends linearly on the population size, that is,

$$\frac{\mathrm{d}n}{\mathrm{d}t}(t) = n(t)(r - dn(t)), \tag{3.3}$$

which is sometimes known as logistic growth. The solution to (3.3) for an initial population size n_0 at time $t = 0$ is

$$n(t) = \frac{r/d}{1 - e^{-r(t-t_0)}}, \tag{3.4}$$

where t_0 is a constant chosen such that $n(0) = n_0$. The asymptotic value of $n(t)$ as $t \to \infty$ is r/d, and cannot be exceeded because of environmental limitations. There are many examples in the literature of laboratory populations that were observed to follow an approximate logistic growth curve. Amongst these are the experiments by Lotka [55, 1925], who described the growth of an experimental population of *Drosophila*; and Gause [28, 1934] who described the growth of a culture of *Paramecium caudatum*.

An example of where the logistic growth process is not well correlated with the growth of a population is described by Smith [72, 1963]. He determined growth rates at a succession of density levels in a laboratory population of *Daphnia magna*. Smith found that the growth rate does not decrease linearly with an increase in population (as would be the case were the population to follow a logistic growth curve), but rather that the relationship is represented by a concave curve. Smith then argued that the growth rate is proportional to the rate of food supply not being used by the population.

Even though the logistic growth process is more realistic than a pure birth process it is still highly simplified. Pielou [68, 1969] lists six assumptions underlying the logistic growth process that are frequently not satisfied in applications. Amongst these is the assumption that crowding affects all population members equally, which is unlikely to be true if individuals are not evenly distributed throughout the available space. The studies of Andrewartha and Birch [3, 1954] on natural and laboratory populations, particularly of insects, indicates the importance of the spatial distribution of populations with respect to its survival.

Fisher [26, 1937] introduced a reaction-diffusion equation of the form

$$\frac{\partial n}{\partial t}(x,t) = D\frac{\partial^2 n}{\partial x^2}(x,t) + r\, n(x,t)(1 - n(x,t)) \tag{3.5}$$

to model the spatial spread of an advantageous gene through a population. In the context of biological populations (3.5) describes a population of organisms assumed to exhibit Brownian random motion and a growth rate depending on the spatially varying population density. Skellam [71, 1951] modelled the expansion of muskrat populations in Europe using a reaction-diffusion equation, where the reaction part was that of a pure birth process. His model predicts that the area occupied by an invader will increase linearly with time.

3.1.3 Competition Systems

Volterra [88, 1931] introduced a system of coupled differential equations of the form (1.2), which, together with suitable initial conditions, model the interaction of n species. A special case of (1.2) is the two-component competition system

$$\left.\begin{aligned} \frac{\mathrm{d}n_1}{\mathrm{d}t}(t) &= n_1(t)(k_1 - a_{11}n_1(t) - a_{21}n_2(t)), \\ \frac{\mathrm{d}n_2}{\mathrm{d}t}(t) &= n_2(t)(k_2 - a_{22}n_2(t) - a_{12}n_1(t)), \end{aligned}\right\} \tag{3.6}$$

where all coefficients are non-negative constants, which, together with initial conditions, models the competition for resources between two biological species.

Of specific interest is the asymptotic behaviour of the population sizes [68] as $t \to \infty$. Figure 3.1 demonstrates the four possible scenarios. In the graphs each point corresponds to a combined two-species population. Projection of such a point onto the x-axis is the population size of the first species, whilst the projection onto the y-axis yields the population size of the second species. The locus of points for which $\mathrm{d}n_i/\mathrm{d}t = 0$ is represented by a solid and a dashed line when $i = 1$ and 2 respectively. For population sizes corresponding to points above the solid line it follows that $n_1(t)$ decreases and for points below the line that $n_1(t)$ increases. The same relationships hold for the dashed line and the population size of $n_2(t)$. Figures 3.1(a) and 3.1(b) demonstrate respectively the scenario where the model parameters are such that either species two or species one eventually becomes extinct. Figures 3.1(c) and 3.1(d) demonstrate scenarios where coexistence equilibrium points exist. That is, a point, other than the origin, where the population sizes are such that both species have zero population growth. The equilibrium point is at the intersection of the solid and the hashed lines. The equilibrium in Figure 3.1(c) is stable, since in the regions above the one line and below the other the joint-population growth rate vector points in the direction of the equilibrium. However, the equilibrium in Figure 3.1(d) is unstable, since in the regions above the one line and below the other the joint-population growth rate vector points away from the equilibrium, and thus one species (depending on the initial conditions) will become extinct if the population densities are perturbed away from the equilibrium point. The parameters of the model in the scenario of Figure 3.1(c) are such that $k_i a_{jj} > k_j a_{ii}$ for $i, j = 1, 2$ and $i \neq j$.

Kereiva *et al.* [47, 1996] use the system (3.6) to investigate the invasiveness of a genetically engineered organism. The organism is a modified strain of the *Pseudomonas syringae*

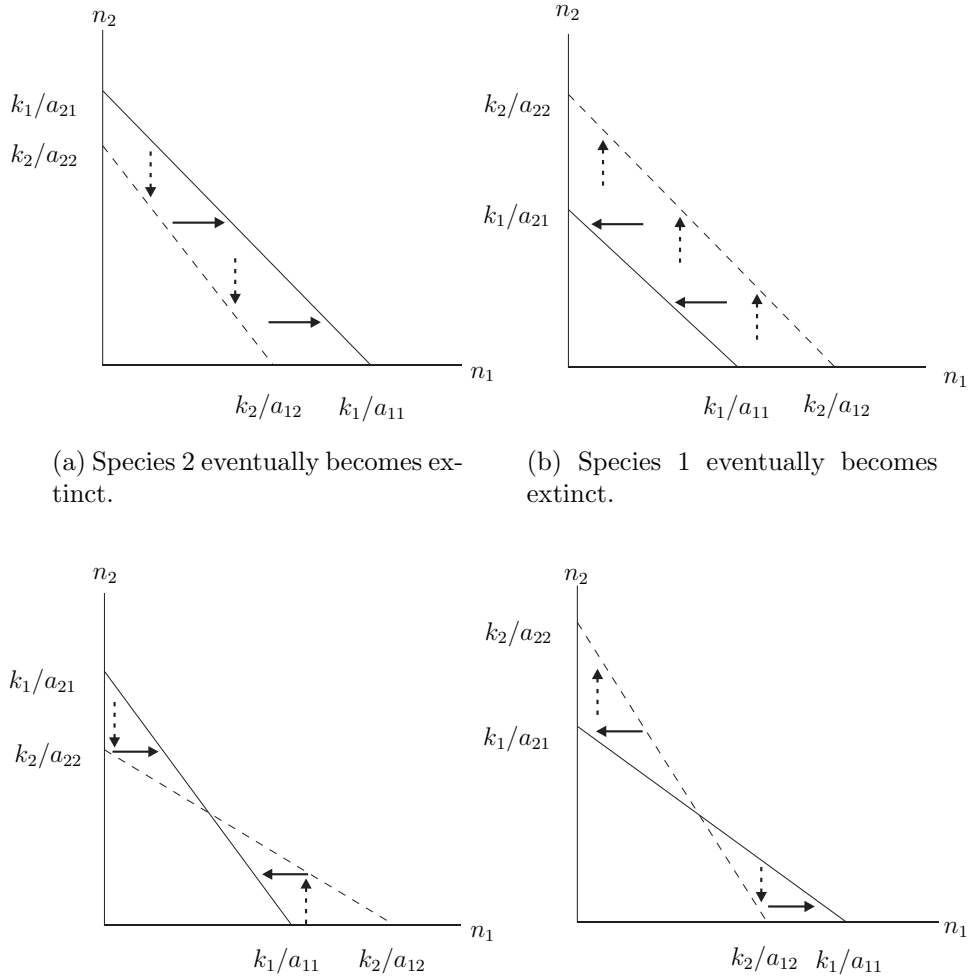

(a) Species 2 eventually becomes extinct.

(b) Species 1 eventually becomes extinct.

(c) A stable coexistence state.

(d) An unstable coexistence state.

Figure 3.1: Lines of zero population growth, or null clines, for the competition system (3.6). The null cline of species one is represented by the solid line and the null cline of species two is represented by the hashed line. In (a) and (b) no coexistent state exists. In (c) and (d) coexistent states exist, but only (c) is stable.

bacteria. The modified bacteria lack ice nucleation activity and hence are less likely to initiate frost damage in plants whose leaves or fruits they coat. The analysis indicates that the modified *Psuedomonas* may maintain locally high population densities if present initially at a sufficient density, but that they were not likely to displace the wild-type *Psuedomonas*. However, Kereiva *et al.* also illustrate the hazards and limitations of viewing invasion ecology as a predictive science. They point out that the invasiveness of any genetically engineered organism will be highly sensitive to local environmental conditions.

3.1.4 The Biological Niche

Grinnell [34, 1917] referred to the "ecological or environmental niche" as the ultimate distributional unit of one species. His conceptualization of a niche was a distribution of individuals over geographical area and among habitat types, but as an idealized distribution of individuals in the absence of their interactions with other species. Elton [21, 1927] stated that, "... the 'niche' of an animal means its place in the abiotic environment, its

relations to food and enemies." Hence early use of the concept of a niche referred to a species' actual place in nature.

Hutchinson [42, 1957] developed the formal notion of the ecological niche as a hypervolume. He began by considering two environmental variables and plotted a population graph against these variables. If, for instance, the variables are temperature and humidity, there is some value of either variable below which a given species cannot exist and some value of either variable above which the species cannot exist. The volume between these values describes the niche of the species. If variables are added the result is a multidimensional space and the hypervolume where species survival describes the niche of the species. Hutchinson's hypervolume description of a niche conceptualizes the *fundamental niche*, that is, where the species could exist. He goes on to describe a *realized niche* as that part of the fundamental niche that remains occupied by the species after interactions with other species. Vandermeer [86, 1972] presented a theoretical framework of niche theory within this context.

However, Whittaker *et al.* [91, 1973] distinguished three senses in which the word 'niche' is used. Firstly, the niche as the position and role of a species within a given community. Secondly, the niche as habitat. And lastly, the niche as a combination of the first two concepts. They suggest that the confusion surrounding the use of the term *niche* may be resolved by referring to that part of the multidimensional space defined by the physical environment as the habitat hyperspace and that space defined by the variables by which a species in a given community are adaptively related as the niche hyperspace. When combined the variables of habitat and niche define the ecotope hyperspace. Figure 3.2 is an abstract representation of the conceptual hyperspace. The n and m dimensional axes of habitat and niche variables have been collapsed into two axes. The plotted volume represents the ecotope hypervolume. The projection of the volume onto the niche variable axis describes the niche of the species.

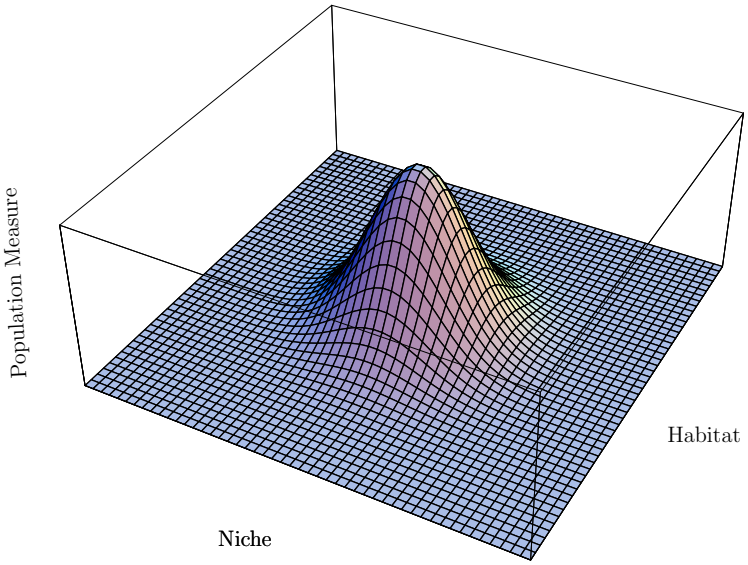

Figure 3.2: A diagrammatic representation of the relations to one another of a system of concepts including niche, habitat, and ecotype [91].

The definition of the notion of a niche used in this thesis is that by Chase and Leibold [9, 2003]. They define the niche of a species as "The joint description of the environmental

conditions that allow a species to satisfy its minimum requirements so that the birth rate of a local population is equal to or greater than its death rate along with the set of per capita effects of that species on these environmental conditions."

They showed that stable coexistence of two species with similar niches requires two trade-offs. Firstly, in the absence of the other species, each species must differ in the factor it finds most limiting. Secondly, each species must have a greater impact on the factor it finds most limiting. In terms of the competition system (3.6) the first condition is similar to requiring that the relative carrying capacities of the two species must be such that neither species has too strong an advantage. Vandermeer [87, 1975], in fact, showed that this condition is necessary for a coexistent state to exist. The condition may be expressed as $a_{ji} < k_j/k_i < 1/a_{ij}$ for $i \neq j$. The second condition ensures local stability and is equivalent to saying that for two species to coexist, locally interspecific competition must be less than intraspecific competition. This condition may be expressed as $a_{ii}a_{jj} > a_{ij}a_{ji}$. Together these two conditions are sufficient to ensure coexistence in the competition system (3.6).

3.2 Reaction-Diffusion Models

Kareiva [46, 1983] used a simple passive diffusion model, that is, (3.5) without a reaction term, to analyse within-habitat dispersal of twelve species of herbivorous insects. The data comprised field mark-recapture studies. For eight of the species, the cumulative frequency distributions of dispersal distances were found to be consistent with a model of movement of organisms assumed to exhibit Brownian random motion.

Kolmogoroff *et al.* [49, 1937] analysed Fisher's equation (3.5). For a certain class of initial values they showed that the solution to (3.5) with appropriate boundary conditions evolves into a travelling wavefront solution with asymptotic wave velocity $\sqrt{4rD}$. The simple form of the equation for the asymptotic invasion velocity holds for a general class of reaction terms, $f(u)$, of which logistic growth is a member. More generally the asymptotic wave velocity is $\sqrt{4f'(u)D}$ [25, 1979].

Such travelling wavefront solutions have been used to model the invasion of an organism into an environment. Lubina and Levin [53, 1988] modelled the range expansion of the California sea otter (which was hunted to near extinction) by means of a reaction-diffusion equation together with an added advection term. The rate of range expansion of the California sea otter as predicted by the model corresponded well with the observed data. The difference in estimated diffusion constants were sufficient to explain the different observed rates of range expansion on the southern and northern fronts.

Lewis and Pacala [52, 2000] derived spatially explicit equations to describe a stochastic invasion process. They derived equations for population moments and used these to analyse the asymptotic permanence of form in the leading edge of the wave of invasion and the patchy structure of the invasion. Lewis [51, 2000] further analysed the effect of intrinsic stochastic factors arising from a finite population reproducing, dying and interacting with other individuals in a probabilistic manner. He derived an upper bound on the rate of spread of the stochastic invasion process that is strictly below the rate of spread of the deterministic model.

Okubo *et al.* [65, 1989] used a two-component reaction-diffusion system coupled in the re-

action terms, in a manner similar to (3.6), to model the competition between the the grey squirrel (which was introduced to Britain at the beginning of the twentieth century) and the smaller indigenous red squirrel. Where possible the model parameters were estimated from field data. The rate of advance of the grey squirrel predicted by their model was typical of the speed of invasion observed in the field. The modelled population distributions were also qualitatively similar to those observed. They suggested that competition alone could explain the observed displacement of the red squirrel by the grey squirrel. Their model predicted a rate of population spread that is slower than the spread of a single species, because competition slows down the advance of the invading species.

Within the context of initial-boundary value problems with governing autonomous reaction-diffusion equations, the notion of a steady state solution means an asymptotic solution that is spatially dependent only. The asymptotic behaviour of solutions may well be more complex than merely convergence to a steady state. Following Cantrell and Cosner [8, 1998] the notion of *coexistence*, or *uniform persistence*, of two species means that there exist some fixed positive population density profiles $n_1^*(x)$ and $n_2^*(x)$ such that the solutions of the initial-boundary value problem will at some point in time, and then for all future time, exceed $n_1^*(x)$ and $n_2^*(x)$ for all x in the considered domain. If further there exist constants N_1 and N_2 such that the solutions remain below these constants, for all x, then the system is said to be *permanent*. A system is called *invasible* if the state where either n_1 or n_2 is present at an equilibrium density in the absence of the other species is unstable to small perturbation in the population density of the hitherto absent species. Cantrell *et al.* [6, 1993] proved that invasibility implies permanence in a reaction-diffusion model system with a rather general (heterogeneous) growth rate function.

Brown [5, 1980] established conditions for the existence and global asymptotic stability of a critical point of the population densities vector with both species coexisting. He provided the result for the two-component homogeneous reaction-diffusion system, with reaction terms given by (3.6), on a region $\Omega \in \mathbb{R}^m$ with sufficiently regular boundary and zero-flux Neumann boundary conditions. He showed that, when the condition holds, the coexistence steady state of the reaction diffusion model is

$$\lim_{t\to\infty} (n_1(x,t), n_2(x,t)) = (n_1^*, n_2^*),$$

uniformly for $x \in \Omega$, where (n_1^*, n_2^*) is the coexistence state of the corresponding system (3.6). Thus diffusion plays no role in the stability of the coexistence steady state. Cosner and Lazer [13, 1984] found sufficient conditions for the existence, uniqueness and stability of a coexistent steady state for the same system when homogeneous Dirichlet boundary conditions are imposed. The work of Conway *et al.* [12, 1978] implies that the asymptotic behaviour of the solution to a homogeneous reaction-diffusion competition system with zero-flux Neumann boundary conditions on a bounded spatial domain and large diffusion coefficients decays exponentially to a spatially homogeneous solution. Thus Conway *et al.* give a sufficient condition for the validity of approximation of a spatially distributed system by solutions of ordinary differential equations. In particular, when their condition holds, they show that all stable coexistent states of the ordinary differential equation are stable as solutions of the partial differential equation as well.

Mimura *et al.* [59, 1991] showed that under strong competition (when the condition for a stable coexistent state to exist for (3.6) does not hold) an appropriate nonconvex domain with zero-flux Neumann boundary conditions may be found in $\mathbb{R}^2$ such that a coexistent state exists for the reaction-diffusion model with constant coefficients. The coexistent

steady state solutions they obtained are spatially inhomogeneous solutions where the species spatially segregate.

3.3 Heterogeneous Environments

Nagylaki [63, 1975] investigated the existence of clines (a spatially varying steady state) in a model similar to Fisher's model (3.5) with zero-flux Neumann boundary condition, but with a spatially heterogeneous selection coefficient that models the frequency of a gene in a population of homogeneous density on a semi-infinite domain. Fleming [22, 1975] studied the existence and stability properties of steady states for a similar model with a spatially heterogeneous selection coefficient on a bounded domain.

Shigesada *et al.* [70, 1986] investigated the travelling (periodic) waves of invasion of a single species reaction-diffusion model similar to Fisher's model (3.5), but with a two-toned spatially varying diffusion coefficient and carrying capacity. The environment represented by the spatially varying parameters comprise of two environment types alternately arranged. The wave front continually changes as the wave travels through the changing environment, though the structure of the wave is periodic in time. A condition for the instability of the trivial solution was found. However, the stability of the travelling periodic wave was only observed in numerical computations. Furthermore, the asymptotic velocity of the travelling periodic wave was calculated.

Pacala and Roughgarden [66, 1982] examine a reaction-diffusion competition system with Lotka-Volterra competition terms generalized with spatially dependent carrying capacities to represent a two-toned heterogeneous environment. The boundary conditions are zero-flux Neumann conditions. Except in special cases the model is solved numerically. An interval with constant carrying capacity is said to be *suitable* if the corresponding system (3.6) allows the invading species to invade whilst still a small initial population when the other species is already established. Otherwise the interval is said to be *unsuitable*. They offered three findings: Firstly, if the one interval is suitable and the other unsuitable then the success of the invasion depends on the length of the suitable interval. Secondly, it is possible for the invading species to invade even though both intervals are unsuitable. Thirdly, it is possible for the invading species to fail to invade even though both intervals are suitable.

Cruywagen *et al.* [15, 1996] sought to quantify the possibility of containment of a genetically engineered organism introduced into a heterogeneous environment. The model equations are an autonomous reaction-diffusion system with Lotka-Volterra competition reaction terms and spatially dependent diffusion coefficients and carrying capacities. In the most general case the diffusion coefficients and carrying capacities are two-toned functions that represent a periodic environment alternating between favourable and unfavourable patches. The invading species represents a genetically engineered organism released into an environment where it competes with a second species that represents the natural, unmodified, organism. In the case where only the diffusion coefficients are two-toned, but the carrying capacities constant, Cruywagen *et al.* found conditions in terms of the model parameters and the length of the unfavourable patch under which the genetically engineered organism will successfully invade. In the general case of two-toned diffusion coefficients and two-toned carrying capacities they found sufficient conditions under which the genetically engineered organism will invade.

Cantrell *et al.* [6, 1993] established conditions for permanence of an autonomous reaction-diffusion system, with either Neumann or Dirichlet boundary conditions, where the growth functions in the reaction terms are spatially dependent and represent predator-prey as well as competition interactions. The conditions for permanence are expressed via the signs of eigenvalues of associated elliptic operators. These eigenvalues themselves depend in non-trivial ways on the model parameters. Cantrell *et al.* [7, 1996] used the results of [6] to investigate the interplay among diffusion, spatial heterogeneity, species interactions and habitat geometry that guarantee coexistence. They considered a number of examples of non-trivial spatial variation where the conditions for permanence are nevertheless exactly calculable. Furthermore they also established conditions in terms of an eigenvalue and the diffusion constant that ensures the existence of a steady state solution for a single species reaction-diffusion equation with zero-flux Neumann boundary conditions. Cantrell *et al.* [8, 1998] demonstrated that competitors may coexist even in the case of strong competition, provided that the populations segregate spatially, with the mechanism for spatial segregation being spatial variation in the growth functions. Furthermore, they also demonstrated that coexistence is possible with no such spatial segregation, provided that strong competition is restricted to small spatial regions. They elaborate on, and explain, observations of numerical computations of Pacala and Roughgarden [66, 1982] indicating that invasion in competition models is possible globally even when it would fail in a homogeneous environment corresponding to any local region of the global environment and that, conversely, invasion may fail globally when it would be possible in a homogeneous environment corresponding to any local region of the global environment.

3.4 Chapter Summary

This chapter contains a concise review of literature pertaining to models that describe populations by means of a coupled system of reaction-diffusion equations. Models describing the growth and decline of homogeneously distributed populations, and the relation of these models to the concept of a biological niche, are reviewed first (§3.1). Thereafter models describing the evolution of populations that are not assumed to be homogeneously distributed are reviewed (§3.2). Finally, models describing the evolution of populations in heterogeneous environments are reviewed (§3.3).

Chapter 4

Numerical Methods

In this chapter the numerical schemes used to approximate solutions to the initial-boundary value problems studied in this thesis are reviewed and motivated in fulfilment of Objectives IV in § 1.3. Two methods are used, that of *finite differences* and the second being *spectral methods*. Prototypical examples of approximating solutions to models that will be studied later in the thesis are compared in this chapter. The initial-boundary value problem in one spatial dimension and in time, with either zero-flux Neumann conditions or imposed periodicity, that will be considered is

$$\left.\begin{aligned} \frac{\partial u}{\partial t}(x,t) &= d_u(x)\frac{\partial^2 u}{\partial x^2}(x,t) + \phi(x,u,v), \\ \frac{\partial v}{\partial t}(x,t) &= d_v(x)\frac{\partial^2 v}{\partial x^2}(x,t) + \theta(x,u,v), \\ u(x,0) = f_u(x) &\quad \text{and} \quad v(x,0) = f_v(x), \end{aligned}\right\} \tag{4.1}$$

where $0 < x < 2\pi$ and $0 < t \leq T$ for some $T \in \mathbb{R}^+$, and where ϕ and θ are the growth terms for each species. The diffusion coefficients $d_u(x)$ and $d_v(x)$ used in the rest of the thesis are two-toned functions. Thus, the system (2.6) reduces to the system (4.1). In the case of zero-flux Neumann boundary conditions the boundary conditions are

$$\left.\begin{aligned} \frac{\partial u}{\partial x}(0,t) = 0, \qquad \frac{\partial v}{\partial x}(0,t) = 0, \\ \frac{\partial u}{\partial x}(2\pi,t) = 0, \qquad \frac{\partial v}{\partial x}(2\pi,t) = 0, \end{aligned}\right\} \tag{4.2}$$

and in the case of periodicity the boundary conditions are

$$\frac{\partial u}{\partial x}(0,t) = \frac{\partial u}{\partial x}(2\pi,t) \quad \text{and} \quad \frac{\partial v}{\partial x}(0,t) = \frac{\partial v}{\partial x}(2\pi,t). \tag{4.3}$$

The non-linear functions ϕ and θ are assumed to have the form

$$\begin{aligned} \phi &= u(x,t)\left(1 - \frac{u(x,t)}{k_u(x,t)} - \frac{\beta_{12}v(x,t)}{k_u(x,t)}\right), \\ \theta &= v(x,t)\left(1 - \frac{v(x,t)}{k_v(x,t)} - \frac{\beta_{21}u(x,t)}{k_v(x,t)}\right). \end{aligned}$$

4.1 The Finite Difference Method

The method of finite differences is used to approximate solutions of initial-boundary value problems on a bounded spatial domain with zero-flux boundary conditions. In this method finite differences are used to approximate derivatives by differentiating local polynomial approximations to a function. While finite difference methods are less accurate than spectral methods for the same number of calculations, there are less complications implementing them for problems on a non-periodic bounded domain.

4.1.1 Finite Difference Approximations of Derivatives

Let $u \in L^2(\mathbb{R})$. Given a set of grid points $\{x_n\}$ with the corresponding set of function values $\{u(x_n)\}$, the question of approximating derivatives of u is addressed in this section.

To be more specific, consider a uniform grid $\{x_1, \ldots, x_N\}$, where $x_{n+1} - x_n = h$ for each $n = 1, \ldots, N$, and a set of corresponding data values $\{u_1, \ldots, u_N\}$. Let w_n denote the approximation to $\frac{\mathrm{d}u}{\mathrm{d}x}(x_n)$, the derivative of u at x_n. Let p_n be the unique polynomial of degree ≤ 2 satisfying $p_n(x_{n-1}) = u_{n-1}$, $p_n(x_n) = u_n$, and $p_n(x_{n+1}) = u_{n+1}$. Then set $w_n = \frac{\mathrm{d}p_n}{\mathrm{d}x}(x_n)$. The interpolating function p_n is defined by

$$p_n(x) = u_{n-1}a_{-1}(x) + u_n a_0(x) + u_{n+1}a_1(x),$$

where $a_{-1}(x) = (x - x_n)(x - x_{n+1})/2h^2$, $a_0(x) = -(x - x_{j-1})(x - x_{j+1})/h^2$, and $a_1(x) = (x - x_{n-1})(x - x_n)/2h^2$. Differentiating p_n and evaluating at $x = x_n$ gives

$$w_n = \frac{\mathrm{d}p_n}{\mathrm{d}x}(x_n) = \frac{u_{n+1} - u_{n-1}}{2h}. \tag{4.4}$$

An alternative way to derive (4.4) is by considering Taylor series expansions of $u(x_{n+1})$ and $u(x_{n-1})$ about x_n. That is

$$u(x_{n+1}) = u_n + w_n h + \frac{\mathrm{d}^2u}{\mathrm{d}x^2}(x_n) + O(h^3) \quad \text{and} \quad u(x_{n-1}) = u_n - w_n h + \frac{\mathrm{d}^2u}{\mathrm{d}x^2}(x_n) + O(h^3).$$

Thus

$$u_{n+1} - u_{n-1} = 2hw_n + O(h^3)$$

and upon division by $2h$ (4.4) follows if the error term is neglected. Thus, for u a thrice continuously differentiable function, the approximation w_n will converge to $\frac{\mathrm{d}u}{\mathrm{d}x}(x_i)$ at the rate $O(h^2)$ as $h \to 0$. If, for simplicity, the function u is assumed periodic, taking $u_0 = u_N$ and $u_1 = u_{N+1}$, then the discrete differentiation process may be represented by means of a matrix-vector multiplication,

$$\begin{pmatrix} w_1 \\ \vdots \\ w_N \end{pmatrix} = \frac{h^{-1}}{2} \begin{pmatrix} 0 & 1 & & & -1 \\ -1 & 0 & \ddots & & \\ & & \ddots & & \\ & & \ddots & 0 & 1 \\ 1 & & & -1 & 0 \end{pmatrix} \begin{pmatrix} u_1 \\ \vdots \\ u_N \end{pmatrix}, \tag{4.5}$$

where omitted entries in the matrix are zero.

The principle of fitting a function to the discrete data points and approximating the derivative by the derivative of the interpolating function again holds for the development of finite difference approximations in multiple dimensions. However, in order to obtain error estimates Taylor series expansions are used.

Let D be the two dimensional domain with grid points $\{(x_n, y_j)\}$ of uniform spacing, where $h = x_{n+1} - x_n$ and $\kappa = y_{j+1} - y_j$ for each $n = 1, \ldots, N$ and $j = 1, \ldots, M$, and corresponding data values $\{u_{n,j} = u(x_n, y_j)\}$. Denote the partial derivative of the function u at (x_n, y_j) in the x direction by $\frac{\partial u_{n,j}}{\partial x}$. The Taylor series expansions for respectively $u_{n+1,j}$ and $u_{n-1,j}$ about the point (x_n, y_j) are

$$u_{n+1,j} = u_{n,j} + h\frac{\partial u_{n,j}}{\partial x} + \frac{h^2}{2!}\frac{\partial^2 u_{n,j}}{\partial x^2} + \frac{h^3}{3!}\frac{\partial^3 u_{n,j}}{\partial x^3} + O(h^4). \tag{4.6}$$

and

$$u_{n-1,j} = u_{n,j} - h\frac{\partial u_{n,j}}{\partial x} + \frac{h^2}{2!}\frac{\partial^2 u_{n,j}}{\partial x^2} - \frac{h^3}{3!}\frac{\partial^3 u_{n,j}}{\partial x^3} + O(h^4). \tag{4.7}$$

Adding (4.6) and (4.7) together and dividing the result by h^2 gives

$$\frac{\partial^2 u_{n,j}}{\partial x^2} = \frac{1}{h^2}(u_{n+1,j} - 2u_{n,j} + u_{n-1,j}) + O(h^2). \tag{4.8}$$

A difference approximation the second order partial derivative of u in the y direction is essentially the same as (4.8).

The equations (4.4) and (4.8) are called *central difference equations*. That is, they approximate a function at a grid point in terms of the values of the function at surrounding grid points. When the domain on which a derivative is approximated by a central difference equation is represented by a finite grid, and appropriate initial and boundary conditions are applied, a solvable linear system such as (4.5) results. However, the question arises how to accommodate the situation where one direction represents time and extends to infinity?

Here a formula is required that is able to advance a solution to time $t = j\kappa$ using only known values, that is, those values of grid points at times $t = (j-1)\kappa, (j-2)\kappa, \ldots, 0$. The simplest method is known as Euler time stepping. A Taylor series expansion of u at time $t_{j+1} = (j+1)\kappa$ about the point (x_n, t_j) is

$$u_{n,j+1} = u_{n,j} + \kappa\frac{\partial u_{n,j}}{\partial t} + O(\kappa^2).$$

After rearrangement of the terms and division by κ, this yields

$$\frac{\partial u_{n,j}}{\partial t} = \frac{1}{\kappa}(u_{n,j+1} - u_{n,j}) + O(\kappa). \tag{4.9}$$

4.1.2 Approximations to Differential Equations

A basic method of approximating a solution to an initial-boundary value problem may be developed by replacing the differentials in the equations by approximating difference equations. Consider the initial-boundary value problem specified in (4.1) and (4.2). Construct a grid of points denoted by $x_n = nh$ and $t_j = j\kappa$, where $n = 1, \ldots, N$ and

$j = 0, \ldots, M$ with $h = x_{n+1} - x_n = 1/N$ and $\kappa = t_{j+1} - t_j = 1/M$. Assume the exact solutions $u(x,t)$ and $v(x,t)$ to the initial-boundary value problem (4.1)–(4.2) are twice continuously differentiable in t and four times continuously differentiable in x, so that the error estimates of the previous subsection are applicable. The true value of u at (x_n, t_j) is denoted by $u_{n,j}$ and the discrete approximation of u at (x_n, t_j) by $U_{n,j}$, and similarly for v. If the partial derivatives in the reaction-diffusion equations are replaced with the difference approximations (4.8) and (4.9) the resulting difference equation for u is

$$\frac{1}{\kappa}(u_{n,j+1} - u_{n,j}) = d_u(x)\frac{1}{h^2}(u_{n+1,j} - 2u_{n,j} + u_{n-1,j}) + \phi(x_n, u_{n,j}, v_{n,j}) + O(\kappa + h^2), \quad (4.10)$$

where $\phi(x_n, u_{n,j}, v_{n,j})$ is the value of ϕ evaluated at (x_n, t_j), for $n = 1, \ldots, N-1$. The equations for $n = 0$ and N are different from (4.10) since, at $x = 0$ and $x = 2\pi$ the boundary conditions hold. Solving for $u_{n,j+1}$ yields the explicit equation

$$u_{n,j+1} = ru_{n-1,j} + (1-2r)u_{n,j} + ru_{n+1,j} + \kappa\phi(x_n, u_{n,j}, v_{n,j}) + O(\kappa^2 + \kappa h^2), \quad (4.11)$$

where $r = \frac{\kappa d_u(x)}{h^2}$. The zero-flux boundary conditions at $x = 0$ and $x = 2\pi$ may be implemented by using (4.9) to approximate $\partial u_{0,j+1}/\partial x$ and $\partial u_{N,j+1}/\partial x$ so as to obtain

$$U_{0,j+1} = U_{N,j+1} \quad \text{and} \quad U_{N+1,j+1} = U_{1,j+1}.$$

The finite difference equations approximating v at the grid points are derived in an analogous manner. The system of difference equations may be written, similarly to (4.5), as a matrix-vector multiplication and vector addition,

$$\begin{pmatrix} U_1 \\ \vdots \\ U_N \end{pmatrix} = \begin{pmatrix} r & (1-2r) & r & & & & & & \\ r & (1-2r) & r & & & & & & \\ & & \ddots & & & & & & \\ & & \ddots & r & & & & & \\ & & \ddots & (1-2r) & \ddots & & & & \\ & & & r & \ddots & & & & \\ & & & & \ddots & & & & \\ & & & & & r & (1-2r) & r & \\ & & & & & r & (1-2r) & r & \end{pmatrix} \begin{pmatrix} U_1 \\ \vdots \\ U_N \end{pmatrix} + \kappa \begin{pmatrix} \phi_{1,j} \\ \vdots \\ \phi_{N,j} \end{pmatrix}, \quad (4.12)$$

where $\phi_{n,j} = \phi(x_n, u_{n,j}, v_{n,j})$. This approach is illustrated below by means of a numerical example.

Example 4.1 *Programming matrix-vector multiplication and vector addition is almost verbatim in a vector based programming language such as Matlab. Time stepping is achieved by simply reapplying (4.12) to the new vector of U values at t_{j+1}.*

Thus, in this example, the initial-boundary value problem (4.1) and (4.2) is approximated by means of the finite difference system (4.12). The spatial grid comprises the $N = 100$ equally spaced points $\{x_i\}_{n=1,\ldots,N}$, where $x_1 = 0$ and $x_{N-1} = 2\pi$. Hence the spatial grid spacing is $h = 2\pi/(N-1) = 0.02\pi$. The grid spacing in the time direction is chosen to satisfy the condition $\kappa \leq \frac{h^2}{2D_{sup}}$, where D_{sup} is the largest value assumed by either of the diffusion coefficients. The reason for this choice will be explained in the next section.

The functions and constants that determine the specific initial-boundary value problem that is solved in this example are as follows. The competition coefficients are $\beta_{12} = 0.75$ *and* $\beta_{21} = 1$. *The carrying capacities* $k_u(x)$ *and* $k_v(x)$ *are two-toned functions that are sampled for use in the finite difference scheme at the grid points. For* $x_i \in [0, 3\pi/2)$, $k_u(x_i) = 1$ *whilst* $k_v(x_n) = 1$. *For* $x_n \in [3\pi/2, 2\pi]$, $k_u(x_n) = 1$ *whilst* $k_v(x_n) = 0.662\,500$. *Similarly* $d_u(x_n) = 0.9$ *and* $d_v(x_n) = 1$ *for* $x_n \in [0, 3\pi/2)$, *whilst* $d_u(x_n) = 0.7$ *and* $d_v(x_n) = 0.8$ *for* $x_n \in [3\pi/2, 2\pi]$.

The solutions $u(x,t)$ *and* $v(x,t)$ *are the population densities of the two competing species at position* x *and time* t. *The convention that will be followed throughout this thesis is that* u *refers to the native species which is at a non-trivial population equilibrium when the second invading species, whose density is denoted by* v, *is introduced. Therefore, in this example, the initial vectors* $\{u_{i,0}\}$ *and* $\{v_{i,0}\}$ *are assigned values* $u_{n,0} = 1$ *and* $v_{n,0} = 0$ *for all* $n \neq N/2$. *When* $n = N/2$, $u_{n,0} = 0.9$ *and* $v_{n,0} = 0.1$. *These initial vectors represent a small initial invasion and are seen in Figure 4.1 as small bumps in the plotted data at* $t = 0$. *The invading population spreads across the whole environment* $[0, 2\pi]$. *On roughly the first three quarters of the environment the invading population manages to eventually suppress the native population to very low densities. Whereas on the last quarter of the environment, the invading population does not gain the upper hand over the native population and only maintains a low density. Around* $x = 3\pi/2$ *there is a transition region where the populations' densities change from high to low and vice versa.* ■

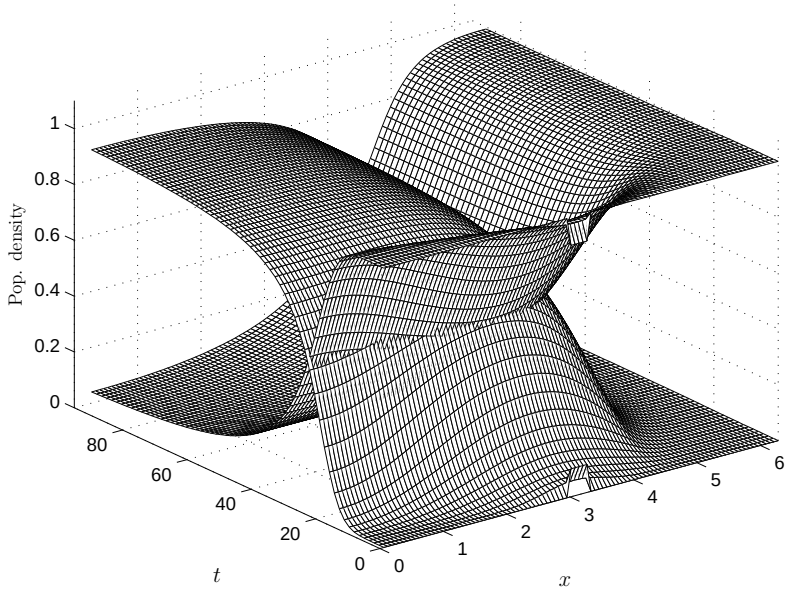

Figure 4.1: The results of applying (4.12) to the initial vectors $\{u_{n,0}\}$ and $\{v_{n,0}\}$, where $u_{n,0} = 1$ and $v_{n,0} = 0$ for all $n \neq N/2$ and $u_{n,0} = 0.9$ and $v_{n,0} = 0.1$ for $n = N/2$. The results are an approximation to the initial-boundary value problem (4.1)–(4.2) with parameter values $\beta_{12} = 0.7$ and $\beta_{21} = 1$, $k_u(x) = 1$, $k_v(x) = 1$, $d_u(x) = 0.9$ and $d_v(x) = 1$ when $x \in [0, 3\pi/2)$ and $k_u(x) = 1$, $k_v(x) = 0.5625$, $d_u(x) = 0.7$ and $d_v(x) = 0.8$ when $x \in [3\pi/2, 2\pi]$.

4.2 The Fourier Spectral Method

In the previous section approximations to derivatives of a function were derived by local interpolation. An increase in the degree of the interpolant brings about an increase in the rate of convergence. Fourier spectral methods take this to the limit. A global interpolant expressed in terms of trigonometric functions is derived and differentiated. Elementary results in Fourier analysis are reviewed in this section and the reader is referred to [90] for a more detailed discussion and for proof of the results presented here.

4.2.1 Approximations of Derivatives

The approximation (4.4) to the derivative of a function $u(x)$ at grid point x_n was derived by differentiating an interpolating polynomial $p_n(x)$ of degree ≤ 2. This derivation by means of local interpolation is easily generalized to higher orders. For instance, for a fourth order method let p_n be the unique polynomial of degree ≤ 4 such that $p_n(x_{n\pm2}) = u_{n\pm2}$, $p_i(x_{n\pm1}) = u_{i\pm1}$, and $p_n(x_n) = u_n$. Then set $w_n = \frac{\mathrm{d}p_n}{\mathrm{d}x}(x_n)$. Again assuming periodic boundary conditions the discrete differentiation process amounts to a matrix-vector multiplication where the matrix is now penta-diagonal instead of tri-diagonal. As may be verified by means of Taylor series expansions, this discrete approximation to $\frac{\mathrm{d}u_n}{\mathrm{d}x}(x_n)$ for a sufficiently smooth function u will converge at the rate $O(h^4)$ as $h \to 0$.

When interpolating polynomials of even higher order are used in approximating the derivative, matrices of greater bandwidth result. Essentially the idea behind a spectral method is allowing the interpolating polynomial's degree to grow without bound. On the infinite grid $h\mathbb{Z}$, a polynomial $p(x)$, independent of n, will be gained, and $\frac{\mathrm{d}u_n}{\mathrm{d}x}(x_n)$ is approximated as $w_n = \frac{\mathrm{d}p_n}{\mathrm{d}x}(x_n)$. This procedure on $h\mathbb{Z}$ amounts to a matrix-vector multiplication where the matrix is an infinite matrix, and hence it is not a practical method. However, it is an intermediate step to deriving a finite spectral differentiation matrix on a bounded discrete domain.

4.2.1.1 An Unbounded Grid

The procedure reviewed here is of discrete differentiation on an unbounded domain. Decomposing a function into its constituent trigonometric functions, or waves, is known as *Fourier analysis*. The Fourier transform of a function $u(x)$, $x \in \mathbb{R}$, is the function

$$\widehat{u}(\xi) = \int_{-\infty}^{\infty} e^{-i\xi x} u(x)\,\mathrm{d}x, \qquad \xi \in \mathbb{R}.$$

The function $\widehat{u}(\xi)$ may be interpreted as the amplitude density of u at wave-number κ. The inverse process of reconstructing u from $\widehat{u}$ is known as *Fourier synthesis*. The inverse Fourier transform is

$$u(x) = \frac{1}{2\pi} \int_{\infty}^{\infty} e^{i\xi x}\, \widehat{u}(\xi)\,\mathrm{d}\xi, \qquad x \in \mathbb{R}.$$

The functions $f = e^{i\xi_1 x}$ and $g = e^{i\xi_2 x}$ are distinct over $\mathbb{R}$ if $\xi_1 \neq \xi_2$. However, if f and g are only sampled on $h\mathbb{Z}$ then the sampled functions are equal if $\xi_1 - \xi_2$ is an integer multiple of

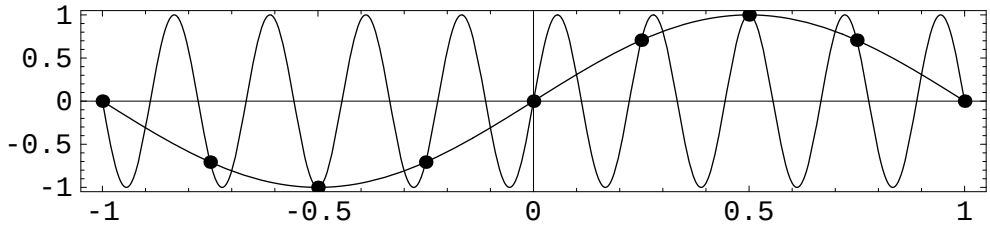

Figure 4.2: An example of aliasing. On the grid $\frac{1}{4}\mathbb{Z}$, the functions $\sin(\pi x)$ and $\sin(9\pi x)$ are identical.

$2\pi/h$. This phenomenon is known as *aliasing* and is demonstrated in Figure 4.2. Thus a function sampled on $h\mathbb{Z}$ has a $2\pi/h$ length domain of distinguishable wave numbers. That is, if a function u sampled on $h\mathbb{Z}$ has a wave amplitude density component of magnitude c for wave number ξ_1, then the sampled function may be synthesised without a ξ_1-wave component by using a ξ_2-wave component of magnitude c, for any ξ_2 such that $\xi_1 - \xi_2$ is an integer multiple of $2\pi/h$. The discretization error of the interpolating function that results is because of those wave-numbers that are neglected. If the continuous function is smooth, that is slowly changing, then the sampled function can retain more of the features of the original function than when the original function were quickly changing and thus exhibits much detail between sample points. Since smoothness is an assumption when discretizing the function, an appropriate choice of a $2\pi/h$ length interval of wave-numbers used to synthesize the function is $(-\pi/h, \pi/h)$ — the low frequency, or slowly changing waves.

Consider the uniform grid $h\mathbb{Z}$ with the set of corresponding function values $\{u_n\}$, where $u_n = u(x_n)$ and $x_n = nh$ for $n \in \mathbb{Z}$. The analogue over the grid $h\mathbb{Z}$ of the continuous Fourier transform is called the *semi-discrete Fourier transform* and by the above the wave-numbers range over the bounded domain $[-\pi/h, \pi/h]$. Since the semi-discrete Fourier variable is used to synthesise an interpolating function, and since it is in the discretization process that errors are introduced, the Fourier variable will be denoted by $\widehat{U}(\xi)$. The semi-discrete Fourier transform is defined by the Fourier series

$$\widehat{U}(\xi) = h \sum_{n=-\infty}^{\infty} e^{-i\xi x_n} u_n, \qquad \xi \in (-\pi/h, \pi/h), \tag{4.13}$$

and the inverse transform is

$$u_n = \frac{1}{2\pi} \int_{-\pi/h}^{\pi/h} e^{i\xi x_n} \widehat{U}(\xi)\, \mathrm{d}\xi, \qquad n \in \mathbb{Z}. \tag{4.14}$$

The following theorem, known as the aliasing formula (see [45, §6.1.15] for a proof), makes clear the relationship between $\widehat{U}(\xi)$ and $\widehat{u}(\xi)$.

Theorem 4.1 (Aliasing Formula) *Let $u \in L^2(\mathbb{R})$ have a first derivative of bounded variation. Then*

$$\widehat{U}(\xi) = \sum_{n=-\infty}^{\infty} \widehat{u}(\xi + 2\pi n/h)$$

for all $\xi \in [-\pi/h, \pi/h]$. ■

From Theorem 4.1 it follows that

$$\widehat{U}(\xi) - \widehat{u}(\xi) = \sum_{\substack{n=-\infty \\ n\neq 0}}^{\infty} \widehat{u}(\xi + 2\pi n/h). \tag{4.15}$$

The error in discretizing u is incurred because high wave-numbers are aliases of low wave-numbers. In order that accuracy be preserved, the Fourier coefficients should decay rapidly as $|\xi| \to \infty$. This is stated in the following theorem, which is proved in [45, §1.4.4].

Theorem 4.2 *If u has $p-1$ continuous derivatives in $L^2(\mathbb{R})$ for some $p \geq 0$ and a $p-th$ derivative of bounded variation, then $\widehat{u}(\xi) = O(|\xi|^{-p-1})$ as $|\xi| \to \infty$.* ■

Now it follows by Theorems 4.1 and 4.2 that the error satisfies

$$|\widehat{U}(\xi) - \widehat{u}(\xi)| \leq \sum_{\substack{n=-\infty \\ n\neq 0}}^{\infty} O(|\xi + \tfrac{2\pi n}{h}|^{-p-1}) = O(h^{p+1}) \qquad \text{as } h \to 0. \tag{4.16}$$

Returning to the idea of differentiating an interpolating function, the interpolating function $p(x)$ is defined by (4.14), evaluated at all $x \in \mathbb{R}$, and not just at $x_j \in h\mathbb{Z}$. By the construction of (4.14), $p(x_j) = u_j$ for every $j \in \mathbb{Z}$ and $p(x)$ is an analytic function.

A sampled function may be written as

$$u_n = \sum_{-\infty}^{\infty} u_m \delta_{n-m}, \tag{4.17}$$

where δ_{n-m} is the Kronecker delta

$$\delta_{n-m} = \begin{cases} 1, & m = n, \\ 0, & m \neq n. \end{cases}$$

The Fourier variable of δ_{n-m} is

$$\widehat{\delta}_{n-m}(\xi) = h \sum_{n=-\infty}^{\infty} e^{-i\xi x_n} \delta_{n-m} = h e^{-i\xi x_m}, \qquad \xi \in (-\pi/h, \pi/h)$$

and therefore the interpolant of δ_{n-m} is

$$S_h(x - x_m) = \frac{h}{2\pi} \int_{-\pi/h}^{\pi/h} e^{i\xi x} e^{-i\xi x_m} \, \mathrm{d}\xi = \frac{h}{2\pi} \int_{-\pi/h}^{\pi/h} e^{i\xi(x - x_m)} \, \mathrm{d}\xi = h \frac{\sin((x - x_m)\pi/h)}{(x - x_m)\pi}.$$

Thus it follows from (4.17) and the linearity of the Fourier transform that an interpolant of the function sampled from u is

$$p(x) = \sum_{m=-\infty}^{\infty} v_m S_h(x - x_m). \tag{4.18}$$

Hence the derivative of the interpolant at x_n is

$$w_n = p'(x_n) = \sum_{m=-\infty}^{\infty} v_m S_h'(x - x_m),$$

where

$$S'_h(x_n - x_m) = \begin{cases} 0, & j-m=0, \\ \frac{(-1)^{n-m}}{(n-m)h}, & n-m \neq 0. \end{cases}$$

To obtain higher order derivatives, $p(x)$ is differentiated several times by differentiating $S_h(x)$ several times. This the differentiation process may be written as the infinite matrix-vector multiplication

$$\begin{pmatrix} \vdots \\ w_{-2} \\ w_{-1} \\ w_0 \\ w_1 \\ w_2 \\ \vdots \end{pmatrix} = h^{-1} \begin{pmatrix} & \vdots & \\ \ddots & \frac{1}{3} & \\ \ddots & -\frac{1}{2} & \\ \ddots & 1 & \\ & 0 & \\ & -1 & \ddots \\ & \frac{1}{2} & \ddots \\ & -\frac{1}{3} & \ddots \\ & \vdots & \end{pmatrix} \begin{pmatrix} \vdots \\ u_{-2} \\ u_{-1} \\ u_0 \\ u_1 \\ u_2 \\ \vdots \end{pmatrix}. \tag{4.19}$$

By Parseval's identity (see Appendix A.2), with appropriately defined norms, $\|\widehat{u}\| = \sqrt{2\pi}\|u\|$ and $\|\widehat{U}\| = \sqrt{2\pi}\|U\|$, where U is the grid function gained by sampling u. It follows then from (4.16) that the functions $u(x)$ and $p(x)$ defined by the inverse Fourier transform over $[-\pi/h, \pi/h]$ of $\widehat{u}$ and $\widehat{v}$ are in agreement with an order of accuracy $O(h^{p+1})$. Moreover, if $w_n = \frac{\mathrm{d}^2}{\mathrm{d}x^2}p(x)$, it follows that

$$\left| w_n - \frac{\mathrm{d}^2}{\mathrm{d}x^2}u(x_n) \right| = O(h^{p-2}) \tag{4.20}$$

as $h \to 0$ by using the fact that $\widehat{\frac{\mathrm{d}^2}{\mathrm{d}x^2}u(x)} = (i\xi)^2\widehat{u}(\xi)$.

4.2.1.2 A Periodic Grid

When a function is sampled on the infinite grid $h\mathbb{Z}$, spectral differentiation results in an infinite differentiation matrix. However, when the grid is restricted to a bounded periodic interval a finite spectral differentiation matrix may be derived. In this subsection the function to be sampled is taken to be periodic over a 2π interval and is sampled on one cycle of the grid of length N, extracted from the infinite grid. The grid is $\{x_1, \ldots, x_N\}$ on the bounded interval $[0, 2\pi]$. The formulae derived here are all for N even. A relationship that will be useful is

$$\frac{\pi}{h} = \frac{N}{2}. \tag{4.21}$$

As in the previous subsection only wave-numbers in the bounded interval $[-\pi/h, \pi/h]$ need to be considered when deriving an interpolating function because the function u is sampled at discrete points. Moreover, since the sample data are now 2π-periodic, only integer wave-numbers need to be considered, because only waves with integer wave-numbers have period 2π. Thus the discrete Fourier transform corresponding to (4.13) of

the previous subsection is the finite sum

$$\widehat{U}_\xi = h\sum_{n=1}^{N} e^{-i\xi x_n} v_n, \qquad \xi = -N/2, -N/2+1, \ldots, N/2. \tag{4.22}$$

The inverse discrete Fourier transform corresponding to (4.14) of the previous subsection is

$$u_n = \frac{1}{2\pi}\sum_{\xi=-N/2}^{N/2} e^{i\xi x_n}\widehat{v}_\xi - \frac{1}{2}\left(e^{ix_nN/2}\widehat{U}_{N/2} + e^{-ix_nN/2}\widehat{U}_{-N/2}\right), \qquad n = 1, \ldots, N.$$

In effect the terms in the Fourier synthesis for $\xi = \pm N/2$ have been multiplied by $\frac{1}{2}$. This was done because the amplitude components for wave-numbers $\xi = \pm N/2$ are indistinguishable on the grid $h\mathbb{Z}$ and thus these amplitude components duplicate each other. A useful notation will be

$$u_n = \frac{1}{2\pi}\sum_{\xi=-N/2}^{N/2\,\prime} e^{i\xi x_n}\widehat{U}_\xi, \qquad n = 1, \ldots, N, \tag{4.23}$$

where the prime indicates that the terms $\xi = \pm N/2$ are multiplied by $\frac{1}{2}$.

As in the previous subsection, an interpolating function is now defined by evaluating (4.23) at $x \in [0, 2\pi]$, instead of just on the grid. Because restricting the Fourier transform to wave-numbers of waves with the desired period incurs no error beyond the aliasing error already introduced, the accuracy bound of the previous subsection remains valid. A periodic delta function is defined by

$$\delta_{n-m} = \begin{cases} 1, & n - m \equiv 0 \pmod N, \\ 0, & n - m \not\equiv 0 \pmod N. \end{cases}$$

By (4.22), $\widehat{\delta}_{n-m}(\kappa) = he^{-i\xi x_m}$ for each ξ. From (4.23) it follows that an interpolant of δ_{n-m} is

$$S_N(x - x_m) = \frac{\sin(\pi(x - x_m)/h)}{(2\pi/h)\tan((x - x_m)/2)}.$$

An expansion of the periodic grid function $\{u_n\}_{n=1,\ldots,N}$ in the basis of periodic delta functions is

$$u_n = \sum_{m=1}^{N} u_m \delta_{n-m}. \tag{4.24}$$

Analogous to (4.18) an interpolating function of an arbitrary sampled periodic function on the interval $[0, 2\pi]$ may thus be written as

$$p(x) = \sum_{m=1}^{N} u_m S_N(x - x_m). \tag{4.25}$$

Moreover, the derivative of $S_N(x - x_m)$ at x_n is

$$S'_N(x_n - x_m) = \begin{cases} 0, & n - m \equiv 0 \pmod N, \\ \frac{1}{2}(-1)^{n-m}\cot((n-m)h/2), & n - m \not\equiv 0 \pmod N, \end{cases}$$

and thus the differentiation process is given by

$$w_n = \frac{\mathrm{d}p_n}{\mathrm{d}x}(x_n) = \sum_{m=1}^{N} u_m S_N'(x_n - x_m).$$

Higher order derivatives may be computed by using higher order derivatives of $S_N(x-x_m)$. The second order derivative at x_n is

$$S_h''(x_n - x_m) = \begin{cases} -\frac{\pi^2}{3h^2} - \frac{1}{6}, & n-m \equiv 0 \pmod N, \\ -\frac{(-1)^{n-m}}{2\cot((n-m)h/2)}, & n-m \not\equiv 0 \pmod N, \end{cases}$$

which results in the matrix-vector multiplication

$$\begin{pmatrix} \vdots \\ w_{N/2-2} \\ w_{N/2-1} \\ w_{N/2} \\ w_{N/2+1} \\ w_{N/2+2} \\ \vdots \end{pmatrix} = \begin{pmatrix} & \vdots & \\ \ddots & -\frac{1}{2}\csc^2(\frac{2h}{2}) & \\ \ddots & \frac{1}{2}\csc^2(\frac{1h}{2}) & \\ \ddots & -\frac{\pi^2}{3h^2} - \frac{1}{6} & \ddots \\ & \frac{1}{2}\csc^2(\frac{1h}{2}) & \ddots \\ & -\frac{1}{2}\csc^2(\frac{2h}{2}) & \ddots \\ & \vdots & \end{pmatrix} \begin{pmatrix} \vdots \\ u_{N/2-2} \\ u_{N/2-1} \\ u_{N/2} \\ u_{N/2+1} \\ u_{N/2+2} \\ \vdots \end{pmatrix} \tag{4.26}$$

with local error $O(h^{p-2})$.

4.2.2 Approximations of Solutions to Initial-Boundary Value Problems

Consider the initial-boundary value problem specified by (4.1) and (4.3). As was done in the previous section, the second order spatial derivative is approximated by the spectral differentiation matrix in (4.26). A perspective which is useful when convergence rates and stability are considered, is that the approximations discretize the problem in space, generating a system of ordinary differential equations. The system of ordinary differential equations is

$$\frac{\mathrm{d}U_n}{\mathrm{d}t}(t) = \sum_{m=1}^{N} U_m(t) S_N(x_n - x_m) + \phi(x, U_n, V_n), \quad n = 1, \ldots, N$$

$$\frac{\mathrm{d}V_n}{\mathrm{d}t}(t) = \sum_{m=1}^{N} V_m(t) S_N(x_n - x_m) + \theta(x, u_n, v_n), \quad n = 1, \ldots, N$$

with initial conditions $U_n(t_0) = f_u(x_0)$ and $V_n(t_0) = f_v(x_0)$ for every $n = 1, \ldots, N$.

Such a system is known as a *semi-discrete approximation* of the partial differential equation system. The system of ordinary differential equations remains to be solved. The numerical method that is used in this thesis to do so is again the simple Euler method. The idea of constructing a semi-discrete approximation and then solving it by a numerical scheme is known as *the method of lines*. This procedure may be represented explicitly for

each time step. Let the grid points on the interval $(0, T)$ be $t_j = j\kappa$. The representation for U is

$$\underline{U}_N^{(j+1)} = \underline{U}_N^{(j)} + \mathbf{D}_N^2 \underline{U}_N^{(j)} + \kappa \phi^{(j)}, \tag{4.27}$$

where $\mathbf{D}_N^2$ is the spectral second order differentiation matrix in (4.26), and where

$$\underline{U}_N^{(j)} = \begin{pmatrix} U_{1,j} \\ \vdots \\ U_{N/2-1,j} \\ U_{N/2,j} \\ U_{N/2+1,j} \\ \vdots \\ U_{N,j} \end{pmatrix} \quad \text{and} \quad \underline{\phi}^{(j)} = \begin{pmatrix} \phi_{1,j} \\ \vdots \\ \phi_{N/2-1,j} \\ \phi_{N/2,j} \\ \phi_{N/2+1,j} \\ \vdots \\ \phi_{N,j} \end{pmatrix}.$$

Let $C(\kappa)$ be the difference operator defined by $C(\kappa)\underline{U}_N^{(j)} = \underline{U}_N^{(j+1)}$. By the expansion of $u(x_i, t_{j+1})$ as a Taylor series about x_i and t_j it follows that the local error of the difference scheme is

$$C(\kappa)\underline{u}_N^{(j)} - \underline{u}_N^{(j+1)} = \kappa \left(\mathbf{D}_N^2 \underline{u}_N^{(t_j)} - \frac{\partial^2 \underline{u}_N^{(t_j)}}{\partial x^2}) \right) + O(\kappa) = O(\kappa h^{p-2} + \kappa). \tag{4.28}$$

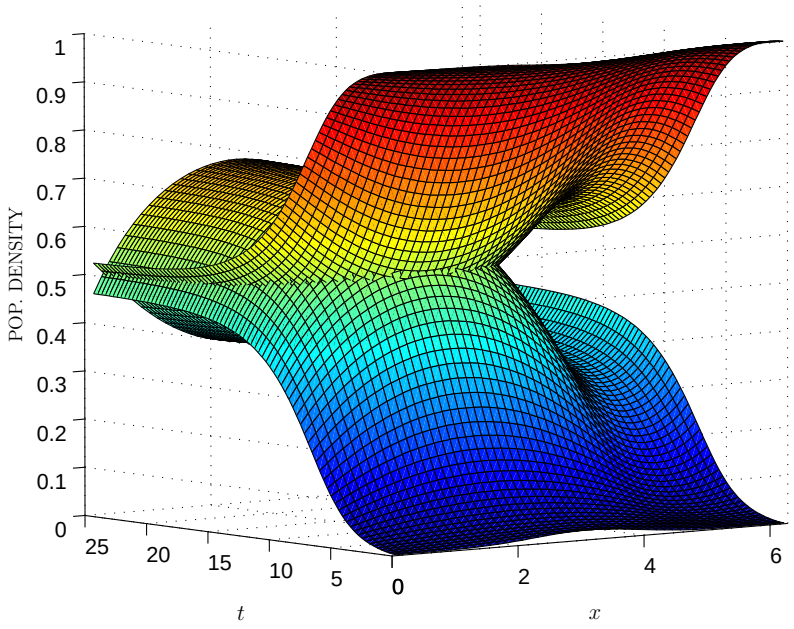

Figure 4.3: Approximations of the solution to the initial-boundary value problem (4.1)–(4.3), with periodic boundary conditions, and parameters as in Example 4.1, computed by applying the spectral difference scheme (4.27).

Example 4.2 (Continuation of Example 4.1)
An approximate solution to the initial-boundary value problem with parameters as considered in Example 4.1 is again computed in this example, but using the spectral difference scheme (4.27). The spatial grid comprising 50 points is used and thus $h = 2\pi/50$. The spacing of the grid in the time direction is $\kappa = 0.1h^2$. The results of the computations are plotted in Figure 4.3. ■

4.3 Convergence, Stability and Consistency

In 1928 Richard Courant, Kurt Friedrichs and Hans Lewy published the famous article "On the partial difference equations of mathematical physics" [14]. The purpose of the article was to investigate the use of finite difference approximations to prove the existence of solutions to boundary value problems governed by partial differential equations. However, the article also laid the theoretical foundation for practical finite difference computations [83].

If $u(x,t)$ is the exact solution of an initial-boundary value problem, and $U_{n,j}$ is the solution of the finite difference equations approximating the solution of the initial-boundary value problem, the error of approximation is $U_{n,j} - u(nh, j\kappa)$. For the approximation to be useful it is required that $|U_{n,j} - u(nh, j\kappa)| \to 0$ for fixed values of $n\kappa$ as $h, \kappa \to 0$. Such a finite difference scheme is said to be *convergent* and the finite difference scheme is said to converge to the initial-boundary value problem. In computations it is hoped that the convergence is quick enough so that for some finite h and κ the solution $U_{n,j}$ of the finite difference equation is close to $u(nh, j\kappa)$.

Courant, Friedrichs and Lewy identified a fundamental necessary condition, which has subsequently become known as the CFL condition, for convergence of a finite difference approximation scheme to an initial-boundary value problem. The CFL condition states that the mathematical domain of dependence is contained in the numerical domain of dependence. The mathematical (or numerical) domain of dependence at (x,t) is the set of all points in space where the initial data may influence the solution $u(x,t)$ (or $u_{n,j}$) in the limit as $h, \kappa \to 0$. In the case of the one dimensional parabolic diffusion equation the mathematical domain of dependence is along the characteristic curves, and these are the whole spatial domain. This is because, as was seen in the derivation of the diffusion equation in Chapter 2, the probability of a particle moving at an infinite speed is small, but not zero. Hence the influence of a point far away from (x,t) may be small, but not zero. The quantities h and κ will thus be required to tend to zero in a manner such that $h = o(\kappa)$. In what follows it will be assumed that h depends on κ in some way. That is, $h = g(\kappa)$ for some relationship g.

A related, and pervasive, concern in numerical solutions to partial differential equations is stability. Stability, however, from a theoretical perspective, is not an obvious problem, as indeed the originator of finite difference methods for partial differential equations, LF Richardson, in [73], proposed an unconditionally unstable method [2, §2.4].

If $C(\kappa)$ is a discrete difference operator, depending on κ, such that

$$u(x_n, t_{j+1}) = C(\kappa)u(x_n, t_j),$$

then the family of operators $\{C(\kappa)\}_\kappa$ is stable if, for some constant $c > 0$,

$$\|C(\kappa)^j\| \leq c$$

for all j and κ satisfying $0 \leq j\kappa \leq T$, where the operator norm is

$$\|C(\kappa)\| = \max_{u \in B} \frac{\|C(\kappa)u(x_n, t_j)\|}{\|u(x_n, t_j)\|},$$

and where B is the set of solutions.

In 1951 W Leutert [32] gave an example of an unstable numerical scheme which is nevertheless in some sense convergent. In 1956 P Lax and RD Richtmyer [74] proved the Lax equivalence theorem, which equates convergence to stability subject to a consistency condition. The *consistency* condition is that the numerical scheme has local order of accuracy $p > 0$, where the local order of accuracy is p if

$$|u(x_n, t_{j+1}) - C(\kappa)u(x_n, t_j)| = O(\kappa^{p+1}) \tag{4.29}$$

as $\kappa \to 0$, for any $t_j \in [0, T]$.

Theorem 4.3 (Lax Equivalence Theorem) *If a numerical scheme has local order of accuracy $p > 0$ then an approximation $\{C(\kappa)\}$ to a well-posed linear initial-boundary value problem is convergent if and only if it is stable.*

By the local errors indicated for the discrete difference operators (4.12) and (4.27) both the finite difference scheme and the spectral difference scheme reviewed in the previous sections are consistent with the initial-boundary value problem (4.1).

In summary, consistency is the assertion that local errors are small, whereas stability is the condition that these errors remain small. Were the initial value problem linear, these two conditions would be enough to ensure that the global error at time step j, which consists of the superposition of the local errors at each step remains small. However, the problem (4.1) is not linear, and thus stability and consistency is not enough to ensure convergence.

4.3.1 . . . of the Finite Difference Scheme

In this subsection the stability and convergence of the finite difference equation (4.11) is established. The Fourier method is used to establish stability and a maximum principle analysis is used to establish convergence. In both cases the boundary conditions are not taken into account.

Example 4.3 (Continuation of Example 4.1) *The finite difference computation of an approximate solution to the initial-boundary value problem considered in Example 4.1 is repeated in this example, but with $\kappa = 7.95h^2$ not satisfying the condition $\kappa \leq \frac{h^2}{2D_{sup}}$. The result of the computation is plotted in Figure 4.4(a). The native population densities are not plotted. Furthermore, the computations were performed over a shorter time interval than in Example 4.1. This was done to produce an attractive plot as the population densities rapidly become very large in unstable computations. The population densities, as computed in Example 4.1, are replotted for comparison purposes in Figure 4.4(b) on the same axes used for Figure 4.4(a). The finite difference calculations on the new grid with an unstable spacing in the time direction and the finite difference equations (4.11) are thus unstable for this value of κ.* ■

4.3.1.1 Stability

Richtmyer and Morton [75, §3.9] proved the following theorem, which states that stability is not destroyed by a small perturbation.

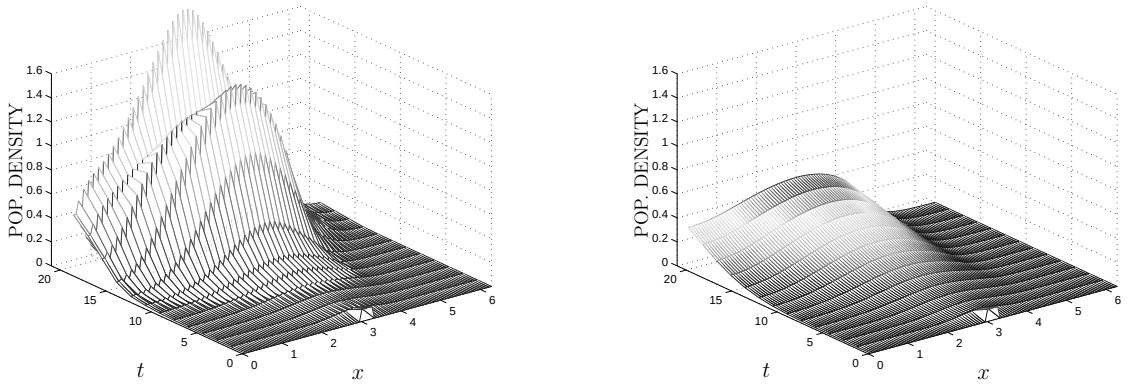

(a) Unstable computation.

(b) Stable computation.

Figure 4.4: Approximations of the solution to the initial-boundary value problem (4.1) and (4.2), with parameters as in Example 4.1, computed by applying (4.12) with two different grid spacings in the time direction.

Theorem 4.4 *If the difference system* $u(x_n, t_{j+1}) = C(\kappa)u(x_n, t_j)$ *is stable, where* $\kappa = t_{j+1} - t_j$, *and* $Q(\kappa)$ *is a bounded family of operators, then the difference system* $u(x_n, t_{j+1}) = (C(\kappa) + \kappa Q)\, u(x_n, t_j)$ *is also stable.* ■

Thus it will be shown that the system of finite difference equations

$$u_{i,j+1} = \frac{d_u(x)\kappa}{h^2}u_{i-1,j} + (1 - \frac{2d_u(x)\kappa}{h^2})u_{i,j} + \frac{d_u(x)\kappa}{h^2}u_{i+1,j}, \quad i = 1, \ldots, M-1, \quad (4.30)$$

known as the *forward difference equations*, approximating the solution of

$$\frac{\partial u}{\partial t}(x,t) = d_u(x)\frac{\partial^2 u}{\partial x^2}(x,t), \quad (4.31)$$

together with suitable initial conditions, but ignoring boundary effects, are stable. Since the non-linear function $\phi^{(u)}(x_i, u_{n,j}, v_{n,j})$ in the finite difference scheme (4.11) is multiplied by κ and is bounded it will follow that stability is retained.

If the difference operator of the forward difference equations is $C(\kappa)$, then applying the operator to a vector $\underline{u}_N$ of function values on the spatial grid may be interpreted as a convolution, $C(\kappa)\underline{u}_N = \underline{a} * \underline{u}$. Thus, in Fourier space, it follows that

$$\widehat{C(\kappa)\underline{u}_N}(\xi) = \widehat{\underline{a} * \underline{u}_N}(\xi) = \widehat{\underline{a}}(\xi)\widehat{\underline{u}_N}(\xi).$$

Repeated application of the difference operator yields

$$\widehat{C(\kappa)^j\underline{u}_N}(\xi) = (\widehat{\underline{a}}(\xi))^j\widehat{\underline{u}_N}(\xi).$$

Inserting the trial solution $u_{n,j} = (g(x,\xi,\kappa))^j e^{i\xi nh}$, of the harmonic of ξ, into the forward difference equation (4.30) yields

$$(g(x,\xi,\kappa))^{j+1}e^{i\xi nh} = (g(x,\xi,\kappa))^j(r(x,\kappa)e^{i\xi(n-1)h} + (1-2r(x,\kappa))e^{i\xi(n+1)h} + r(x,\kappa)e^{i\xi nh}),$$

or, after factoring out $(g(x,\xi,\kappa))^j e^{i\xi nh}$,

$$g(x,\xi,\kappa) = 1 + r(x,\kappa)(e^{i\xi(n-1)h} + e^{i\xi(n+1)h} - 2),$$

which may be rewritten as

$$g(x,\xi,\kappa) = 1 + 2r(x,\kappa)(\cos(\xi h) - 1).$$

Now, if $r(x,\kappa) \leq 1/2$ then $|g(x,\xi,\kappa)| \leq 1$ for $\xi \in [-\pi,\pi]$, and $g(x,0,\kappa) = 1$. Thus $|(g(x,\xi\kappa))^n e^{i\xi nh}| \leq |e^{i\xi nh}| = 1$ for the harmonic of every $\xi \in [-\pi,\pi]$. If g did not depend on x it would follow for any initial function $u_{n,0}$ with a convergent Fourier representation that

$$\frac{\|(C(\kappa))^j \underline{u}_N(0)\|}{\|\underline{u}_N(0)\|} \leq 1$$

and hence that the finite difference scheme (4.30) is stable.

However, g does indeed depend on x. In this case stability still holds. Theorem 4.5 here under follows from a result also proved by Richtmyer and Morton [75, §5.3].

Theorem 4.5 *If the coefficient $d_u(x)$ is piecewise constant and if $|g(x,\xi,\kappa)| < 1$ for all x and all $\xi \in (-\pi,\pi)$, $\xi \neq 0$, with $g(x,0,\kappa) = 1$, then the difference scheme is stable.* ■

Hence the finite difference scheme (4.30) is stable by Theorem 4.5 and so by Theorem 4.4 the finite difference system (4.11) is also stable.

4.3.1.2 Convergence

It is convenient to define a *central difference operator* as

$$\delta_x u_{n,j} = u_{n+\frac{1}{2},j} - u_{n-\frac{1}{2},j}.$$

Using this operator the central difference approximation (4.8) may be rewritten as

$$\frac{\partial^2 u_{n,j}}{\partial x^2} = \frac{1}{h^2}\delta_x^2 u_{n,j} + O(h^2).$$

Let $u_{n,j} = u(x_n,t_j)$ be the solution at $x = x_n$ and $t = t_j$ of the initial-boundary value problem (4.1), with boundary conditions specified by (4.2). Also write $U_{n,j}$ for the solution of the finite difference scheme at $x = x_n$ and $t = t_j$. A Taylor series expansion of (4.1) about t_j yields

$$u_{i,j+1} = u_{i,j} + \kappa\left(\frac{d_u(x_n)}{h^2}\delta^2 u_{n,j} + \phi^{(u)}(x_n,u_{n,j},v_{n,j}) + O(h^2)\right) + O(\kappa^2), \tag{4.32}$$

where the first order partial derivative in t was replaced by the right hand side of the partial differential equation for u in (4.1) and the consequent second order spatial differential is replaced by the spatial difference operator (4.8). The explicit finite difference scheme derived for u in §4.1.2 was just

$$U_{n,j+1} = U_{n,j} + \kappa\left(\frac{d_u(x_n)}{h^2}\delta^2 U_{n,j} + \phi^{(u)}(x_n,U_{n,j},V_{n,j})\right). \tag{4.33}$$

Thus the error of the approximation at (x_n, t_{j+1}) is $u_{n,j} - U_{n,j}$. Hence, define $z^{(u)}_{n,j} = u_{n,j} - U_{n,j}$, and similarly define $z^{(v)}_{n,j} = v_{n,j} - V_{n,j}$. From (4.32) and (4.33) it follows that

$$\begin{aligned} z^{(u)}_{n,j+1} &= z^{(u)}_{n,j} + \kappa\frac{d_u(x_n)}{h^2}(z^{(u)}_{n-1,j} - 2z^{(u)}_{n,j} + z^{(u)}_{n+1,j}) \\ &\quad +\kappa(\phi^{(u)}(u_{n,j}, v_{n,j}) - \phi^{(u)}(U_{n,j}, V_{n,j})) + O(\kappa^2 + \kappa h^2). \end{aligned}$$

If it is assumed that $u_{n,j}, v_{n,j}, U_{n,j}$ and $V_{n,j}$ all remain non-negative and smaller than 1 for all x_n and t_j, as is expected of the analytical solution, then it holds that

$$|\phi^{(u)}(u_{n,j}, v_{n,j}) - \phi^{(u)}(U_{n,j}, V_{n,j})| \leq |z^{(u)}_{n,j}| + |z^{(v)}_{n,j}|.$$

Thus

$$\begin{aligned} |z^{(u)}_{n,j+1}| &\leq \left(1 - 2k\frac{d_u(x_n)}{h^2}\right)|z^{(u)}_{n,j}| + \kappa\,\frac{d_u(x_n)}{h^2}\left(|z^{(u)}_{n-1,j}| + |z^{(u)}_{n+1,j}|\right) \\ &\quad + \kappa\left(|z^{(u)}_{n,j}| + |z^{(v)}_{n,j}|\right) + O(\kappa^2 + \kappa h^2), \end{aligned}$$

if $(1 - 2\kappa\frac{d_u(x_n)}{h^2}) \geq 0$ and $\kappa\frac{d_u(x_n)}{h^2}) \geq 0$. Define $||z^{(u)}_j|| = \max_i |z^{(u)}_{n,j}|$ $||z^{(v)}_j|| = \max_n |z^{(v)}_{n,j}|$, and $||z_j|| = ||z^{(u)}_j|| + ||z^{(u)}_j||$. Now it follows that

$$||z^{(u)}_{j+1}|| \leq ||z^{(u)}_j|| + \kappa||z^{(u)}_j|| + \kappa||z^{(v)}_j)|| + O(\kappa^2 + \kappa h^2),$$

and a similar inequality holds for $||z^{(v)}_{j+1}||$. Thus

$$||z_{j+1}|| \leq (1 - 2k)||z_j|| + [\kappa^2 + \kappa h^2]A,$$

for some constant A. Now

$$||z_j|| \leq (1+2\kappa)||z_{j-1}||+[\kappa^2+\kappa h^2]A \leq (1+2\kappa)\left((1 + 2\kappa)||z_{j-2}|| + [\kappa^2 + \kappa h^2]A\right)+[\kappa^2+\kappa h^2]A,$$

and, completing the recursive expansion to z_0, it follows, because $||z_0|| = 0$ and since $U_{n,0}$ and $V_{n,0}$ are known for every n, that

$$||z_j|| \leq (1 + (1 + b\kappa) + (1 + b\kappa)^2 + \ldots + (1 + b\kappa)^{j-1})A(\kappa h^2 + \kappa^2).$$

Using the facts that $j\kappa \leq M\kappa = T$ and that

$$(1 + 2\kappa)^M = \left(1 + \frac{2T}{M}\right)^M < e^{2T}$$

it follows that

$$||z_j|| \leq e^{2T} j\kappa(\kappa + h^2)A \leq Te^{2T}(\kappa + h^2)A,$$

and hence the errors tend to zero as h and κ tend to zero, since T and A are constants.

4.3.2 ... of the Spectral Difference Scheme

Let D_N^2 be the spectral difference operator on the grid $\{x_j\}_{j=1,\ldots,N}$ defined in (4.26) approximating the second order spatial differential. Then the diffusion equation

$$\frac{\partial}{\partial t}u(x,t) = \frac{\partial^2}{\partial x^2}u(x,t), \tag{4.34}$$

with periodic boundary conditions at $x = 0$ and $x = 2\pi$ may be approximated by the semi-discrete system of ordinary differential equations

$$\frac{\mathrm{d}}{\mathrm{d}t}\underline{U}_N(t) = \mathbf{D}_N^2\underline{U}_N(t),$$

where $\underline{U}_N(t)$ is the vector of function values $U(x_n,t)$ for every x_n on the grid. Using the matrix exponential, the solution of this system is

$$\underline{U}_N(t) = e^{\mathbf{D}_N^2 t}\underline{U}_N(0)$$

where $\underline{U}_N(0)$ is the vector of initial values. The matrix $\mathbf{D}_N^2$, as defined in (4.26), may be written as $\mathbf{D}_N^2 = \mathbf{C}^{-1}\mathbf{D}\mathbf{C}$ where $\mathbf{C}$ is a unitary matrix and $\mathbf{D}$ is diagonal. The matrix $\mathbf{C}$ is the projection of $\underline{U}_N$ into Fourier space, that is

$$C_{\xi',l} = \sqrt{h}e^{i\xi x_l}$$

where $\xi' \in [-N/2+1,\ldots,N/2]$. The matrix $\mathbf{D}$ is such that $\mathbf{D}\mathbf{C}\underline{U}_N$ are the Fourier coefficients of $\underline{w}_N$ where $w_n = \frac{\partial^2}{\partial x^2}U(x_n,t)$. Thus, it follows that

$$D_{\xi',l} = (i\xi)^2\delta_{\xi'-l}, \tag{4.35}$$

since $\widehat{\frac{\partial^2}{\partial x^2}U(x,t)} = (i\xi)^2\widehat{U}(\xi,t)$. And finally, $\mathbf{C}^{-1}[\mathbf{D}\mathbf{C}\underline{U}_N]$ is the projection from Fourier space back to the original space. Hence it follows that $\underline{U}_N = \mathbf{C}^{-1}e^{\mathbf{D}t}\mathbf{C}\underline{U}_N(0)$ and that $e^{\mathbf{D}t}$ is the diagonal matrix with diagonal entries $e^{-(\xi/2)^2 t}$ for $\xi = -(N/2)+1,\ldots,N/2$. Thus

$$\max_{\underline{U}_N(0)}\frac{\|e^{\mathbf{D}_N^2 t}\underline{U}_N(0)\|}{\|\underline{U}_N(0)\|} < c$$

for some constant c.

It follows that the eigenvalues of $\mathbf{D}_N^2$ determine whether the solution $\underline{U}_N(t)$ remains bounded. The method of lines, introduced earlier, was to solve the semi-discrete system of ordinary differential equations in t by a finite difference scheme. The rule of thumb [84, pp. 103] is that the method of lines is stable if the eigenvalues of the spatial discretization operator, scaled by κ, lie in the stability region of the time discretization operator.

The stability region of the Euler scheme is the region of the complex plane consisting of those $\lambda \in \mathbb{C}$ for which the scheme applied at time step κ to the problem $\frac{\mathrm{d}}{\mathrm{d}t}u(t) = \lambda u(t)$ produces bounded solutions. The Euler time stepping scheme reduces to the recurrence relation

$$U((j+1)\kappa) = (1+\lambda\kappa)U(j). \tag{4.36}$$

At time $j\kappa$, $U(j\kappa) = (1+\kappa\lambda)^j U(0)$, where $U(0)$ is the initial value. The fixed point of the recurrence relation (4.36) is $z = 1+\kappa\lambda$. That is $z^j = (1+\kappa\lambda)^j z$. Any initial value may be written in terms of z, that is $U(0) = bz$ for some constant b. Thus it follows

that $U(j\kappa) = (1+\kappa\lambda)^n)U(0) = b(1+\kappa\lambda)^j z = bz^j$. Hence the solution of the Euler finite difference scheme remains bounded for all initial values if and only if z^j remains bounded as $j \to \infty$. This will be the case if and only if $|z| = |1+\kappa\lambda| \leq 1$.

Therefore the spectral difference scheme approximating the linear diffusion problem with Euler time stepping and the spatial discretization operator $\mathbf{D}_N^2$ is expected to be stable if the eigenvalues $\lambda = -\xi^2$ of $\mathbf{D}_N^2$ are such that $|1+\kappa\lambda| \leq 1$. The largest eigenvalue is $\lambda = -(N/2)^2$. Hence the stability condition is satisfied if $|1-\kappa(N/2)^2| \leq 1$. That is, the condition for the difference scheme to be stable is

$$\kappa \leq 2N^{-2} = 2h^2. \tag{4.37}$$

Since the difference scheme is consistent with the initial-boundary value problem (4.34) it follows by Theorem 4.3 (the Lax equivalence theorem) that the difference scheme is also convergent to the initial-boundary value problem (4.34). Furthermore, by Theorem (4.4) it follows that the difference scheme (4.27) for the non-linear initial boundary-value problem (4.1) is stable. Conditions for the convergence of the difference scheme (4.27) to the non-linear system (4.1) will, however, not be pursued.

4.4 Chapter Summary

In this chapter numerical schemes used to approximate solutions to the initial-boundary value problems studied in this thesis were reviewed and motivated. The first numerical method used was that of finite differences (§4.1). Finite differences employ local approximating polynomials which are differentiated to approximate derivatives. This method was applied to approximate solutions to initial-boundary value problems when the boundary values are described by zero-flux Neumann conditions, in fulfilment of part (a) of Objective IV in § 1.3.

The second method used was that of spectral differences (§4.2). This method employs a basis of periodic functions on the grid to approximate periodic functions on an interval. These approximating grid functions are then differentiated to approximate derivatives of the functions on the interval. Spectral differences were employed to approximate solutions to initial-boundary value problems where periodicity of solutions is imposed, in fulfilment of part (b) of Objective IV in § 1.3.

Both numerical schemes were shown to be consistent with the respective initial-boundary value problems (§4.3). Furthermore, conditions for the stability of each numerical scheme were derived. Finally, the finite difference scheme was shown to converge to the solution of the initial value problem with zero-flux Neumann boundary conditions.

Chapter 5

Invasibility and Coexistence of Two Competing Species

In this chapter the system of equations

$$\frac{\partial N_1^*}{\partial t^*} = \frac{\partial}{\partial x^*}\left(D_1^*(x^*)\frac{\partial N_1^*}{\partial (x^*)}\right) + r_1^* N_1^*\left(1 - \frac{1}{k_1^*(x^*)}N_1^* - \frac{\beta_{21}^*}{k_1^*(x^*)}N_2^*\right), \tag{5.1}$$

$$\frac{\partial N_2^*}{\partial t^*} = \frac{\partial}{\partial x^*}\left(D_2^*(x^*)\frac{\partial N_2^*}{\partial (x^*)}\right) + r_2^* N_2^*\left(1 - \frac{1}{k_2^*(x^*)}N_2^* - \frac{\beta_{12}^*}{k_2^*(x^*)}N_1^*\right) \tag{5.2}$$

is considered on a one dimensional habitat R. R is partitioned into intervals of length ℓ_1 and ℓ_2, respectively referred to as type 1 and type 2 intervals. The functional coefficients $D_i(x)$ and $k_i(x)$ have constant values on each interval. That is, they are two-toned functions. In particular, a functional coefficient has a constant value on every interval of type 1 and a possibly different constant value on every interval of type 2. These coefficients have significance as environmental parameters. The functions $D_i^*(x^*)$ are diffusion coefficients. The coefficient functions $k_i^*(x^*)$ are environmental carrying capacities. The functions $k_i^*(x^*)$ are assumed to achieve maximum values on the intervals of type 1. In the case that R is finite, R comprises exactly one interval of type 1 and one interval of type 2, and the length of R is $\ell = \ell_1 + \ell_2$. In the case that R is infinite the intervals of type 1 and type 2 alternate and $\ell = \ell_1 + \ell_2$ is said to be the period of the habitat.

In the model $N_1^*(x^*, t^*)$ and $N_2^*(x^*, t^*)$ represent the population densities of two competing species at point $x^* \in \mathbb{R}$ and at time $t^* \geq 0$. $N_2^*(x^*, t^*)$ represents a new species introduced to the habitat at a low density at time $t^* = 0$ and $N_1^*(x^*, t^*)$ represents the native species to the habitat, assumed already to be at a non-trivial population equilibrium at time $t^* = 0$. The coefficients r_1^* and r_2^* are their respective linear growth rates at small population densities and the coefficients β_{ij}^* represent interspecific competition intensities.

5.1 Nondimensionalisation of the Model

In this section the model is nondimensionalised. The spatial variable x^* is scaled so that the focus of the model is at the scale of the diffusion coefficient. Upon introduction of the nondimensional parameters

$$t = r_1^* t^*, \quad x = x^*\left(\frac{r_1^*}{D_2}\right)^{1/2}, \quad \beta_{21} = \beta_{21}^*\frac{m_2}{m_1}, \quad \beta_{12} = \beta_{12}^*\frac{m_1}{m_2},$$

$$r = \frac{r_2^*}{r_1^*}, \quad k_i(x) = \frac{k_i^*(x^*)}{m_i}, \quad D_i(x) = \frac{D_i^*(x^*)}{D_2} \quad \text{and} \quad N_i(x,t) = \frac{N_i^*(x^*,t^*)}{m_i},$$

where $D_2 = \sup_x(D_2^*(x))$ and where $m_i = \sup_x(k_i^*(x))$, it follows that $\frac{\mathrm{d}x}{\mathrm{d}x^*} = \left(\frac{r_1^*}{D_2}\right)^{1/2}$ and $\frac{\mathrm{d}t}{\mathrm{d}t^*} = r_1^*$. By applying the chain rule it therefore follows that

$$\frac{\partial N_i^*(x^*,t^*)}{\partial t^*} = m_i r_1^* \frac{\partial N_i(x,t)}{\partial t}$$

and

$$\frac{\partial N_i^*(x^*,t^*)}{\partial x^*} = m_i \left(\frac{r_1^*}{D_2}\right)^{1/2} \frac{\partial N_i(x,t)}{\partial x}.$$

Furthermore, by applying the product and chain rules,

$$\begin{aligned}
\frac{\partial}{\partial x^*}\left(D_i^*(x^*)\frac{\partial N_i^*(x^*,t^*)}{\partial (x^*)}\right) &= D_i^*(x^*)\frac{\partial^2 N_i^*(x^*,t^*)}{\partial (x^*)^2} + \frac{\mathrm{d}D_i^*(x^*)}{\mathrm{d}x}\frac{\partial N_i^*(x^*,t^*)}{\partial (x^*)} \\
&= D_2 m_1 D_i(x)\frac{\partial^2 N_i(x,t)}{\partial x^2}\left(\frac{r_1^*}{D_2}\right) \\
&\quad + m_1 D_2 \frac{\mathrm{d}D_i^*(x^*)}{\mathrm{d}x}\left(\frac{r_1^*}{D_2}\right)^{1/2}\frac{\partial N_i(x,t)}{\partial x}\left(\frac{r_1^*}{D_2}\right)^{1/2} \\
&= m_1 r_1^* \frac{\partial}{\partial x}\left(D_i(x)\frac{\partial N_i(x,t)}{\partial x}\right).
\end{aligned}$$

Hence the system (5.1) and (5.2) becomes

$$\begin{aligned}
m_1 r_1^* \frac{\partial N_1}{\partial t} &= m_1 r_1^* \frac{\partial}{\partial x}\left(D_1(x)\frac{\partial N_1}{\partial x}\right) + m_1 r_1^* N_1\left(1 - \frac{m_1 N_1}{m_1 k_1(x)} - \frac{\beta_{21} m_2 N_2 m_1}{m_1 k_1(x) m_2}\right), \\
m_2 r_1^* \frac{\partial N_2}{\partial t} &= m_2 r_1^* \frac{\partial}{\partial x}\left(D_2(x)\frac{\partial N_2}{\partial x}\right) + m_2 r_2^* N_2\left(1 - \frac{m_2 N_2}{m_2 k_2(x)} - \frac{\beta_{12} m_1 N_1 m_2}{m_2 k_2(x) m_1}\right),
\end{aligned}$$

which reduces to

$$\frac{\partial N_1}{\partial t} = \frac{\partial}{\partial x}\left(D_1(x)\frac{\partial N_1}{\partial x}\right) + N_1\left(1 - \frac{N_1}{k_1(x)} - \frac{\beta_{21} N_2}{k_1(x)}\right), \tag{5.3}$$

$$\frac{\partial N_2}{\partial t} = \frac{\partial}{\partial x}\left(D_2(x)\frac{\partial N_2}{\partial x}\right) + r N_2\left(1 - \frac{N_2}{k_2(x)} - \frac{\beta_{12} N_1}{k_2(x)}\right). \tag{5.4}$$

5.2 Linearized Model

The stability of the steady state representing a dominant native species and an absent second species in the habitat is investigated in this section, by introducing a small population of the second species in order to consider the possibility of invasion of the habitat by the latter species. To this end $n_1(x,t)$ and $n_2(x,t)$ are assumed to be small perturbations from the steady state solution of the system where the population $\hat{N}_2(x)$ is zero everywhere and where $\hat{N}_1(x)$ is found by solving the ordinary differential equation obtained by setting $\frac{\partial}{\partial t}N_1(x,t) = 0$ in (5.3). Thus

$$\begin{aligned}
N_1(x,t) &= \hat{N}_1(x) + n_1(x,t) \text{ and} \\
N_2(x,t) &= 0 + n_2(x,t).
\end{aligned}$$

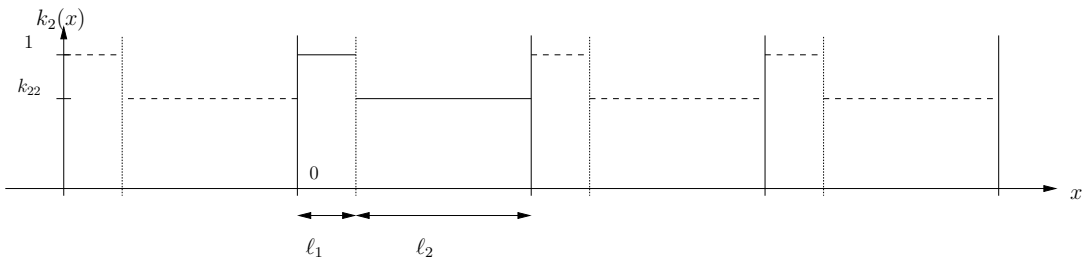

Figure 5.1: The spatial pattern of $k_2(x)$.

Due to the nondimensionalisation process the carrying capacities $k_i(x)$ assume a unit value on the intervals of type 1 and a value of $k_{i2} \leq 1$ on the intervals of type 2, as illustrated in Figure 5.1 for $k_2(x)$. The diffusion coefficients $D_i(x)$ take the positive constant values D_{i1} on the intervals of type 1 and the positive constant values D_{i2} on the intervals of type 2. Since the functions $D_i(x)$ are constant on the partition intervals of R the derivatives $\frac{\mathrm{d}D_i(x)}{\mathrm{d}x}$ vanish almost everywhere, and hence, inside each interval

$$\frac{\partial}{\partial x}\left(D_i(x)\frac{\partial N_i}{\partial x}\right) = \frac{\mathrm{d}D_i(x)}{\mathrm{d}x}\frac{\partial N_i}{\partial x} + D_i(x)\frac{\partial^2 N_i}{\partial x^2} = D_i(x)\frac{\partial^2 N_i}{\partial x^2}$$

and between intervals $N_i(x,t) \in C^1(\mathbb{R},\mathbb{R})$. Substituting $N_i(x,t)$ with $\hat{N}_i(x) + n_i(x,t)$ for $i = 1,2$ in (5.4) and ignoring higher order terms, since $n_1(x,t)$ and $n_2(x,t)$ are small, results in the equation

$$\frac{\partial n_2}{\partial t} = D_2(x)\frac{\partial^2 n_2}{\partial x^2} + s(x)n_2, \tag{5.5}$$

where

$$s(x) = r\left(1 - \frac{\beta_{12}\hat{N}_1(x)}{k_2(x)}\right).$$

Notice that (5.5) is independent of n_1. Thus the behaviour of the population N_2 near the zero population steady state is independent of small perturbations from the equilibrium population density distribution of the other species. A separable solution to this equation is now sought in the form $n_2(x,t) = y(x)T(t)$. Substituting this functional structure for n_2 into (5.5) yields the equation

$$y(x)T^{'}(t) = D_2(x)y^{''}(x)T(t) + s(x)y(x)T(t),$$

which may be rewritten as

$$\frac{T^{'}(t)}{T(t)} = \frac{D_2(x)y^{''}(x) - s(x)}{y(x)} = -\mu.$$

The latter equality with a constant $-\mu$ is justified by noting that the left hand side of the first equality is dependent on t only, whilst the right hand side of the same equality is dependent on x only. A solution of $T'(t) = -\mu T(t)$ is $T(t) = ce^{-\mu t}$ for some constant $c \in \mathbb{R}$ dependent on the initial conditions. Hence a separable solution is of the form $n_2(x,t) = ce^{-\mu t}y(x;\mu)$. From this solution structure it may be seen that if a solution exists for some $\mu < 0$, then the trivial steady state with a zero second species population density is unstable.

Substituting $n_2(x,t) = ce^{-\mu t}y(x)$ into (5.5) gives

$$-\mu ce^{-\mu t}y(x) = D_2(x)ce^{-\mu t}y''(x) + s(x)ce^{-\mu t}y(x),$$

which reduces to Hill's equation

$$y''(x) + (S(x) + \lambda)y(x) = 0, \tag{5.6}$$

where

$$S(x) = \begin{cases} \frac{s(x)}{D_{21}}, & n\ell \le x < n\ell + \ell_1, \\ \frac{s(x)}{D_{22}} + \left(\frac{\mu}{D_{22}} - \frac{\mu}{D_{21}}\right), & n\ell + \ell_1 < x < (n+1)\ell, \end{cases}$$

where $y(x) \in C^1(\mathbb{R}, \mathbb{R})$, and where $\lambda = \frac{\mu}{D_{21}}$. The boundary conditions that together with (5.5) describe an initial boundary value problem translate to conditions, that, together with (5.6), describe an eigenvalue problem. Only for the eigenvalues λ of the eigenvalue problem will solutions of the form $n_2(x,t) = ce^{-\mu t}y(x)$ satisfy the required boundary conditions, where $\mu = \lambda D_{21}$.

5.3 Stability and Invasibility Conditions

In §5.2 it was demonstrated that the sign of the smallest eigenvalue of Hill's equation determines the stability of a small invading population. In this section bounds on model parameters are derived for which the corresponding smallest eigenvalue λ_0 of Hill's equation is negative and hence the invading population density distribution unstable.

A basis of solutions of the initial value problem (5.6) has dimension two. The two linearly independent solutions are denoted $y_1(x)$ and $y_2(x)$. The solutions are said to be normalized if $y_1(0) = 1$, $y_1'(0) = 0$, $y_1(0) = 0$ and $y_2'(0) = 1$.

Three cases of restrictions on the environmental variables and habitat are considered in this section, in order of increasing complexity. In all three cases $D_1(x)$, $D_2(x)$, and $k_2(x)$ are two-toned functions. However, in the first case the environment considered is finite with zero-flux Neumann boundary conditions and $k_1(x)$ constant value over the whole environment. The second case is that of a periodic environment, but still with $k_1(x)$ constant over the whole environment. The final case is where the environment is periodic and $k_1(x)$ is two-toned. These three cases are

- A finite habitat with $k_1(x)$ constant.
- A periodic habitat with $k_1(x)$ constant.
- A periodic habitat with $k_1(x)$ a two-toned function.

5.3.1 A Finite Habitat with $k_1(x)$ Constant

In this subsection the simplifying assumption is made that $k_1(x) = 1$ for all $x \in R$. The steady state population density distribution of the native species in the absence of an

invading species therefore reduces to $\hat{N}_1(x) = 1$. Moreover, the function $S(x)$ in Hill's equation also reduces to a two-toned function. For notational convenience, let

$$S(x) = \begin{cases} s_1 & \text{for all } n\ell \le x < n\ell + \ell_1, \\ s_2, & \text{for all } n\ell + \ell_1 < x < (n+1)\ell. \end{cases}$$

Since $S(x)$ is constant on each interval of type 1 or 2 the solution of (5.6), with initial conditions $y(0) = \beta$ and $y'(0) = \omega$, on an interval of type i, is

$$y(x) = \beta \cos(x\sqrt{s_i + \lambda}) + \frac{\omega}{\sqrt{s_i + \lambda}} \sin(x\sqrt{s_i + \lambda}),$$

by Theorem B.1. By Theorem B.2 $y(x)$ may be written as

$$y(x) = \gamma \cos((x + \alpha)\sqrt{s_i + \lambda}),$$

where $\frac{\omega}{\sqrt{s_i+\lambda}} = \gamma \sin(x + \alpha)$ and $\beta = \gamma \sin(x + \alpha)$.

Additionally, in this subsection, R is a finite habitat and consists of the partition intervals $[0, \ell_1]$ and $(\ell_1, \ell\,]$ with zero flux boundary conditions at $x = 0$ and $x = \ell$. This assumption translates to the initial condition $y'(0) = 0$ of the initial value problem for the differential equation (5.6). Of the two independent normalized solutions only y_1 satisfies this initial condition. Thus, on the interval $[0, \ell_1]$, $y(x) = \cos(\sqrt{s_1 + \lambda}\, x)$. Furthermore, let $y(x) = A\cos(\sqrt{s_2 + \lambda}\,(x + \alpha_1))$ on the interval $(\ell_1, \ell\,]$, where A and α_1 are constants. Then, by the boundary condition at $x = \ell$,

$$y_1'(\ell) = -A \sin(\sqrt{s_2 + \lambda}(\ell + \alpha_1))\sqrt{s_2 + \lambda} = 0$$

and hence

$$\sqrt{s_2 + \lambda}(\ell + \alpha_1)) = n\pi,$$

so that

$$\alpha_1 \sqrt{s_2 + \lambda} = n\pi - \ell\sqrt{s_2 + \lambda}.$$

Therefore the solution on R of the initial value problem (5.6), with initial conditions as dictated by the boundary assumptions in this subsection, is

$$y_1(x) = \begin{cases} \cos(\sqrt{s_1 + \lambda}\, x) & 0 \le x < \ell_1, \\ A\cos(\sqrt{s_2 + \lambda}(\ell - x)), & \ell_1 < x < \ell. \end{cases}$$

At $x = \ell_1$, the population density is not expected to be discontinuous just because the carrying capacity is. Hence it is required that

$$\lim_{x \to \ell_1^-} y_1(x) = \lim_{x \to \ell_1^+} y_1(x). \tag{5.7}$$

Furthermore, at the discontinuity of the carrying capacity, members of the population should not disappear. Hence the flux across this point should be continuous, and because the flux is proportional to the slope of the population density it is thus required that

$$\lim_{x \to \ell_1^-} D_2(x) y_1'(x) = \lim_{x \to \ell_1^+} D_2(x) y_1'(x). \tag{5.8}$$

Consequently

$$\cos(\sqrt{s_1+\lambda}\ell_1) = A\cos(\sqrt{s_2+\lambda}\ell_2) \tag{5.9}$$

$$\text{and } D_{21}\sqrt{s_1+\lambda}\sin(\sqrt{s_1+\lambda}\ell_1) = D_{22}A\sqrt{s_2+\lambda}\sin(\sqrt{s_2+\lambda}\ell_2). \tag{5.10}$$

Dividing (5.9) by (5.10) eliminates the constant A, rendering the single condition

$$\frac{D_{22}}{D_{21}}\sqrt{s_1+\lambda}\tan(\sqrt{s_1+\lambda}\ell_1) = \sqrt{s_2+\lambda}\tan(\sqrt{s_2+\lambda}\ell_2). \tag{5.11}$$

That is, if λ satisfies (5.11) then $y_1(x;\lambda)$ is a solution of (5.6) satisfying conditions (5.9) and (5.10) together with the zero-flux Neumann boundary conditions.

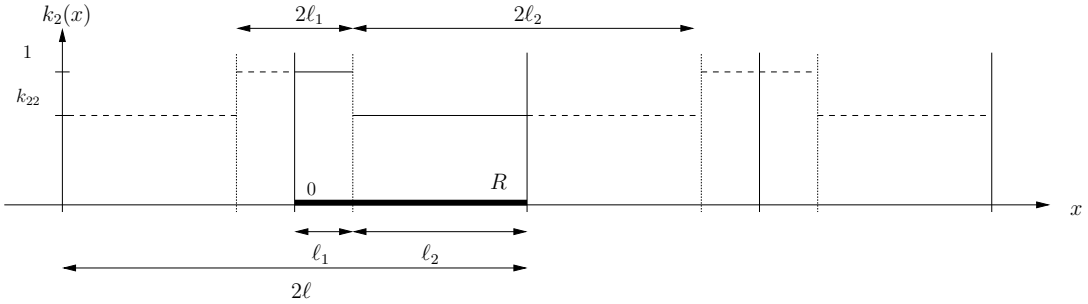

Figure 5.2: The spatial pattern of $k_2(x)$ when reflected about the origin and then extended periodically.

If the carrying capacity $k_2(x)$ is reflected about the point $x = 0$ and then extended periodically, as illustrated in Figure 5.2, then the resulting extended function $k_E(x)$ is periodic with a period of 2ℓ. Hence $S(x)$ is also 2ℓ-periodic. If a solution of (5.6) is reflected about the point $x = 0$ and then extended periodically, the extended solution will also have a period of 2ℓ. With $S(x)$ periodic, (5.6) is known as Hill's equation and there exists a $\lambda^* \in \mathbb{R}$ such that Hill's equation has no periodic solutions for $\lambda \leq \lambda^*$ (see Theorem B.6). Therefore there exists a smallest λ for which $y_1(x;\lambda)$ exists in this periodically extended case.

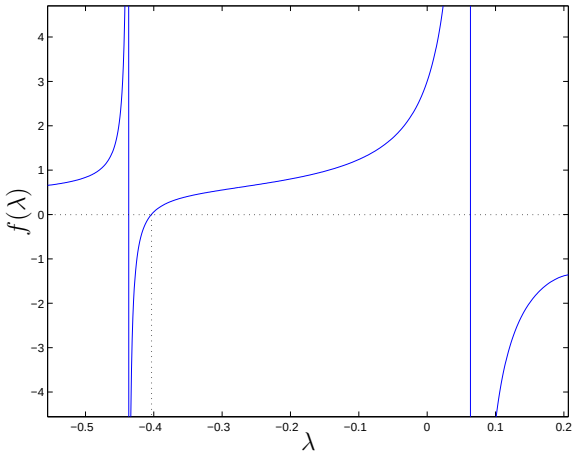

Figure 5.3: Smallest zero of (5.11) as considered in Example 5.1.

Example 5.1 *Take the spatial domain to be of length* 4π *and let* $\ell_1 = 2\pi$. *Furthermore, let* $k_{22} = \frac{10}{24}$, $D_1 = D_2 = 1$, $r = 1$, *and* $\beta_{12} = \beta_{21} = 0.5$.

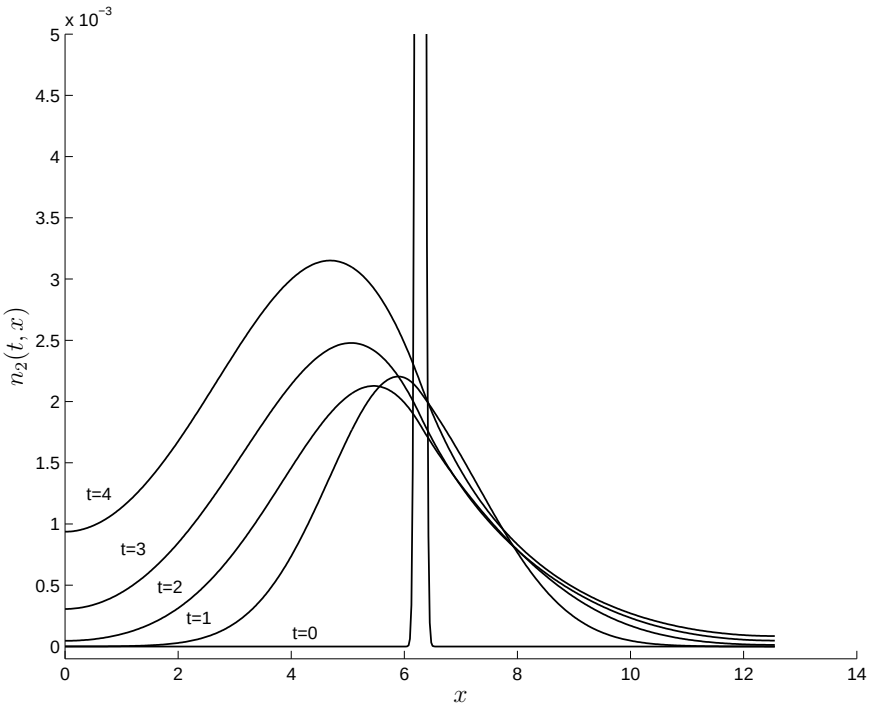

Figure 5.4: Numerical approximation at discrete points over the time interval $(0, 4)$ of the solution to the system (5.3)–(5.4) for parameter values considered in Example 5.1.

Therefore $s_1 = (1 - \frac{(0.5)(1)}{1}) = 0.5$ *and* $s_2 = (1 - \frac{(0.5)(24)}{10}) = -0.2$. *The result in Appendix B.3 shows that the smallest zero of (5.11) will be larger than* -0.5 *and indeed the plot of* $f(\lambda; \ell_1) = \sqrt{s_2 + \lambda}\tan(\sqrt{s_2 + \lambda}\ell_2) - \sqrt{s_1 + \lambda}\tan(\sqrt{s_1 + \lambda}\ell_1)$ *in Figure 5.3 confirms that the first zero is in the interval* $(-0.5, 0)$. *The zero is near* $-0.403\,574$.

A numerical approximation of the solution to the system (5.3)–(5.4) over the time interval $[0, 20]$ *for a small population introduced at* $x = \ell_1$, *as shown in Figure 5.5(a), suggests that a small initial population would successfully invade the habitat for these parameter values. Furthermore, the solution over a longer time interval, as shown in Figure 5.5(b), suggests that the two populations will reach a stable coexistent equilibrium. The behaviour of the small invading population is shown in Figure 5.4 over a short initial time interval.* ■

At the critical value $\lambda = 0$ (where $\lambda < 0$ is unstable and $\lambda > 0$ is stable) the condition (5.11) becomes

$$\ell_1^* = \frac{1}{\sqrt{s_1}} \arctan\left(\frac{\sqrt{s_2}}{\sqrt{s_1}} \tan\left(\ell_2\sqrt{s_2}\right)\right).$$

This value is a critical length for the interval $(0, \ell_1)$ in the sense that, if $\ell_1 < \ell_1^*$, then the trivial population is stable, whereas if $\ell_1 > \ell_1^*$, then it is unstable. In other words, the invading population survives in the habitat when $\ell_1 > \ell_1^*$, but does not survive in the habitat when $\ell_1 < \ell_1^*$.

Example 5.2 (Continuation of Example 5.1) *If* ℓ_2 *is set at a length of* 2π, *then* $\ell^* \approx 0.303\,293$. *The plot of* $f(\lambda; \ell_1)$ *in Figure 5.3.1 where* $\ell_1 = 0.2 < \ell^*$ *indicates that for these values of the parameters* s_1, s_2, ℓ_1 *and* ℓ_2 *the first zero of (5.11) is larger than* 0. *It is close to* $0.217\,490$.

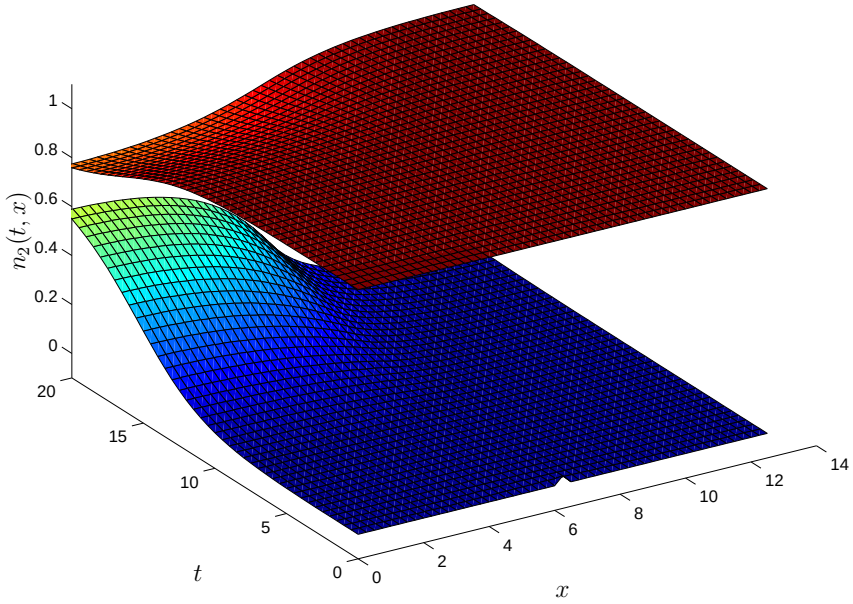

(a) Medium-time dynamics of both the native and invading species.

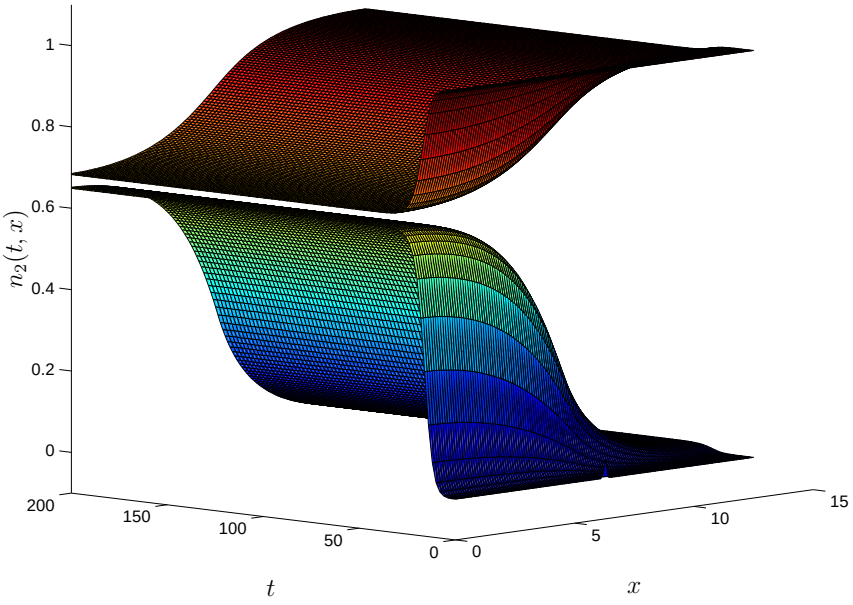

(b) Long-time dynamics of both the native and invading species.

Figure 5.5: Numerical approximations of the solution to the system (5.3)–(5.4) for parameter values considered in Example 5.1.

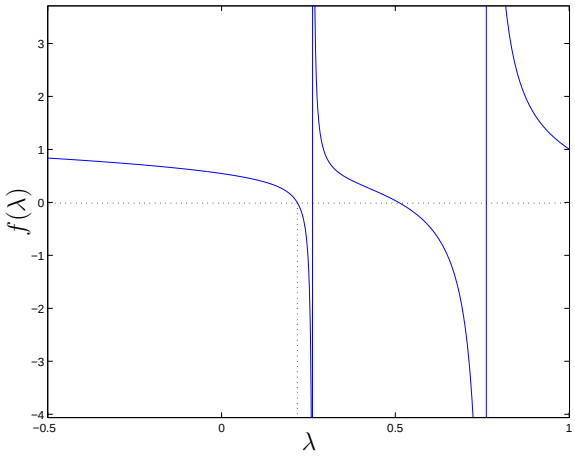

Figure 5.6: Smallest zero of (5.11) as considered in Example 5.2.

A numerical approximation of the solution to the system of equations for parameter values as in Example 5.1, but only now with $\ell_1 = 0.2 < \ell^*$ and the small population introduced at $x = \ell_1$, suggests that the population introduced would not be able to invade. Figure 5.7(a) shows the distribution of the species introduced in the region of the introduction over a short time interval after the initial time $t = 0$. The long-time behaviour of the dying population is shown at discrete times in Figure 5.7(b). ■

5.3.2 A Periodic Habitat with $k_1(x)$ Constant

The problem of determining whether a small initial population of the species represented by n_2 in the system (5.3)–(5.4) will survive when introduced into a two-toned environment where it competes with an established population of a different species, represented by n_1, was reduced in § 5.2 to the question of whether there exists a negative eigenvalue λ of Hill's equation. In this subsection $k_1(x)$ is again assumed constant over the whole environment, as it was in the previous subsection. Thus the function $S(x)$ of (5.6) is ℓ-periodic and takes two values, $s_1 > s_2$, as shown in Figure 5.8, with both s_1 and s_2 possibly negative. However, the environment R is here assumed periodic with period ℓ. These boundary conditions translate to the requirement of ℓ-periodic solutions of Hill's equation. If ℓ-periodic solutions to (5.6) do exist for a $\lambda < 0$, then the trivial equilibrium of the introduced species population is unstable and the species will invade successfully, that is, survive. By Theorem B.6 bounded real solutions to (5.6) can only exist for $\lambda > -\sup_x S(x)$. Thus the problem is to determine whether $-s_1 < \lambda < 0$ exists such that (5.6) has ℓ-periodic solutions.

The first order system of ordinary differential equations associated with (5.6) is

$$\underline{X}'(x) = \mathbf{A}(x) \cdot \underline{X}(x) \tag{5.12}$$

with coefficient matrix

$$\mathbf{A} = \begin{pmatrix} 0 & 1 \\ -(S(x) + \lambda) & 0 \end{pmatrix} \in PC\left(\mathbb{R}, M_2(\mathbb{R})\right),$$

where $PC\left(\mathbb{R}, M_2(\mathbb{R})\right)$ is the set of piecewise continuous functions from $\mathbb{R}$ to the 2×2 matrices on $\mathbb{R}$. By [10, Theorem 7.8], when $\mathbf{A} \in PC\left(\mathbb{R}, M_2(\mathbb{R})\right)$, given any $\underline{\chi} = (\beta, \omega)^T \in$

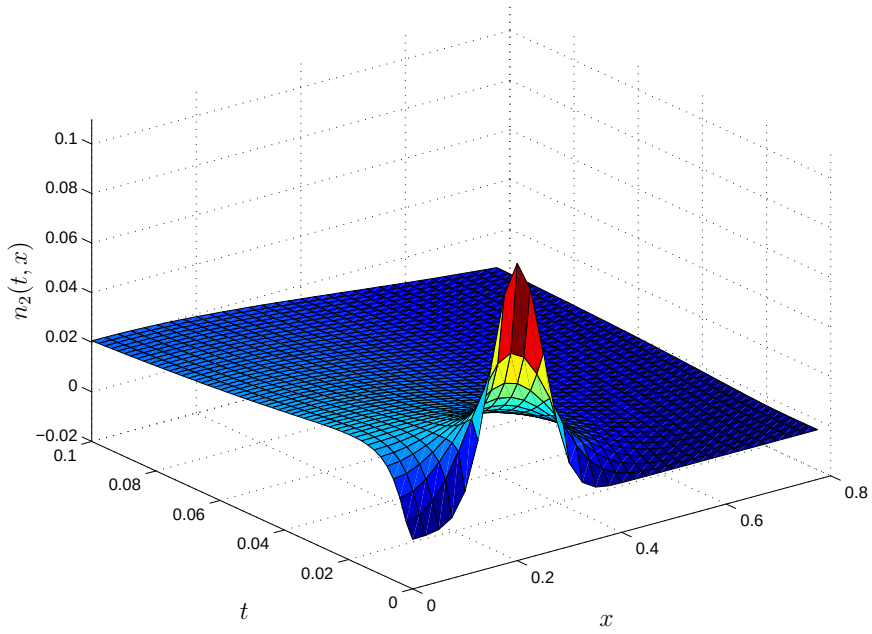

(a) Short-time dynamics of introduced species.

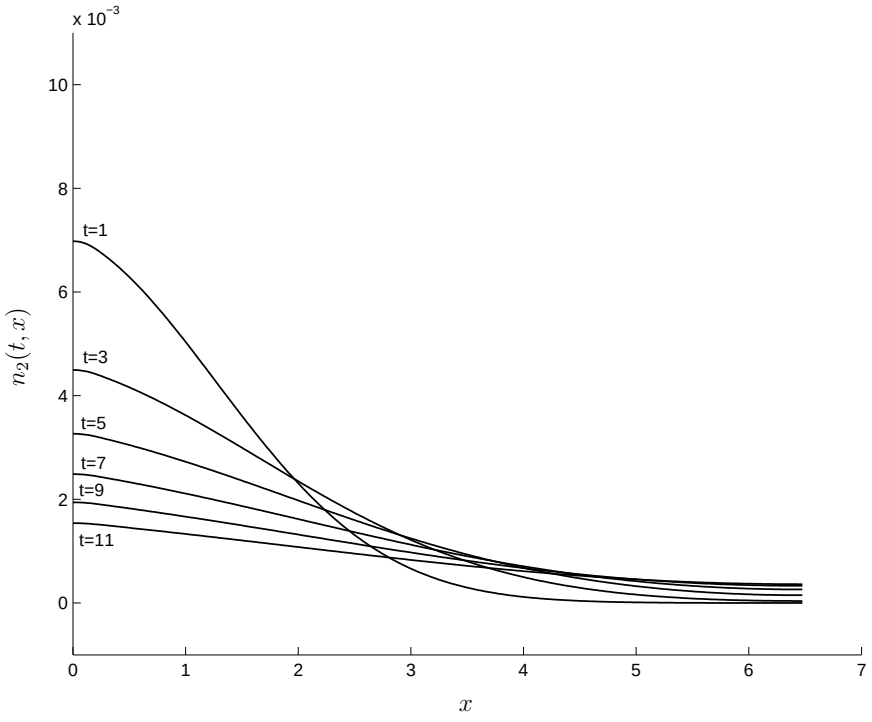

(b) Long-time dynamics of introduced species.

Figure 5.7: Numerical approximations of the solution to the system (5.3)–(5.4) for parameter values considered in Example 5.2.

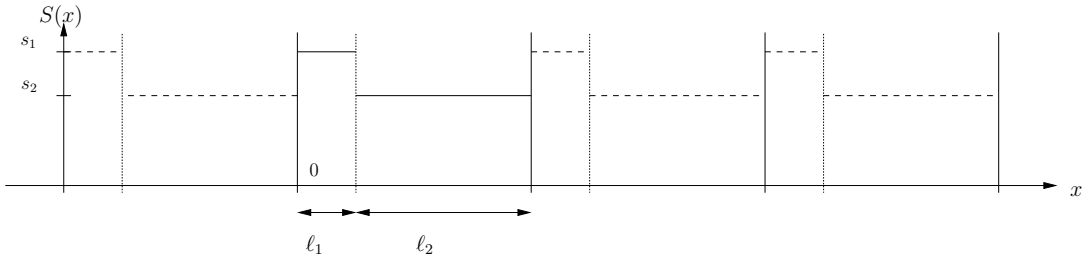

Figure 5.8: The spatial pattern of $S(x)$.

$\mathbb{R}^2$ and $\varsigma \in \mathbb{R}$, there exists a unique solution $Z \in C(\mathbb{R}, \mathbb{R}^2)$ of (5.12) satisfying $\underline{Z}(\varsigma) = \underline{\chi}$. $\underline{Y} = (y_1, y_2)^T \in C(\mathbb{R}, \mathbb{R}^2)$ is a basis of solutions of (5.6) if and only if

$$\mathbf{X} = \begin{pmatrix} y_1 & y_2 \\ y_1' & y_2' \end{pmatrix}$$

is a basis of solutions of (5.12). By Floquet's theorem (Theorem B.3) each basis of solutions of (5.12) can be represented as

$$\mathbf{X}(x) = \mathbf{P}(x) \cdot e^{\mathbf{R}x},$$

where $\mathbf{P} \in C^1(\mathbb{R}, M_2(\mathbb{R}))$, $\mathbf{P}(x)$ is invertible, $\mathbf{P}(x + \ell) = \mathbf{P}(x)$ for all $x \in \mathbb{R}$, and $\mathbf{R} \in M_2(\mathbb{R})$. Since $\mathbf{Z}(x) = \mathbf{X}(x + \ell) = \mathbf{X}(x) \cdot \mathbf{C}$ is also a basis for some invertible $\mathbf{C} \in M_2(\mathbb{R})$ it follows that $\mathbf{C} = \mathbf{X}^{-1}(0) \cdot \mathbf{X}(\ell)$, and, from the proof of Floquet's theorem, $\mathbf{C} = e^{\mathbf{R}\ell}$. If $\mathbf{X}_1$ is another basis for (5.12), then $\mathbf{X}_1(x) = \mathbf{X}(x) \cdot \mathbf{T}$ for some invertible $\mathbf{T} \in M_2(\mathbb{R})$, and if $\mathbf{X}_1(x + \ell) = \mathbf{X}_1(x) \cdot \mathbf{C}_1$, then

$$\mathbf{C}_1 = \mathbf{X}_1^{-1}(0) \cdot \mathbf{X}_1(\ell) = \mathbf{T}^{-1} \cdot \mathbf{X}^{-1}(0) \cdot \mathbf{X}(\ell) \cdot \mathbf{T} = \mathbf{T}^{-1} \cdot \mathbf{C} \cdot \mathbf{T}.$$

Thus $\mathbf{C}_1$ is similar to $\mathbf{C}$. That is, the eigenvalues of $\mathbf{C}$ together with their multiplicities are independent of the basis chosen and depend only on $\mathbf{A}$. The eigenvalues of $\mathbf{C}$ are known as the *multipliers* of the system (5.12).

Theorem 5.1 (Multipliers) *A solution $\underline{Z} = \mathbf{X} \cdot \xi$ of (5.12) satisfies $\underline{Z}(x + \ell) = \mu \underline{Z}(x)$ for every $x \in \mathbb{R}$ if and only if μ is a multiplier of (5.12).*

Proof.
If a solution $\underline{Z}(x) = \mathbf{X}(x) \cdot \underline{\xi}$ satisfies $\underline{Z}(x + \ell) = \mu \underline{Z}(x)$, then

$$\underline{X}(x) \cdot \mathbf{C} \cdot \underline{\xi} = \mathbf{X}(x + \ell) \cdot \underline{\xi} = \underline{Z}(x + \ell) = \mu \underline{Z}(x) = \mu \mathbf{X}(x) \cdot \underline{\xi},$$

which implies that $\mathbf{C} \cdot \underline{\xi} = \mu \underline{\xi}$. Conversely, if $\mathbf{C} \cdot \underline{\xi} = \mu \underline{\xi}$, then

$$\underline{Z}(x + \ell) = \mathbf{X}(x + \ell) \cdot \underline{\xi} = \mathbf{X}(x) \cdot \mathbf{C} \cdot \underline{\xi} = \mu \mathbf{X}(x) \cdot \underline{\xi} = \mu \underline{Z}(x). \qquad \blacksquare$$

In particular, (5.12) has a nontrivial ℓ-periodic solution $\underline{Z}(x) = \mathbf{X}(x) \cdot \underline{\xi}$ if and only if $\mu = 1$ is an eigenvalue of $\mathbf{C}$ and $\underline{\xi}$ is a corresponding eigenvector.

Suppose the basis $\mathbf{X}$ is chosen for (5.12) such that it satisfies $\mathbf{X}(0) = \mathbf{I}_2$. Then the multipliers of (5.12) are the eigenvalues μ_1, μ_2 of $\mathbf{C} = \mathbf{X}(\ell)$. These eigenvalues are the zeros of

$$\det(\mu \mathbf{I}_2 - \mathbf{X}(\ell)) = \mu^2 - 2a\mu + b = 0, \tag{5.13}$$

where $2a = \mathrm{tr}(\mathbf{X}(\ell))$ and $b = \det(\mathbf{X}(\ell))$. By Theorem B.4 it follows that the Wronskian $W_{\mathbf{X}} = \det(\mathbf{X})$ satisfies $\det(\mathbf{X}(\ell)) = e^{\int_0^x tr(\mathbf{A}(s))\,\mathrm{d}s} = 1$. Hence $b = 1$. Solving for the zeros of (5.13) with $b = 1$ gives

$$\mu_1 = a + \sqrt{a^2 - 1} \quad \text{and} \quad \mu_2 = a - \sqrt{a^2 - 1}.$$

Thus $\mu_1\mu_2 = a^2 - a^2 + 1 = 1$. If $a^2 \neq 1$, then $\sqrt{a^2 - 1} \neq 0$. Hence neither μ_1 nor μ_2 is unity, and by Theorem 5.1 no ℓ-periodic solutions of (5.12) exists. If $a^2 = 1$ then $\mu_1 = \mu_2 = 1$ and by Theorem 5.1 ℓ-periodic solutions exist. Conversely, if $\mu_1 = 1$ then $\mu_2 = 1/\mu_1 = 1$; hence $a = 1$, and thus $\mathrm{tr}(\mathbf{X}(\ell)) = 2a = 2$. Consequently, ℓ-periodic solutions of (5.12) exist if and only if $\mathrm{tr}(\mathbf{X}(\ell)) = 2$. The ℓ-periodic solutions are $\underline{Z}(x) = \mathbf{X}(x)\cdot\xi$, where ξ is an eigenvector corresponding to the eigenvalue $\mu = 1$. The trace $\mathrm{tr}(\mathbf{X}(\ell)) = y_1(\ell, \lambda) + y_2'(\ell, \lambda)$ as a function of λ is known as the discriminant. Denote this descriminant by $\Delta(\lambda)$. Then $\Delta(\lambda)$ is an entire function of λ [57, Theorem 2.2].

Since $S(x) = s_1$ is constant on the interval I, by Theorem B.1, the solution of (5.6) associated with $\underline{Z}$ is

$$y(x) = \beta\cos(x\sqrt{s_1 + \lambda}) + \frac{\omega}{\sqrt{s_1 + \lambda}}\sin(x\sqrt{s_1 + \lambda}).$$

By Theorem B.2 $y(x)$ may be written as

$$y(x) = \gamma\cos((z + \alpha)\sqrt{s_1 + \lambda}),$$

where $\frac{\omega}{\sqrt{s_1+\lambda}} = \gamma\sin(x + \alpha)$ and $\beta = \gamma\sin(x + \alpha)$. Hence the solution $y_1(x)$ of (5.6) on $\mathbb{R}$ that satisfies $y_1(0) = 1$ and $y_1'(0) = 0$ is

$$y_1(x) \;=\; \begin{cases} \cos(\sqrt{s_1 + \lambda}\, x), & n\ell \le x < n\ell + \ell_1, \\ \gamma_1\cos(\sqrt{s_2 + \lambda}(x + \alpha_1)), & n\ell + \ell_1 < x < (n + 1)\ell, \end{cases}$$

for $n \in \mathbb{N}$. A second solution, independent of the first, because it satisfies $y_2(0) = 0$ and $y_2'(0) = 1$, is

$$y_2(x) \;=\; \begin{cases} \frac{1}{\sqrt{s1+\lambda}}\sin(\sqrt{s_1 + \lambda}\, x), & n\ell \le x < n\ell + \ell_1, \\ \gamma_2\sin(\sqrt{s_2 + \lambda}(x + \alpha_2)), & n\ell + \ell_1 < x < (n + 1)\ell. \end{cases}$$

The solution basis of (5.12) corresponding to the solution basis $\underline{Y} = (y_1, y_2)$ of (5.6) is

$$\mathbf{X} = (\underline{X}_1, \underline{X}_2) = \begin{pmatrix} y_1 & y_2 \\ y_1' & y_2' \end{pmatrix},$$

satisfying

$$\mathbf{X}(\varsigma) = \begin{pmatrix} 1 & 0 \\ 0 & 1 \end{pmatrix}$$

at $\varsigma = 0$. The continuity of $\underline{X}_1$ at $x = \ell_1$ determines the coefficients γ_1 and α_1. The system of equations to be satisfied is

$$\begin{aligned} \cos(\ell_1\sqrt{s_1 + \lambda}) &= \gamma_1\cos(\sqrt{s_2 + \lambda}(\ell_1 + \alpha_1)) \\ \sqrt{s_1 + \lambda}\sin(\ell_1\sqrt{s_1 + \lambda}) &= \gamma_1\sqrt{s_2 + \lambda}\sin(\sqrt{s_2 + \lambda}(\ell_1 + \alpha_1)). \end{aligned}$$

Thus

$$\gamma_1 = \frac{\cos(\ell_1\sqrt{s_1+\lambda})}{\cos(\sqrt{s_2+\lambda}(\ell_1+\alpha_1))} \tag{5.14}$$

and

$$\alpha_1 = \frac{1}{\sqrt{s_2+\lambda}}\tan^{-1}\left(\frac{\sqrt{s_1+\lambda}}{\sqrt{s_2+\lambda}}\tan(\ell_1\sqrt{s_1+\lambda})\right) - \ell_1. \tag{5.15}$$

Similarly, the continuity of $\underline{X}_2$ at $x = \ell_1$ determines the coefficients γ_2 and α_2. The system of equations to be satisfied is

$$\begin{aligned}\frac{1}{\sqrt{s_1+\lambda}}\sin(\ell_1\sqrt{s_1+\lambda}) &= \gamma_2\sin(\sqrt{s_2+\lambda}(\ell_1+\alpha_2))\\ \cos(\ell_1\sqrt{s_1+\lambda}) &= \gamma_2\sqrt{s_2+\lambda}\cos(\sqrt{s_2+\lambda}(\ell_1+\alpha_2)).\end{aligned}$$

Thus

$$\gamma_2 = \frac{\cos(\ell_1\sqrt{s_1+\lambda})}{\cos(\sqrt{s_2+\lambda}(\ell_1+\alpha_2))} \tag{5.16}$$

and

$$\alpha_2 = \frac{1}{\sqrt{s_2+\lambda}}\tan^{-1}\left(\frac{\sqrt{s_2+\lambda}}{\sqrt{s_1+\lambda}}\tan(\ell_1\sqrt{s_1+\lambda})\right) - \ell_1. \tag{5.17}$$

Now, $\Delta(\lambda) = y_1(\ell,\lambda) + y_2'(\ell,\lambda)$, and the condition for ℓ-periodic solutions of (5.12) to exist is

$$\Delta(\lambda) = \gamma_1\cos(\sqrt{s_2+\lambda}(\ell+\alpha_1)) + \gamma_2\sqrt{s_2+\lambda}\cos(\sqrt{s_2+\lambda}(\ell+\alpha_2)) = 2. \tag{5.18}$$

Substituting (5.14) and (5.16) into (5.18) yields

$$\Delta(\lambda) = \cos(\ell_1\sqrt{s_1+\lambda})\frac{\cos(\sqrt{s_2+\lambda}(\ell+\alpha_1))}{\cos(\sqrt{s_2+\lambda}(\ell_1+\alpha_1))} + \cos(\ell_1\sqrt{s_1+\lambda})\frac{\cos(\sqrt{s_2+\lambda}(\ell+\alpha_2))}{\cos(\sqrt{s_2+\lambda}(\ell_1+\alpha_1))}.$$

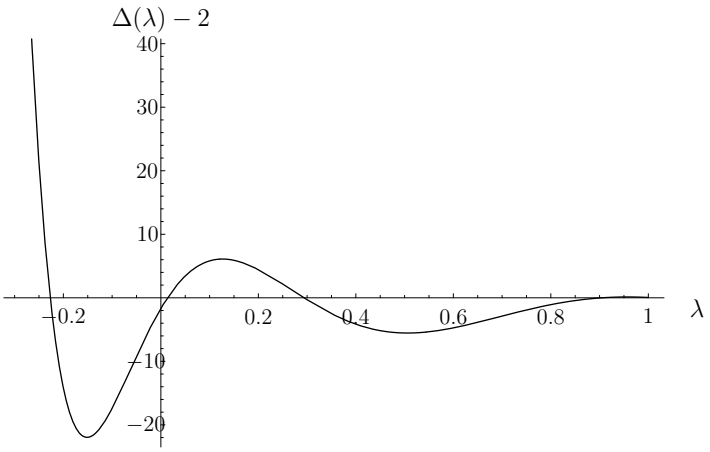

Figure 5.9: A plot of $\Delta(\lambda) - 2$ for parameter values $s_1 = 0.3$, $s_2 = -0.5$, $\ell_1 = 2.9\pi$. The smallest zero occurs at $\lambda = -0.226\,857$.

Example 5.3 (A Periodic Solution of Hill's Equation) *In this example a periodic solution of (5.12) is exhibited for a negative value of λ, given that $\ell = 4\pi$ and $\ell_1 = 2.9\pi$.*

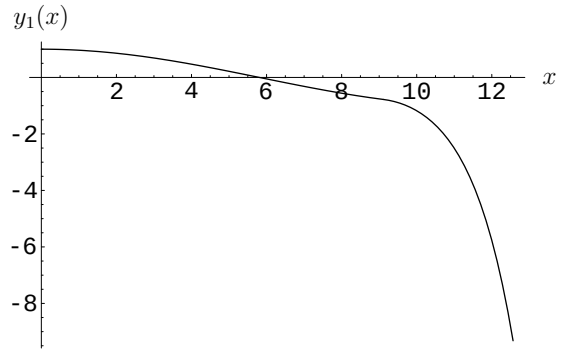

(a) The function $y_1(x)$.

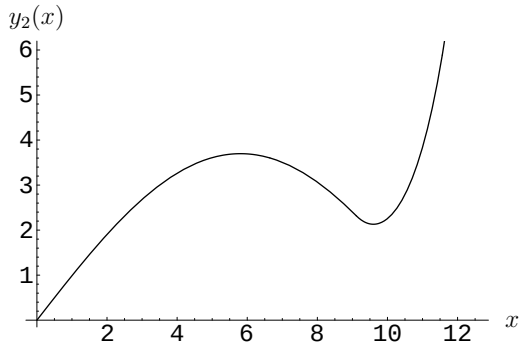

(b) The function $y_2(x)$.

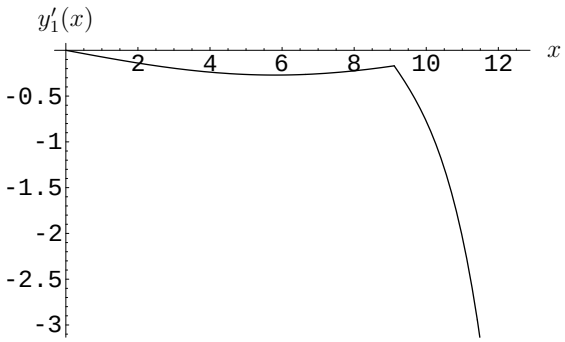

(c) The function $y_1'(x)$.

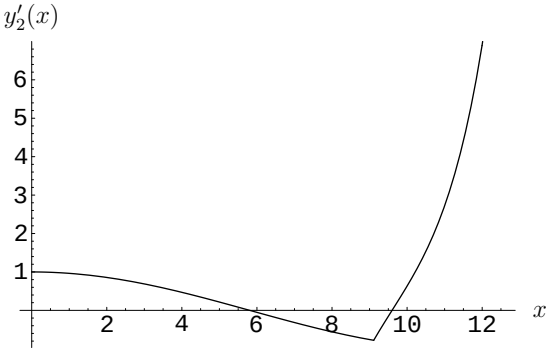

(d) The function $y_2'(x)$.

Figure 5.10: Graphs, over one period, of the functions in the basis of solutions of (5.12) with parameters as in Example 5.3.

In an interval where $S(x) + \lambda$ is positive and constant (5.6) is the equation governing simple harmonic motion. Intuitively then periodic solutions of (5.12) may be expected to exist if $S(x)+\lambda$ is positive over the whole period of the domain. Ignoring, for the moment, that (5.12) follows from a system of partial differential equations, let $s(x)$ take the values $s_1 = 0.300\,000$ and $s_2 = -0.500\,000$, where s_2 is specifically chosen negative so that this example does not merely support the above intuition.

A value $\lambda = \lambda_0$ such that $\Delta(\lambda_0) = 2$ is approximated via Newton's method by successively calculating values of $\gamma_1, \alpha_1, \gamma_2$, and α_2 from (5.14)–(5.17) for every candidate value of λ. Figure 5.9 is a graph of the function $\Delta(\lambda) - 2$ over the interval $\lambda \in (-0.3, 1)$. As may be seen in the figure, $\Delta(\lambda_0) = 2$ for some value $\lambda_0 < 0$. Indeed $\Delta(\lambda_0) = 2$ for $\lambda_0 = -0.226\,857$.

The values of $\gamma_1, \alpha_1, \gamma_2$, and α_2 for λ_0 determine the functions $y_1(x), y_2(x), y_1'(x)$ and $y_2'(x)$. These functions are graphed in Figures 5.10(a)–5.10(d). The value of $\mathbf{X}$ at $x = \ell$ is approximately

$$\mathbf{C} = \mathbf{X}(\ell) = \begin{pmatrix} y_1(\ell) & y_2(\ell) \\ y_1'(\ell) & y_2'(\ell) \end{pmatrix} = \begin{pmatrix} -9.332\,380 & 13.450\,300 \\ -7.921\,890 & 11.322\,400 \end{pmatrix}.$$

An eigenvector of $\mathbf{C}$, the eigenvector of Theorem 5.1 corresponding to the eigenvalue $\mu = 1$ with multiplicity 2, is $\xi = (0.793\,307, -0.608\,822)^T$. Thus a periodic solution of (5.12) is $Z(x) = (z(x), z'(x))^T = \mathbf{X}(x) \cdot \xi$. The solution $Z(x)$ is graphed in Figure 5.11. Both $z(x)$

and $z'(x)$ appear to be periodic and continuous. ■

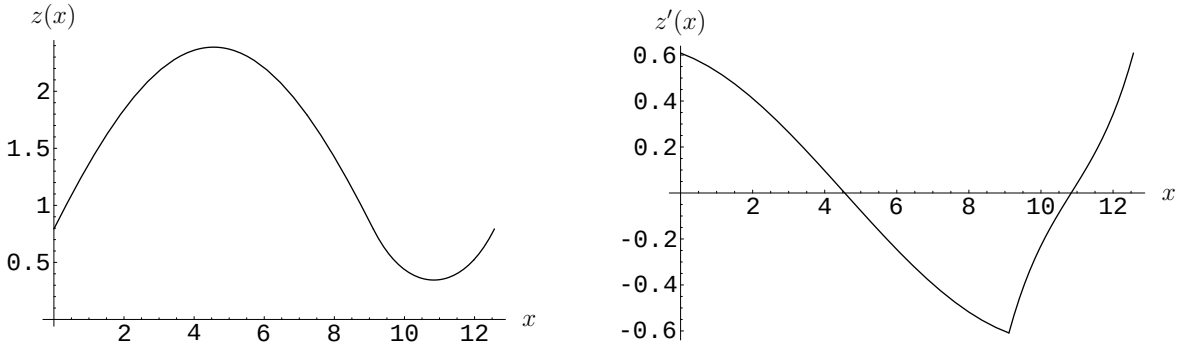

(a) The function $z(x)$. (b) The function $z'(x)$.

Figure 5.11: Graphs, over one period, of a periodic solution of (5.12) with parameters as in Example 5.3.

In Example 5.3 a periodic solution of Hill's equation was found to exist for a negative value of λ. Thus, by the analysis of this section, if the parameter values of the system (5.3)–(5.4) are such that $s_1 = 0.3$ and $s_2 = -0.5$ then the invading species will invade successfully in the presence of an already established species.

Example 5.4 (Successful Invasion) *In this example the spectral method described in Chapter 4 is used to find a numerical approximation to the solution of the system (5.3)–(5.4) with parameters such that $s_1 = 0.3$ and $s_2 = -0.5$.*

Let the length of the type 1 environment be $\ell_1 = 2.9\pi$ and that of a single period of the environment $\ell = 4\pi$. Due to the nondimensionalization process $D_2(x) = 1$ for x in a type 1 environment patch and $\sup_x k_i(x) = 1$, $i = 1, 2$, for $x \in \mathbb{R}$. Moreover, due to the simplifying assumption in this section, $k_1(x) \equiv 1$. In this example $k_2(x) = 0.662\,500$ and $D_2(x) = 0.8$ for x in an type 2 environment patch. Let the other parameter values be $D_1(x) \equiv 1$, $\beta_{21} = 1$, $\beta_{12} = 0.75$ and $r = 1.2$. Thus,

$$s_1 = \frac{r}{1}\left(1 - \frac{\beta_{12}}{1}\right) = 0.3 \quad \text{and} \quad s_2 = \frac{r}{D_2(x)}\left(1 - \frac{\beta_{12}}{k_2(x)}\right) = -0.5.$$

Figure 5.9 is a plot of the function $\Delta(\lambda) - 2$ over the interval $\lambda \in (-0.3, 01)$. As may be seen in this figure, $\Delta(\lambda) = 2$ for some value of $\lambda < 0$. Indeed $\Delta(\lambda) = 2$ for $\lambda = -0.256\,238$. Hence it is expected that a small initial population introduced into the environment where the other species is already at a population equilibrium should invade successfully. Figure 5.12 shows a numerical approximation to the solution of the system (5.3)–(5.4) when a point population is introduced at time $t = 0$ and position $x = 2\pi$. As was the conclusion drawn from the behaviour of the function $\Delta(\lambda)$, the numerical approximations also indicate that the introduced population will invade successfully. ■

The value of the discriminant $\Delta(\lambda)$ determines the value of the parameter λ for which Hill's equation has periodic solutions. The value of the discriminant depends also on the

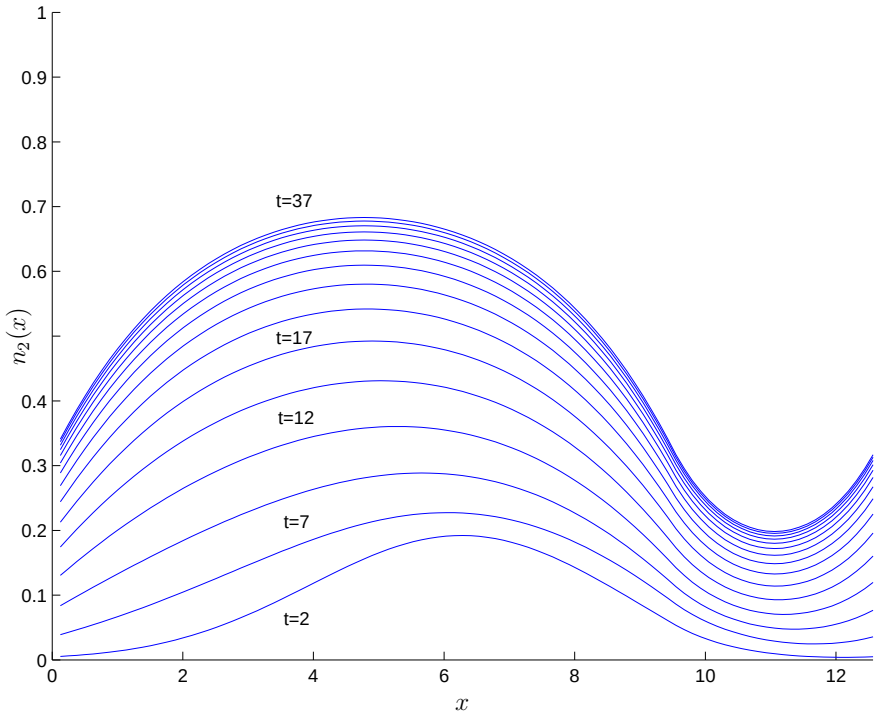

(a) The Invading Species' population distribution as time t progresses.

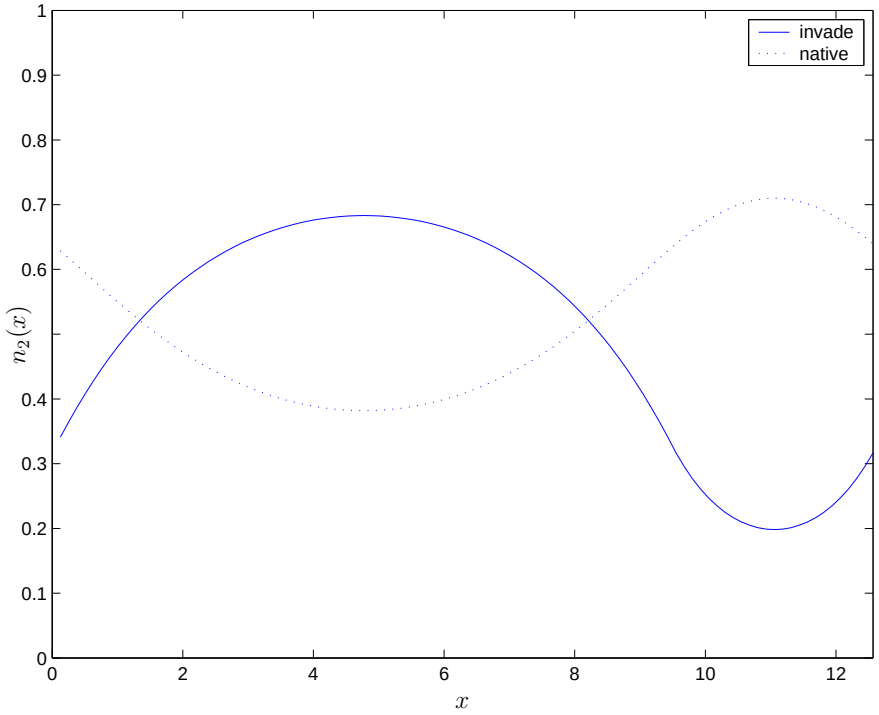

(b) Both Invading and Native Species' population distributions at time $t = 40$.

Figure 5.12: Numerical approximations over the time interval $(0, 40)$ of the solution of the system (5.3)–(5.4) with parameters as in Example 5.4.

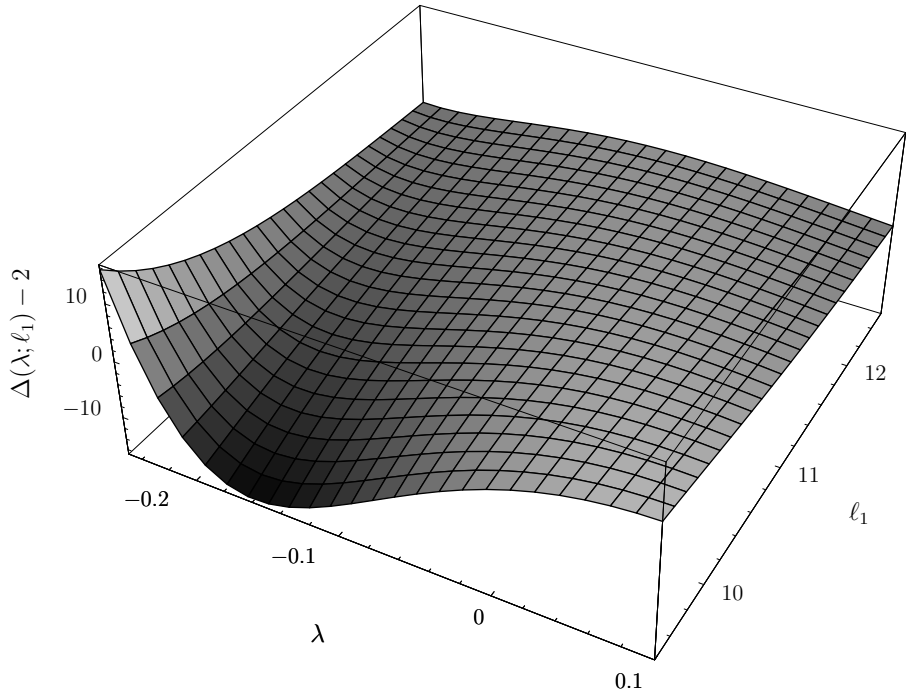

(a) The function $\Delta(\lambda;\ell_1)-2$ for $\lambda \in (-0.3, 0.1)$ and $\ell_1 \in (3\pi, 4\pi)$.

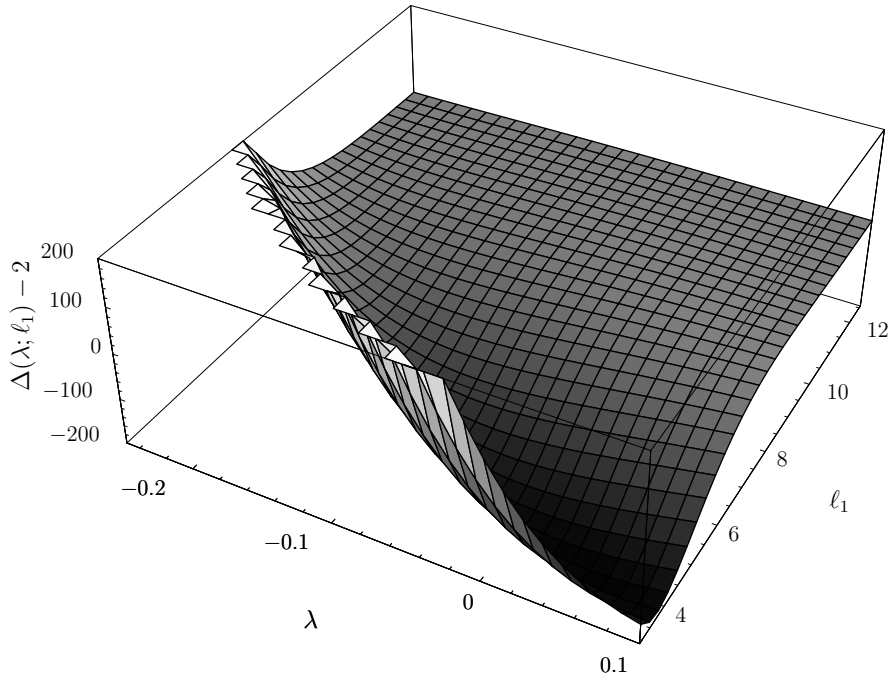

(b) The function $\Delta(\lambda;l1)-2$ for $\lambda \in (-0.3, 0.1)$ and $\ell_1 \in (\pi, 4\pi)$.

Figure 5.13: 3D Graphs of the function $\Delta(\lambda;\ell_1)-2$ with parameters as in Example 5.5.

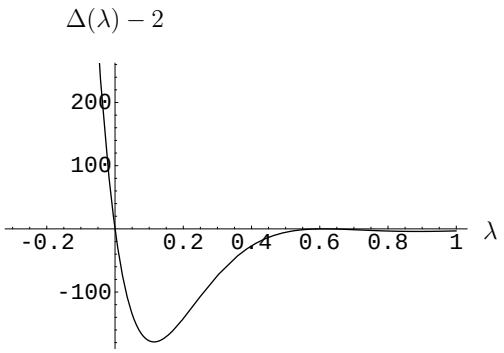

(a) No negative zeros exist for the discriminant $\Delta(\lambda;\ell_1) = 2$ when $\ell_1 = 1.058\,080\pi$.

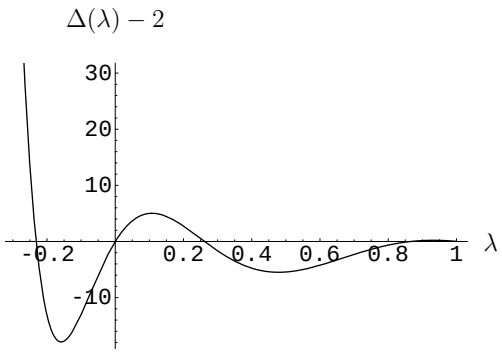

(b) One negative zero exists for the discriminant $\Delta(\lambda;\ell_1) = 2$ when $\ell_1 = 3.005\,210\pi$.

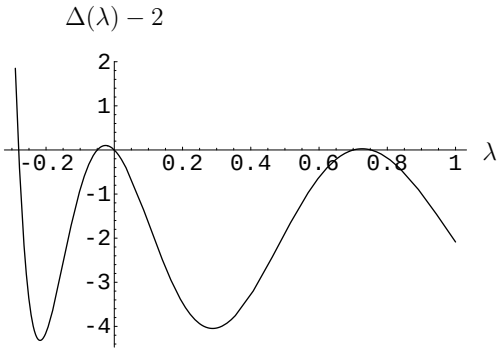

(c) Two negative zeros exist for the discriminant $\Delta(\lambda;\ell_1) = 2$ when $\ell_1 = 3.867\,770\pi$.

Figure 5.14: Zeros of the discriminant $\Delta(\lambda;\ell_1) = 2$ for fixed values of ℓ_1 and parameters as in Example 5.5.

ratio ℓ_1/ℓ. Thus the values of λ for which periodic solutions exist depend on this ratio, and hence, so does the persistence of the invading species. The model (5.3)–(5.4) where the ratio ℓ_1/ℓ is variable describes the situation where the environment may be tailored to either inhibit or facilitate the invading species.

Example 5.5 (The Discriminant) *Let $\ell = 4\pi$ and the parameters of the system (5.3)–(5.4) be as in Example 5.4, but leave ℓ_1 variable. Since $s(x)$ does not depend on ℓ_1, the values $s_1 = 0.3$ and $s_2 = -0.5$ are determined and are the same as in examples 5.3 and 5.4.*

Figure 5.13(a) shows the discriminant plotted for $\lambda \in (-0.3, 0.1)$ and $\ell_1 \in (3\pi, 4\pi)$. Since the positions of zeros are the primary concern, it makes sense to study the graph in terms of where the zeros are. It may be seen that the smallest value of λ for which $\Delta(\lambda;\ell_1)$ is zero decreases as ℓ_1 increases. What may be less evident from Figure 5.13(a), since this feature is masked by the general decrease of the absolute value of the discriminant for an increase in ℓ_1, is that values of λ at which larger zeros occur also decreases with increase in ℓ_1. The 2D graphs of Figure 5.14 make this more obvious. The graphs of Figure 5.14 are for successively increasing values of ℓ_1.

The 3D graph in Figure 5.13(b) is of the discriminant for $\ell_1 \in (\pi, 4\pi)$ and $\lambda \in (-0.3, 0.1)$.

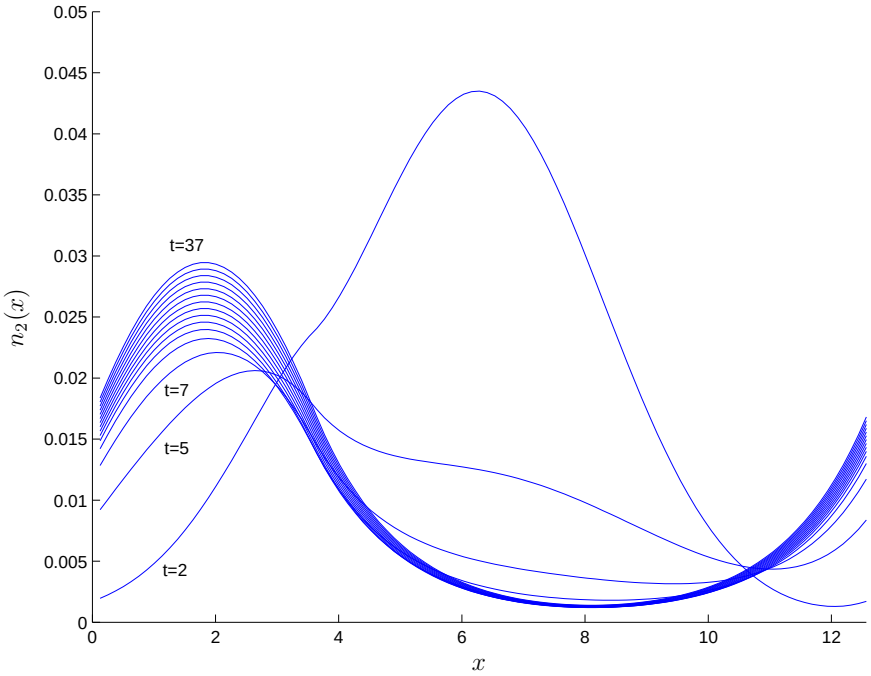

(a) The Invading Species' population distribution at times $t \in (0, 37)$.

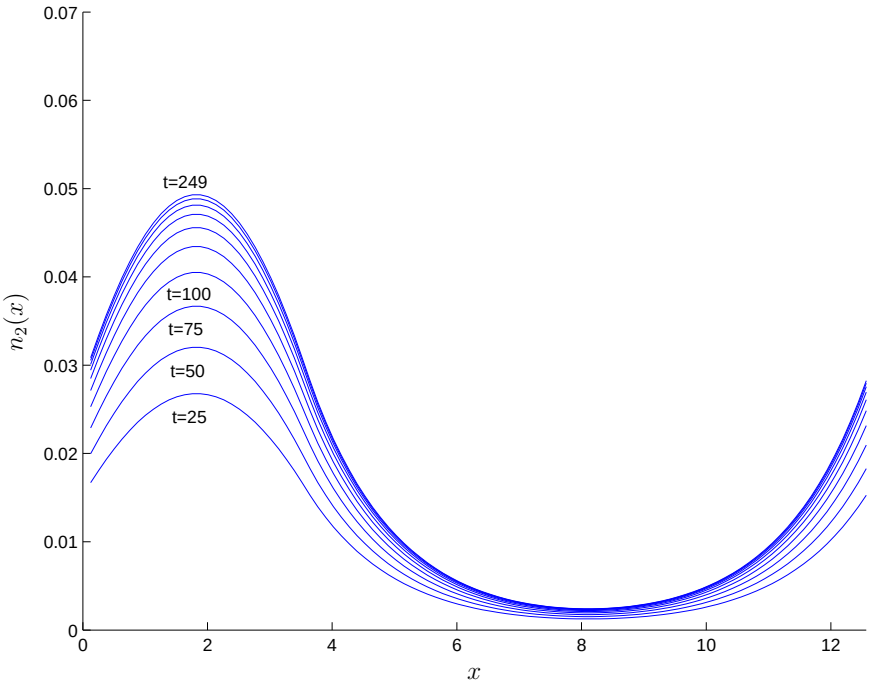

(b) The Invading Species' population distribution at times $t \in (0, 249)$.

Figure 5.15: Numerical approximations of the invading species' population distribution for solutions of the system (5.3)–(5.4) with parameters as in Example 5.6. The length of the type 1 environment is $\ell_1 = 1.121\,740\pi$.

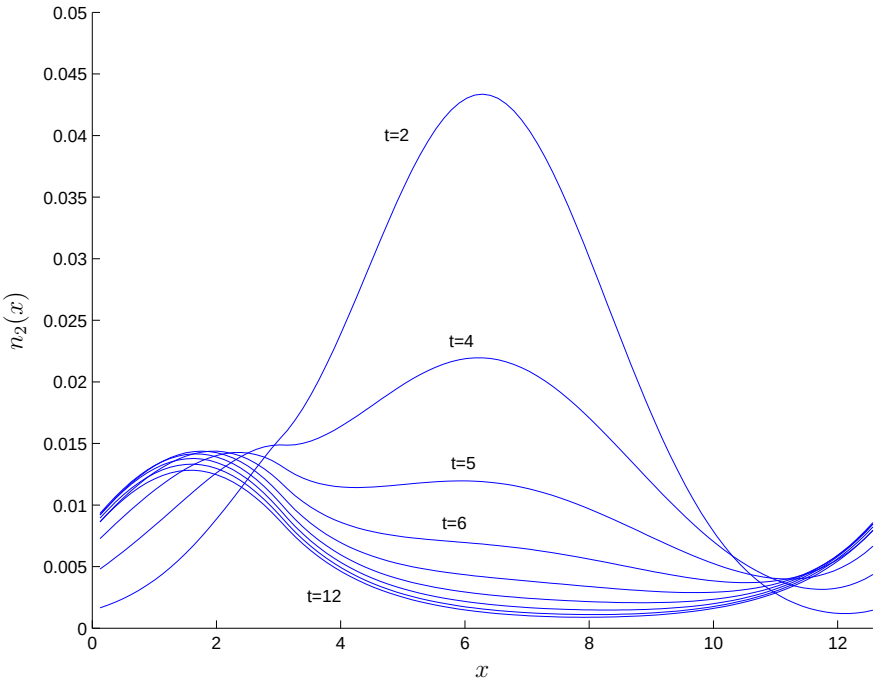

(a) The Invading Species' population distribution at times $t \in (0, 12)$.

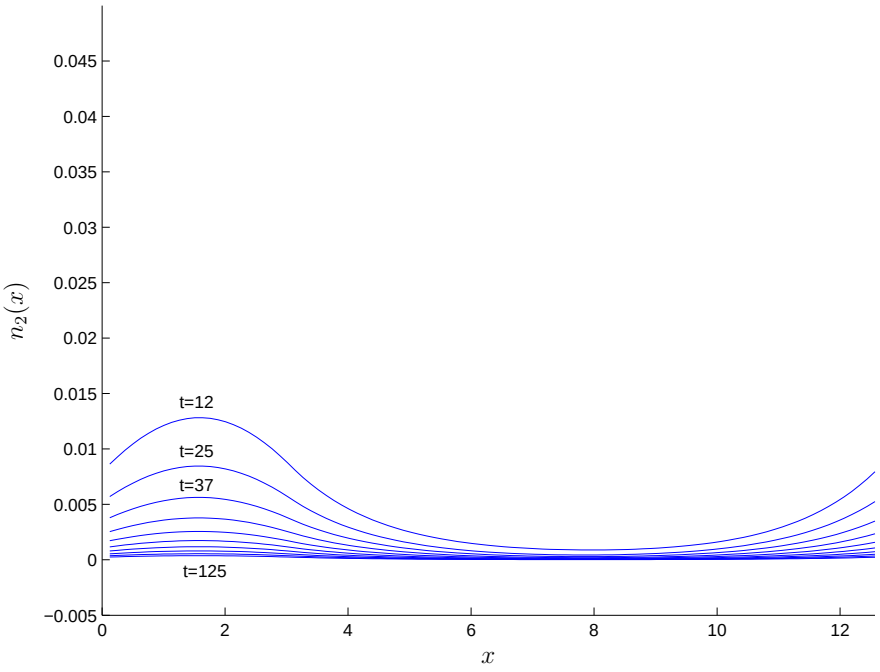

(b) The Invading Species' population distribution at times $t \in (0, 125)$.

Figure 5.16: Numerical approximations of the invading species' population distribution for solutions of the system (5.3)–(5.4) with parameters as in Example 5.6. The length of the type 1 environment is $\ell_1 = 0.994\,421\pi$.

The features of the graph for ℓ_1 close to 4π are masked by the relatively large values of the discriminant when $\ell_1 < 3\pi$. What is apparent from Figure 5.13(b) is that the smallest zero eventually occurs for λ positive when ℓ_1 is small enough. The 2D slices in Figure 5.14 taken from the 3D graphs in Figure 5.13 of $\Delta(\lambda;\ell_1)-2$ for fixed values of ℓ_1 are such that in each a zero occurs at $\lambda = 0$. From Figure 5.14(a) it can be seen that the smallest zero will occur at a positive value of λ when $\ell_1 > 1.058\,080\pi$. ■

The zero occurring at the value of $\lambda = 0$ in Figure 5.14(a) is critical in the sense that it is the smallest zero and if ℓ_1 is increased, then it occurs at a negative value of λ. Equally, if ℓ_1 were decreased it would occur at a positive value of λ and because it is the smallest zero no periodic solution of Hill's equation would exist. The zero in Figure 5.14(b) when $\ell_1 = 3.005\,210\pi$ is not critical in this sense. Example 5.4 demonstrates this situation where ℓ_1 is decreased slightly to 2.9π and the zero that occurred at $\lambda = 0$ subsequently occurs at $\lambda = 0.013\,577$, but because there is still a smaller zero, occurring at a negative value of λ, the invading species persists.

The following example demonstrates that the critical zero that exists when $\ell_1 = 1.058\,080\pi$ is indeed critical by solving the system (5.3)–(5.4) for ℓ_1 at a slightly larger value and then at a slightly smaller value.

Example 5.6 (Critical Zero) *Let the length of a single period of the environment again be $\ell = 4\pi$. The parameters of the system (5.3)–(5.4) are as in the preceding three examples, that is, $D_2(x) = 1$, $k_2(x) = 1$ for x in a type 1 environment patch, $D_1(x) \equiv 1$ and $k_1(x) \equiv 1$, $D_2(x) = 0.8$ and $k_2(x) = 0.562\,500$ for x in an type 2 environment patch, $\beta_{21} = 1$, $\beta_{12} = 0.75$, and $r = 1.2$.*

The grid used to discritize one period of the environment has 101 grid points. Thus the spaces between grid points are of length $\pi 4/100$. In order that the numerical model distinguishes the chosen values of ℓ_1, the respective values of ℓ_1 must therefore be increased or decreased by at least $\pi 4/100$.

In the first case let $\ell_1 = 1.121\,174$. For this value the smallest zero of the discriminant occurs at $\lambda = -0.0186\,727$. Figure 5.15(a) shows the population distribution over one period of the environment at a number of times $t \in (0, 37)$. An initial point population was released at time $t = 0$ and position $x = 2\pi$. The population moves to the type 1 environment as time progresses and all but dies out in the type 2 environment. Figure 5.15(b) shows the population distribution over a longer time period. The population increases progressively less quickly until at time $t = 249$ it is practically settled at a population equilibrium.

In the second case let $\ell_1 = 0.994\,421\pi$. For this value of ℓ_1 the smallest zero of the discriminant occurs at $\lambda = 0.020\,392$. Figure 5.16(a) shows the population distribution over one period of the environment at a number of times $t \in (0, 12)$. Again an initial point population was released at time $t = 0$ and position $x = 2\pi$. During the initial migration the population increases in the type 1 environment. However, eventually the population starts to decrease here too. Figure 5.16(b) shows the population distribution over a longer time period. The population decreases steadily and in the long term seems to tend to extinction, which is in agreement with what was established in the prior analysis.■

5.3.3 A Periodic Domain with $k_1(x)$ a Two-Toned Function

In §5.3.1 and §5.3.2 the function $S(x)$ in Hill's equation, (5.6), is two-toned, that is, it is piecewise constant. However, the function $S(x)$, depends on the steady state native population distribution. In those sections $S(x)$ is constant only because of the assumption that the environmental carrying capacity is constant over the whole environment, which results in a constant steady state population distribution $\hat{N}_1$. Without the assumption of a constant environmental carrying capacity for the native species the steady state population distribution of the native species in the absence of the invading species is the solution to the boundary value problem

$$D_1(x)\frac{\mathrm{d}^2\hat{N}_1}{\mathrm{d}x^2}(x) + \hat{N}_1(x)\left(1 - \frac{\hat{N}_1(x)}{k_1(x)}\right) = 0 \tag{5.19}$$

with periodic boundary conditions. These solutions are no longer constant; moreover, the ordinary differential equation (5.19) is semi-linear and elliptic and hence a solution is difficult to obtain.

Yet, as was demonstrated in §5.3.1, the sign of the smallest eigenvalue λ_0 for which Hill's equation has a periodic solution determines the stability of a small invading population, and, in turn, the value of λ_0 is determined by $\hat{N}_1(x)$. Thus, to determine a stability bound on λ_0, for a given set of model parameters, an approximation to $\hat{N}_1(x)$ is sought.

An approximation to the steady state population distribution of the native species is achieved by a perturbation solution. Define the small perturbation parameter $\epsilon = 1 - k_{12}$, where k_{12} is the value of the carrying capacity $k_1(x)$ in an interval of type 2. Thus ϵ is the difference between the carrying capacities in a type 1 and a type 2 environment. To obtain an approximate solution on the whole environment R, solutions satisfying (5.19) on an interval of respectively type 1 or type 2 are derived and then the continuity conditions are introduced. As a convenience the general solution of (5.19) is represented by $\nu(x)$ on an interval of type 1 and by $\eta(x)$ on an interval of type 2. It is assumed that these functions have power series representations of the form

$$\nu(x) = 1 + \epsilon\,\nu_1(x) + \epsilon^2\,\nu_2(x) + O(\epsilon^3)$$

and

$$\eta(x) = k_{12} + \epsilon\,\eta_1(x) + \epsilon^2\,\eta_2(x) + O(\epsilon^3).$$

Upon substituting these into (5.19) and collecting terms of the same order of ϵ, the $O(\epsilon)$ equations

$$D_{11}\frac{\mathrm{d}^2\nu_1}{\mathrm{d}x^2}(x) - \nu_1(x) = 0 \tag{5.20}$$

and

$$D_{12}\frac{\mathrm{d}^2\eta_1}{\mathrm{d}x^2}(x) - \eta_1(x) = 0 \tag{5.21}$$

result on intervals of respectively type 1 and type 2. The $O(\epsilon^2)$ equations are

$$D_{11}\frac{\mathrm{d}^2\nu_1}{\mathrm{d}x^2}(x) - \nu_2(x) = (\nu_1(x))^1 \tag{5.22}$$

and

$$D_{12}\frac{\mathrm{d}^2\eta_2}{\mathrm{d}x^2}(x) - \eta_2(x) = \frac{(\eta_1(x))^2}{k_{12}} \tag{5.23}$$

for intervals of type 1 and type 2 respectively. Since the carrying capacity and the diffusion coefficients of (5.19) are symmetric about $\ell_1/2 + n\ell$ and $-\ell_2/2 + n\ell$ for $n \in \mathbb{N}$, it follows by the uniqueness of the solution of (5.19) (see [62, §3.3]) that the general solution is symmetric about $\ell_1/2+n\ell$ and $-\ell_2/2+n\ell$. Hence, also, $\nu_i(x)$ is symmetric about $\ell_1/2+n\ell$ and $\eta_i(x)$ is symmetric about $-\ell_2/2 + n\ell$, for $i \in \mathbb{Z}^+$. Therefore, the general solution to (5.20) on the interval $(0, \ell_1)$ is

$$A_1 \cosh\left(\frac{1}{\sqrt{D_{11}}}(x - \ell_1/2)\right)$$

and the general solution to (5.21) on the interval (ℓ_1, ℓ) is

$$A_2 \cosh\left(\frac{1}{\sqrt{D_{12}}}(x + \ell_2/2 - \ell)\right).$$

The continuity conditions (5.7) and (5.8) hold for $\nu(x)$ and $\eta(x)$ for the same seasons as discussed in §5.3.1. Hence the continuity conditions also hold for every $\nu_i(x)$ and $\eta_i(x)$, where $i \in \mathbb{Z}^+$. The constants A_1 and A_2 are determined by the continuity conditions

$$\lim_{x\to\ell_1^-} 1 + \epsilon\nu_1(x) = \lim_{x\to\ell_1^+} k_{12} + \epsilon\eta_1(x)$$

and

$$\lim_{x\to\ell_1^-} \frac{d\nu_1}{\mathrm{d}x}(x) = \lim_{x\to\ell_1^+} \frac{d\eta_1}{\mathrm{d}x}(x).$$

These constants are

$$A_1 = -\frac{\frac{1}{\sqrt{D_{12}}}\sinh\left(\frac{\ell_2}{2}\frac{1}{\sqrt{D_{12}}}\right)}{\frac{1}{\sqrt{D_{11}}}\cosh\left(\frac{\ell_2}{2}\sqrt{\frac{1}{\sqrt{D_{12}}}}\right)\sinh\left(\frac{\ell_1}{2}\frac{1}{\sqrt{D_{12}}}\right) + \frac{1}{\sqrt{D_{12}}}\cosh\left(\frac{\ell_1}{2\sqrt{D_{11}}}\right)\sinh\left(\frac{\ell_2}{2}\frac{1}{\sqrt{D_{12}}}\right)} \tag{5.24}$$

and

$$A_2 = \frac{\frac{1}{\sqrt{D_{11}}}\sinh\left(\frac{\ell_1}{2\sqrt{D11}}\right)}{\frac{1}{\sqrt{D_{11}}}\cosh\left(\frac{\ell_2}{2}\frac{1}{\sqrt{D_{12}}}\right)\sinh\left(\frac{\ell_1}{2}\frac{1}{\sqrt{D_{12}}}\right) + \frac{1}{\sqrt{D_{12}}}\cosh\left(\frac{\ell_1}{2\sqrt{D_{11}}}\right)\sinh\left(\frac{\ell_2}{2}\frac{1}{\sqrt{D_{12}}}\right)}. \tag{5.25}$$

Example 5.7 (Perturbation Solution) *In this example the steady state population distribution of the native species in the absence of a competing species is approximated by a perturbation solution to $O(\epsilon)$. The steady state population distribution is the solution to (5.19) with periodic boundary conditions. The parameters of (5.19) are $D_1(x)$ and $k_1(x)$. By the non-dimensionalisation in §5.1 $k_{11} = 1$. The other parameters are chosen as $k_{12} = 0.7$, $D_{11} = 1$ and $D_{12} = 0.8$. The length of the type 1 and type 2 environments are respectively $\ell_1 = 2.9\pi$ and $\ell_2 = 1.1\pi$.*

The perturbation parameter is $\epsilon = 1 - k_{12} = 0.3$. At $O(\epsilon)$ the approximation is

$$\hat{N}_1(x) \approx \begin{cases} 1 + \epsilon\,\nu_1(x), & n\ell \le x < n\ell + \ell_1, \\ k_{12} + \epsilon\,\eta_1(x), & n\ell + \ell_1 < x < (n+1)\ell. \end{cases}$$

The approximation over one period of the environment is shown in Figure 5.17(a). ■

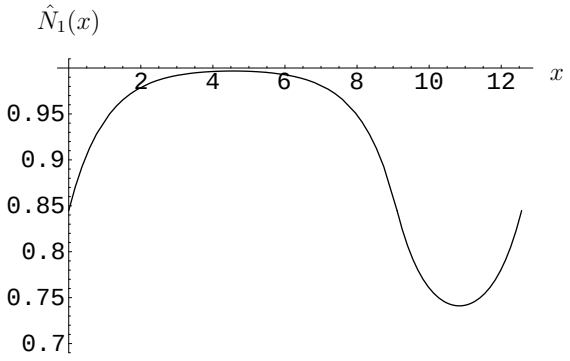

(a) The perturbation solution to $O(\epsilon)$ of the steady state population distribution of the native species in the absence of a competing species.

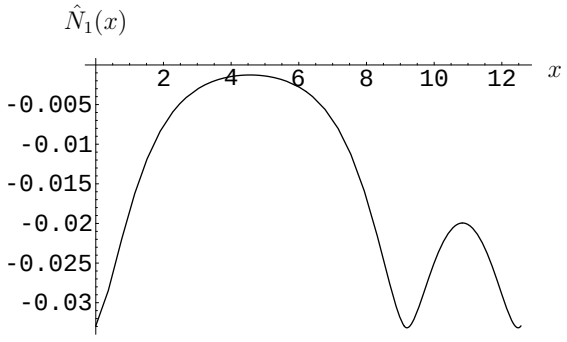

(b) The perturbation solution at $O(\epsilon^2)$.

Figure 5.17: A perturbation solution approximating the solution to (5.19) with periodic boundary conditions. The parameter values are as in Example 5.7.

The general solutions to (5.22) and (5.23) have a slightly more complex form since the ordinary differential equations are inhomogeneous. Using the solutions of $\eta_1(x)$ and $\nu_1(x)$ the general solution to (5.22) on the interval $(0, \ell_1)$ is

$$\nu_2(x) = B_1 \cosh\left(\frac{1}{\sqrt{D_{11}}}(x - \ell_1/2)\right) + \frac{A_1^2}{6}\cosh\left(\frac{2}{\sqrt{D_{11}}}(x - \ell_1/2)\right) - \frac{A_1^2}{2}$$

and the general solution to (5.23) on the interval (ℓ_1, ℓ) is

$$\eta_2(x) = B_2 \cosh\left(\frac{1}{\sqrt{D_{12}}}(x + \ell_2/2 - \ell)\right) + \frac{A_2^2}{6k_{22}}\cosh\left(\frac{2}{\sqrt{D_{12}}}(x + \ell_2/2 - \ell)\right) - \frac{A_2^2}{2k_{22}},$$

where A_1 and A_2 are as given in (5.24) and (5.24). Once again the constants B_1 and B_2 are determined by continuity considerations. The expressions for these constants are similar to those for A_1 and A_2, only more complex, and are therefore omitted.

Example 5.8 (Continuation of Example 5.7.) *This example extends the perturbation approximation of Example 5.7 to $O(\epsilon^2)$. Again the parameters of (5.19) are $k_{12} = 0.7$, $D_{11} = 1$, $D_{12} = 0.8$, and the type 1 and type 2 environment lengths are $\ell_1 = 2.9\pi$ and $\ell_2 = 1.1\pi$ respectively.*

The perturbation solution to $O(\epsilon)$ is just the perturbation solution to $O(\epsilon)$ plus $\epsilon\,\nu_1(x)$ in the type 1 environment and $\epsilon\,\eta_1(x)$ in the type 2 environment. The additional part of the approximation at $O(\epsilon^2)$ is shown in Figure 5.17(b). From the figure it is apparent that the additional part of the approximation is very small relative to the magnitude of the perturbation solution to $O(\epsilon)$. Indeed, the solution to $O(\epsilon)$ numerically integrated over one period of the environment gives a nondimensional area of 11.467 565 in comparison with the nondimensional area under the additional part of the solution which is 0.063 277. From Figure 5.17(a) the magnitude of the largest addition at a point is around 0.03, which is small relative to the smallest magnitude of the perturbation solution to $O(\epsilon)$, around 0.75.

The steady state population distribution as approximated by means of a numerical spectral method is shown in Figure 5.18. The representation of the perturbation solution to $O(\epsilon)$ in Figure 5.17(a) corresponds remarkably well with this numerical approximation. This further suggests that the perturbation solution is already relatively accurate taken only to $O(\epsilon)$. ■

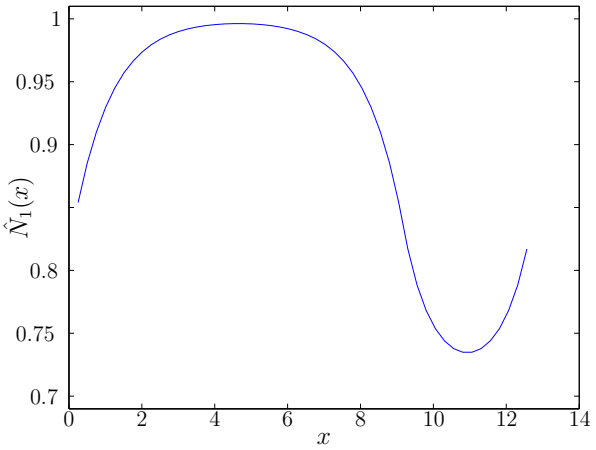

Figure 5.18: An approximation of the solution to (5.19) with periodic boundary conditions obtained by means of a spectral method. The parameter values are as in Example 5.7.

Even for the relatively large value of ϵ used in Example 5.8 the perturbation solution taken to $O(\epsilon)$ seems reasonably accurate. In the analysis that follows a perturbation solution to $O(\epsilon)$ is employed. Rewrite (5.6) as

$$\frac{\mathrm{d}}{\mathrm{d}x}\left(D(x)y'(x)\right) + (Q(x) + \lambda + S)y(x) = 0, \tag{5.26}$$

where S is a constant and

$$Q(x) = s(x) - S,$$

where, as before,

$$s(x) = r\left(1 - \frac{\beta_{12}\hat{N}_1(x)}{k_2(x)}\right).$$

The constant S is chosen such that

$$\int_0^\ell Q(x)\,\mathrm{d}x = 0.$$

Hence

$$S = \int_0^\ell s(x)\,\mathrm{d}x,$$

and using the perturbation solution to $O(\epsilon)$,

$$S = r\ell_1(1-\beta_{12}) - r\ell_2(1-\beta_{12}\frac{k_{12}}{k_{22}}) - \epsilon r\beta_{12}\left(A_1\sqrt{D_{11}}\sinh(\frac{\ell_1}{2\sqrt{D_{11}}}) + A_2\frac{k_{12}}{k_{22}}\sqrt{\frac{D_{12}}{k_{12}}}\sinh(\frac{\ell_2\sqrt{k_{12}}}{2\sqrt{D_{12}}})\right).$$

By Theorem B.6 there exists a smallest eigenvalue $\lambda_0 + S$ such that (5.26) has a periodic solution.

Theorem 5.2 *If $D(x)$ and $Q(x)$ are ℓ-periodic,*

$$\int_0^\ell Q(x)\,\mathrm{d}x = 0,$$

and $y(x) = y_0(x)$ is the ℓ-periodic solution corresponding to the smallest eigenvalue $\sigma = \sigma_0$ of Hill's equation

$$\frac{\mathrm{d}}{\mathrm{d}x}\left(D(x)y'(x)\right) + (\sigma + Q(x))y(x) = 0,$$

then $\sigma_0 \leq 0$.

Proof.
According to Magnus and Winkler [57, Theorem 2.14] it is proved in Haupt [38] that, since $y_0(x)$ is the ℓ-periodic solution corresponding to the smallest eigenvalue of Hill's equation, $y_0(x)$ has no zeros. Assume that $y_0(x) > 0$ for all x. From Hill's equation it follows that

$$\frac{\mathrm{d}}{\mathrm{d}x}(D(x)y_0'(x))\frac{1}{y_0(x)} = D'(x)\frac{y_0'(x)}{y_0(x)} + \frac{D(x)}{y_0(x)}y_0''(x) = -\sigma_0 - Q(x).$$

Since $y_0(x) > 0$, let $h(x) = \frac{\mathrm{d}}{\mathrm{d}x}\left(\ln y_0(x)\right) = \frac{y_0'(x)}{y_0(x)}$. Then

$$y_0''(x) = \frac{\mathrm{d}}{\mathrm{d}x}\left(y_0'(x)\frac{1}{y_0(x)}y_0(x)\right) = y_0(x)h'(x) + y_0'(x)h(x),$$

so that

$$\begin{aligned} D'(x)\frac{y_0'(x)}{y_0(x)} + \frac{D(x)}{y_0(x)}y_0''(x) &= h(x)D'(x) + \frac{D(x)}{y_0(x)}\left(y_0(x)h'(x) + y_0'(x)h(x)\right) \\ &= \frac{\mathrm{d}}{\mathrm{d}x}\left(D(x)h(x)\right) + D(x)(h(x))^2. \end{aligned}$$

It therefore follows that

$$\frac{\mathrm{d}}{\mathrm{d}x}\left(D(x)h(x)\right) + D(x)(h(x))^2 = -\sigma_0 - Q(x).$$

Integrating this relationship over one period of length ℓ yields

$$\int_0^\ell D(x)h^2(x)\,\mathrm{d}x = -\ell\sigma_0,$$

since $D(x)$, $h(x)$ and $Q(x)$ are periodic. Thus $\sigma_0 = 0$ if the integral over $h^2(x)$ vanishes; otherwise $\sigma_0 < 0$, because $D(x) > 0$. ■

It follows by Theorem 5.2 that $\lambda_0 + S < 0$. Since an unstable invading species population corresponds to a periodic solution of (5.6) for which $\lambda = \lambda_0 < 0$, a sufficient condition for $\lambda_0 < 0$ to hold is $S \geq 0$.

Example 5.9 *In this example the sufficiency bound $S \geq 0$ is tested. The parameters of the system (5.3)–(5.4) of two competing species are $D_{11} = 1$, $D_{12} = 0.8$, $k_{11} = 1$, $k_{12} = 0.7$, $D_{21} = 1$, $D_{22} = 1$, $k_{21} = 1$, $k_{22} = 0.5$, $\beta_{12} = 0.8$ and $r = 0.6$.*

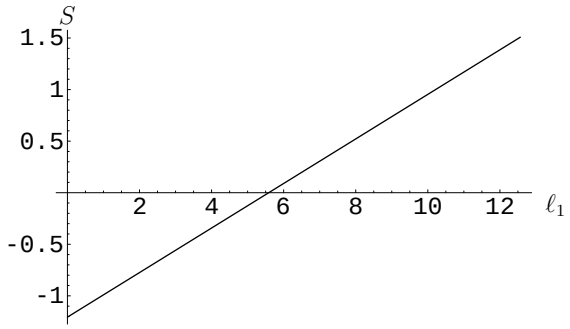

Figure 5.19: S as a function of ℓ_1 for a model with parameters as in Example 5.9.

S is shown as a function of ℓ_1 in Figure 5.19. According to the analysis the values of ℓ_1 for which S is positive are the values of ℓ_1 for which the invading species is successful. However, since this is only a sufficiency bound there may be smaller values of ℓ_1 for which the invading species is still successful. From the figure the invading species should successfully invade if the type 1 environment has length $\ell_1 > 6$.

Figure 5.20(a) represents the population distributions of the two competing species where the length of the type 1 environment is $\ell_1 = 6.3$. The long and short dashed lines represent the native population at respectively times $t = 0$ and $t = 57$. The solid lines represent the invading species' population density at different times in the interval $[0, 57]$. As expected from the preceding analysis the invading species is able to invade, since the type 1 environment has a length larger than 6.

However, the populations' distributions at time $t = 57$ are shown in Figure 5.20(b) for the case where the type 1 environment has length $\ell_1 = 4.7$. Although the invading species' population is very small the invading species nevertheless manages to invade and survive. The observation shows that the condition that $S \geq 0$ is certainly not necessary for the survival of the invading species. ■

5.4 Invasion Time

The analysis of the preceding section yields conditions that, when satisfied, ensure that the invading species survives. That is, for a given environment and competitor in that environment a small population of the invading species will persist if these conditions are satisfied. In terms of the model governing system (5.3)–(5.4), persistence of the invading species means that the integral of the population density function of the invading species is strictly positive for all $t > 0$.

The system (5.3)–(5.4) is a deterministic model. However, in reality, the species' populations are subject to stochastic perturbations. Arguing heuristically, the rate at which the invading species' population grows may contribute to the ability of the invading species to persist in a stochastic environment [58]. That is, a quickly recovering population has a larger chance of surviving multiple population perturbations. When the invading species does persist, Cantrell and Cosner [8] show that if the model does not admit a coexistent steady state, then the invading species excludes the native species. Hence, in this section a relative measure of how quickly a population recovers to population equilibrium

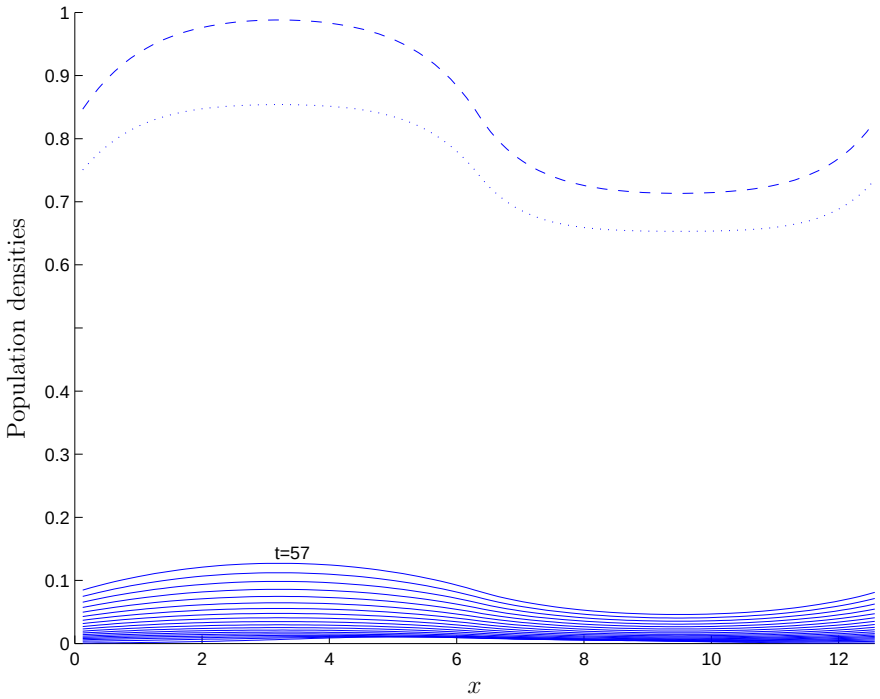

(a) Numerical approximation of species population densities when the type 2 environment has length $\ell_1 = 6.3$.

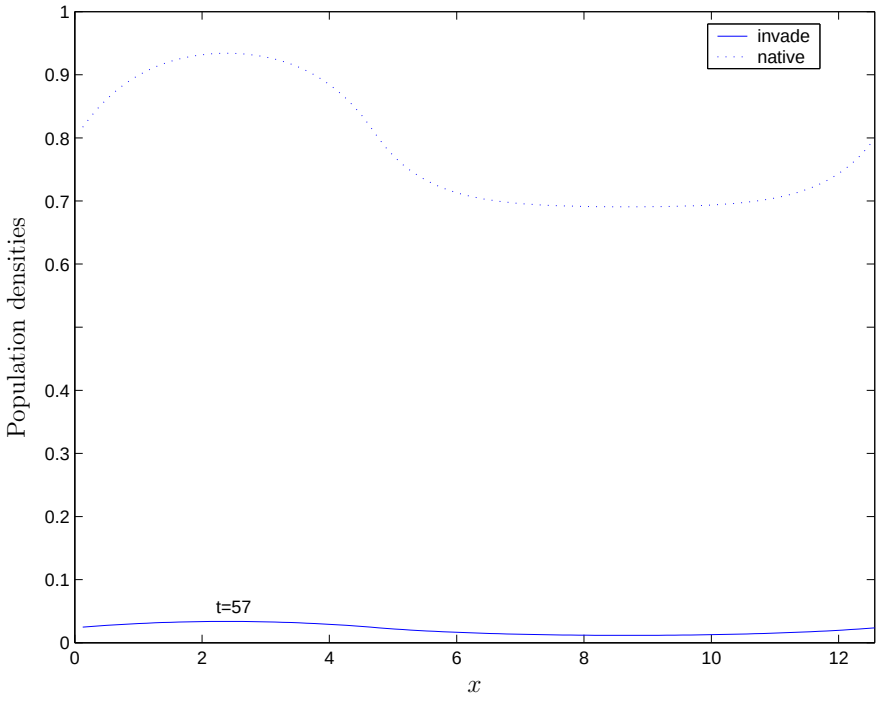

(b) Numerical approximation of species population densities when the type 2 environment has length $\ell_1 = 4.7$.

Figure 5.20: Numerical approximations of the solution to the system (5.3)–(5.4), with periodic boundary conditions, for parameters as in Example 5.9.

is introduced by quantifying when a population has "reached" a population equilibrium. The time at which an invading species introduced as a small initial population "reaches" a steady state is said to be the *invasion time*.

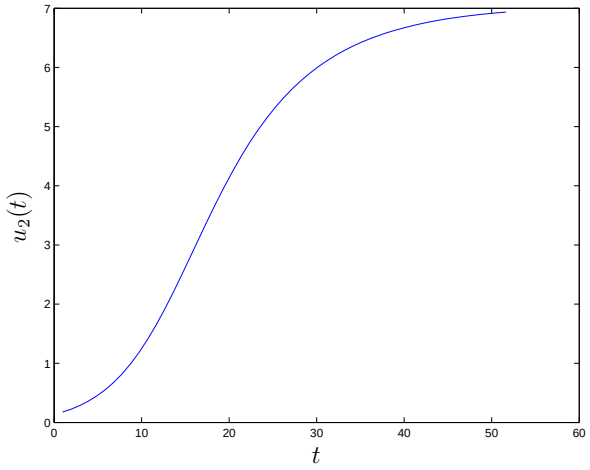

(a) The total population, with respect to time, on one period of the environment.

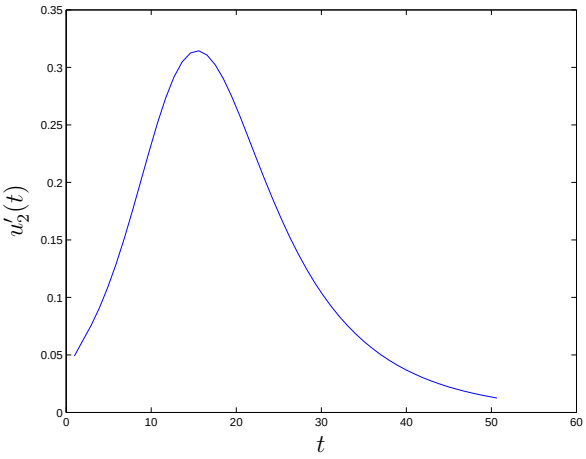

(b) The rate of population growth, with respect to time, on one period of the environment.

Figure 5.21: Numerical approximations of $u_2(t)$ and $u_2'(t)$ of the solution of the system (5.3)–(5.4) with parameters as in Example 5.4.

Toward a sensible and useful mathematical definition of invasion time consider that the steady state, which may be a coexistent or a one-species dominant state, is not a known function. The steady state can, however, be approximated numerically by means of the methods of Chapter 4.

Let

$$u_i(t) = \int_R n_i(x,t)\,\mathrm{d}x$$

denote the total population of species i at time t in the environment R. The total population size with respect to time of the invading species considered in Example 5.4 is plotted in Figure 5.21(a). The invading population invades successfully and increases to a relatively high density at a coexistent steady state. Figure 5.21(b) shows the rate of population growth as numerically approximated by means of the finite difference $u'(t_j) \approx (u(t_j) - u(t_{j-1}))/\mathrm{d}t$. From Figure 5.21(b) it follows that the population size growth slows down as the population approaches the steady state. This observation will be incorporated into the definition of invasion time.

However, a steady state may well be a limit state, in which case the population may continue to grow yet never reach the steady state. Thus, quantifying when the population is sufficiently close to a steady state is inherently arbitrary. In this respect defining invasion time only in terms of population growth rate is unsatisfactory, since a population with little variance in its population growth rate may grow very slowly yet still be far from a population equilibrium.

Figure 5.22(a) shows the total population size, on one period of the environment, of the invading species considered in Example 5.6 when the favourable environment is of length $\ell_1 = 0.994\,421\pi$. For comparison purposes, see Figure 5.16, which represents the

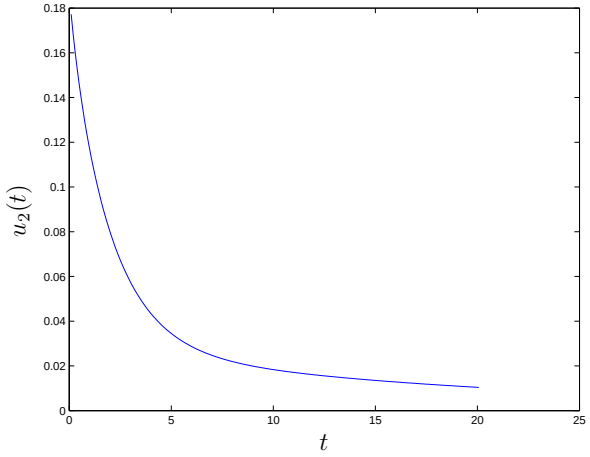

(a) The total population, with respect to time, on one period of the environment.

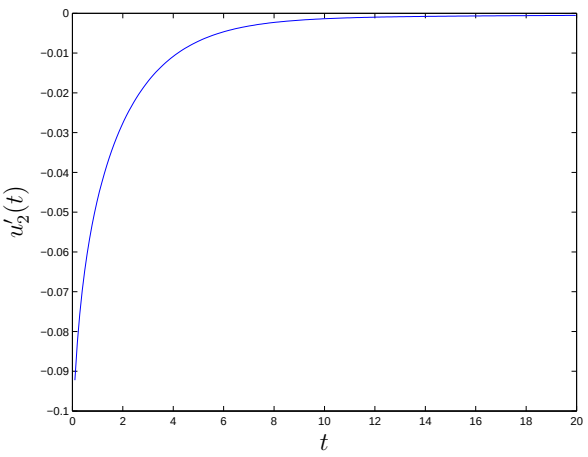

(b) The rate of population growth, with respect to time, on one period of the environment.

Figure 5.22: Numerical approximations of $u_2(t)$ and $u_2'(t)$ of the solutions of the system (5.3)–(5.4) with parameters as in Example 5.6. The length of the type 1 environment is $\ell_1 = 0.994\,421\pi$.

population densities of the invading species. It follows from Figure 5.16 that the invading species is not successful, since the population density tends to zero everywhere. Figure 5.22(b) represents the rate of population growth, which remains negative, although the decline does slow down. Since it is assumed that the initial population of the invading species is small, even if the population were to reach a steady state at a population volume below the initial population volume, such a small population will not be considered a successfully invading population. Because of the assumption that the initial population is small, a time t can only be the invasion time if the rate of population growth is positive at t.

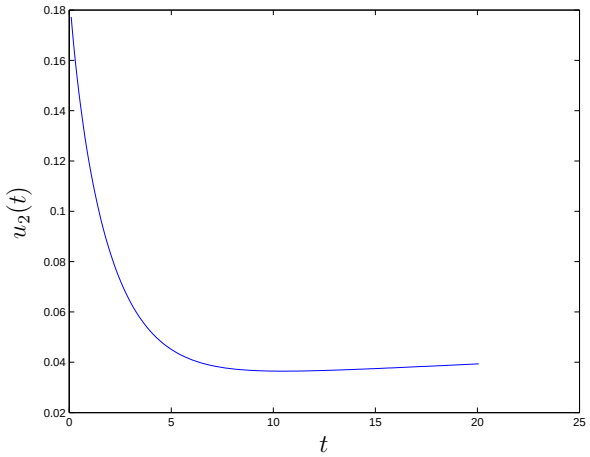

(a) The total population, with respect to time, on one period of the environment.

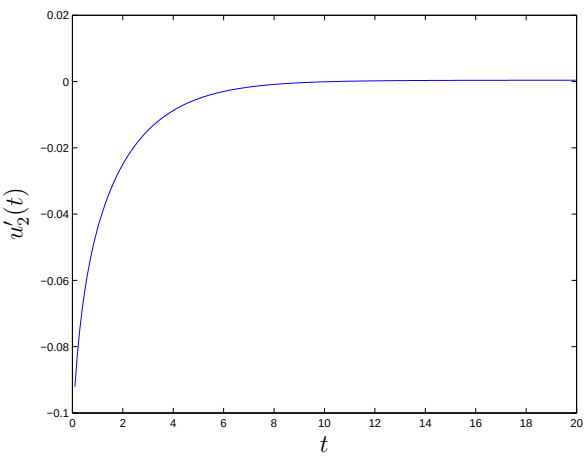

(b) The rate of population growth, with respect to time, on one period of the environment.

Figure 5.23: Numerical approximations of $u_2(t)$ and $u_2'(t)$ of the solutions of the system (5.3)–(5.4) with parameters as in Example 5.6. The length of the type 1 environment is $\ell_1 = 1.121\,740\pi$.

Figure 5.23(a) shows the total population size, on one period of the environment, of the invading species considered in Example 5.6 when the favourable environment is of length $\ell_1 = 1.121\,740\pi$. Figures 5.23(a) and 5.23(b) demonstrate the situation where the population volume first declines as the population decreases faster in the unfavourable environment than it increases in the favourable environment and then increases again when the population density growth rate in the favourable environment becomes larger. That is, the population growth becomes positive at some time t_0 after the introduction of the initial invading population.

For the definition of invasion time, set $t_0 = 0$ by shifting the time axis. Let the invasion time of an invading species be the smallest time t at which the instantaneous rate of change of the total population of the invading species is such that if that rate of population change were maintained for the interval of time $(t, 2t)$ the total population would have changed by less than a fraction c of the change in population in the interval $(0, t)$. The arbitrary designation of c is introduced due to the steady state being a limit state, as discussed above. A species that fails to invade is assigned an invasion time $t_i = \infty$.

Definition 5.1 (Invasion Time) *Invasion time is the smallest time t_i such that*

$$t_i \frac{\mathrm{d}u_2}{\mathrm{d}t}(t_i) \leq c\,(u_2(t_i) - u_2(0))$$

and $\frac{\mathrm{d}u_2}{\mathrm{d}t}(t) > 0$ *for* $0 < t \leq t_i$. ■

By approximating the derivative $u_2'(t)$ by means of numerical methods, such as those discussed in Chapter 4, invasion time may be determined by numerical computation. The magnitude of invasion time for a species in a specific competition system may be regarded as a measure of the dominance of the invading population in its niche compared to other similar species in similar systems.

5.5 Chapter Summary

In this chapter a linear stability analysis was performed for the model of two competing species derived in Chapter 2. The model was non-dimensionalised (§5.1) and then linearized about the steady state solution where the first species has reached a population equilibrium and the second species is absent (§5.2). Thereafter the stability of the population densities was analysed about this steady state with respect to small perturbations of the linearised model (§5.3). The situation represented by this scenario is that of a small population of an invading species introduced into a habitat containing an already established native species. The question answered by the stability analysis is whether or not the introduced species will successfully invade the habitat.

The linear stability analysis was performed for three successively more complex scenarios. In the first case (§5.3.1) the habitat has finite length and the carrying capacity of the native species is constant on the entire habitat. In the second case (§5.3.2) the habitat is periodic, but the carrying capacity of the native species is still constant on the entire habitat. In the final case (§5.3.3) the habitat is periodic and the carrying capacity of the native species is a two-toned function.

The results emanating from the analysis of the first two scenarios are necessary and sufficient conditions for successful invasion of small initial populations. However, the result of the analysis of the third scenario is only a sufficient condition for successful invasion. This linear stability analysis was performed in fulfilment of Objective VI in § 1.3. Also, instances of the model were solved in this chapter via the numerical techniques derived in Chapter 4, in order to verify the results of the linear stability analysis.

Finally the notion of invasion time was established and motivated as a measure of the dominance of the invading population in its niche compared to other similar species in similar systems (§5.4), in fulfilment of Objective VII in § 1.3.

Chapter 6

Case Study: Barley

A barley field.

In this chapter the model derived in Chapter 2 is instantiated with parameter values derived from real data with respect to two cultivars of *barley* with discriminating traits. In particular, the yield of the one cultivar is less influenced by drought than that of the other cultivar. The competing species in the model represent these two cultivars in an environment characterised by varying water availability. The linear stability analysis of Chapter 5 is then applied to the instance of the model, in fulfilment of Objective VII. The scenario of two competing species in a heterogeneous environment, as represented by the model, nonetheless remains hypothetical in the sense that the results gained from the model are not tested against real data gained from observation of a heterogeneous environment.

6.1 Introduction

Cultivating of barley has been traced back to the earliest remains of agricultural activity about 10 000 years ago [39]. Only a few other species, such as *einkorn*, *emmer wheat* and *lentils*, accompanied barley in the transitional phase from preferential reaping of wild plants to purposely performed cultivation [93]. The four main types of cultivated barley, namely, *hulled* versus *naked kernels* and *two-row* versus *six-row* ear types, appeared during the early phases of plant cultivation when agriculture was confined to the fertile crescent region incorporating the *Levant*, *Ancient Mesopotamia*, and *Ancient Egypt* [93]. However, the two-row ear types of hulled kernels dominated the early forms of cultivated barley and often represent larger percentages of archaeological remains than either einkorn or emmer wheat.

Already during the sixth and fifth millennium BC cultivated barley, together with einkorn, emmer wheat and weedy forms of wild barley, spread to the Aegean and consequently the eastern part of the Mediterranean Basin [93]. Remains of cultivated barley from Egypt and the Nile delta date back to the fifth millennium BC. From Egypt cultivated barley spread to Ethiopia. However, Ethiopia is considered the secondary centre of genetic diversity of barley. Perhaps this is as a result of the diverse range of ecological conditions under which barley was cultivated en route to Ethiopia [50].

Remains of cultivated barley indicate that an old world type of agriculture was practised in the highlands of the Indian subcontinent during the fifth millennium BC [11]. Cultivated barley reached central and northern Europe during the third millennium BC and China during the second half of the second millennium BC [40].

During the earliest phases of agricultural activity barley occurred as a large percentage of all cultivated crops. A characteristic change during the later phases is associated with a preference for wheat. The exceptions, where barley occupied the prime position, were mainly at locations characterised by less favourable growing conditions. Hulled barleys are more tolerant of nutritional depletion of cultivated soils and also salinity [93]. It is for this reason that during the fourth Millennium BC the largest part of agricultural activity involved growing barley in the Mesopotamian basin [93].

Currently barley assumes the fourth place, after wheat, rice and maize, in the world's total cereal acreage [40]. And even though barley cultivation is more tolerant of poor environmental conditions, its importance as a food for human nutrition has diminished since ancient times. The main use of barley today is as animal feed. The second largest use of barley is malting barley for brewing purposes [79].

The use of barley in the production of fermented beverages probably originated between 3 000 and 5 000 years BC. There is some archaeological evidence originating from barley grain found in Egypt suggesting selective breeding for malting [67]. Until the nineteenth century AD selection within locally adapted barley was the only practised method of improvement. Selection was largely based on physical appearance of the grain; plump, well-filled grains with fine husk were favoured. Although certain geographical areas became renowned for the brewing quality of their local barley, it was not until the 1930s that crosses were made between barley types of different areas [56].

Laboratory malting systems that mimic the commercial process were first designed toward the end of the nineteenth century. As breeding programmes began to evolve, laboratory malting became a means of progeny evaluation. However, even laboratory malting re-

quired large quantities of grain which meant laboratory malting was viable only during the later stages of the breeding programmes.

Breeders have many objectives besides malting quality. For example, yield and disease resistance are also important objectives pursued in breeding programmes. Some of the desirable characteristics are controlled by single dominant genes, and others by multiple genes. Selection for characteristics that were easy to observe sometimes led to inadvertent selection of closely linked characteristics. An example of this was the selection for mildew and brown rust resistance that led to the production of cultivars that were high yielding, but not suitable for malting [82].

Malting quality derives from the complex interactions of a wide range of characteristics. However, the four main aspects of the malting process are the *hormone control system*, the *production of certain enzymes*, the *substrate of starch, protein and cell walls within the endosperm*, and the *transport of soluble material to the embryo* [80]. Barley breeders are now able to exploit the knowledge gained about these factors so as to affect malting quality and to use DNA markers for selection of desired traits.

6.2 The Hypothetical Scenario

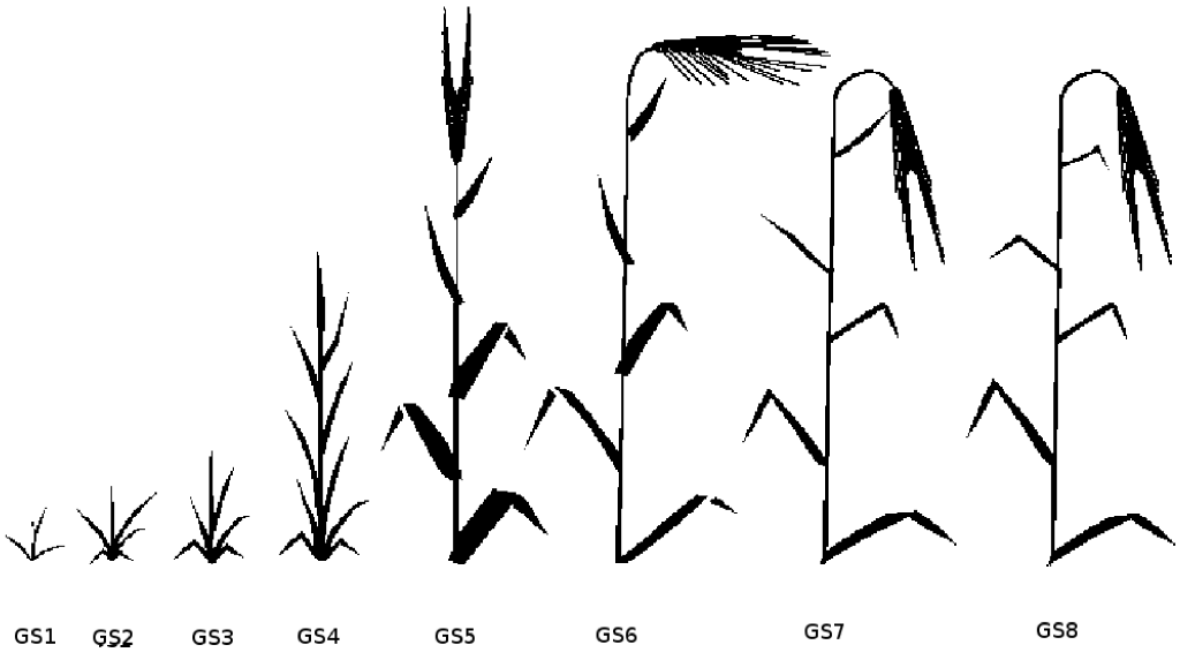

Figure 6.1: Growth stages — (GS1) seedling growth, (GS2) tillering, (GS3) stem elongation, (GS4) booting, (GS5) ear emergence, (GS6) flowering, (GS7) milk development and (GS8) Ripening.

Figure 6.1 shows the main growth stages of barley. These are *seedling growth*, *tillering*, *stem elongation*, *booting*, *ear emergence*, *flowering*, *milk development* and *ripening*. During seedling growth the first leaves develop. The second stage is tillering; this is when shoots other than the main shoot develop. Tillering is affected by temperature, water and nutrients and the number of shoots that develop have a large impact on yield. During stem elongation and booting much of the crop's green surface develops. The number of ears that emerge again greatly influences yield [41]. Development in each of these stages

affects the crop yield. The most important environmental factors affecting crop growth in each stage differs, ranging from adequate heat, sufficient soil nitrogen to enough moisture [79].

Whereas there are systems simulating barley growth that incorporate a wide range of factors affecting the development of barley at the different growth stages, the interest in this chapter is on a longer time scale. The primary concern is the competition between two cultivars and the influence of diffusion over many seasons. The parameters of the reaction-diffusion model derived in Chapter 2 have no direct relation to the availability or characteristics of the environment, nor to the impact of the species on the available resources. Population growth in the model is simply a function of overcrowding. To determine the population density when overcrowding occurs for a given species in a given environment, the species has to be observed in that specific environment. In some sense this dependence on overcrowding summarises the intricate dependencies of the growth of barley.

The hypothetical scenario modelled in this chapter is that of two cultivars competing for resources in a resource heterogeneous environment. The cultivars that are represented in the model differ in their response to drought. Once again the response of each cultivar to drought is more intricate than can be expressed by a simple dependence on overcrowding. Insufficient moisture at different stages of the development of the barley plant influences each cultivar differently [69]. However, ultimately, the response of a barley crop to a given rainfall pattern is evident in the crop yield.

Practically the scenario of a resource heterogeneous environment, where the important varying resource is water, may be created by watering some regions more than others. The environment in the model analysed in Chapter 5 is represented by a two-toned variation in carrying capacities of each of the two competing species. Creating such a two-toned environment amounts to selectively watering a field in lanes. The type 1 habitat of the model corresponds to the lanes that receive more water.

6.2.1 The Cultivars

The final crop yield per square metre comprises three components: the *number of ears* per square metre, the *number of grains* per ear and the *average grain weight*. The number of ears per square metre is the product of the *establishment* [1] of the sowed grains and the number of ears per plant. Of these three components, in general the average grain weight of a barley cultivar is the least influenced by adverse growing conditions.

The South African barley brewers institute registered the cultivar $SSG\,506$ in 1996. $SSG\,506$ is specifically a malting barley and was breed for malting and not an increased yield or drought resistance. In terms of the three components of crop yield the average grain weight of $SSG\,506$ is 46mg, the average number of grains per ear under favourable conditions is 16, establishment of 220 grains per square metre, under favourable conditions, is about 80% and each plant has an average of three ears [69]. Of the three components of yield the average number of grains per ear of $SSG\,506$ is most effected by drier conditions, and may be as low as 8. $SSG\,506$ is represented by the invading species in the model.

[1] The percentage of sowed grains that mature to barley plants is known as *establishment*.

		Year						
		2001	2002	2003	2004	2005	2006	mean
Clipper	Caledon			4 676	3 493	5 280	4 687	4 248
	Greyton	3 814	3 930	2 942	3 535	4 406	4 782	3 902
*SSG*506	Caledon			4 534	3 730	4 980	4 687	4 483
	Greyton	3 261	3 596	2 859	3 692	4 013	4 308	3 622

Table 6.1: Kilograms of grain yield per hectare per year [69].

The other species in the model, the native species, represents the sub-saharan cultivar *Clipper*. Clipper is characteristically less influenced by drought, which makes it a successful cultivar in drier regions. The average grain weight of *Clipper* is 38mg in a favourable environment, its grain per ear ratio in a favourable environment is 20, establishment of 220 grains per square metre, under favourable conditions, is also about 80% and each plant has an average of three ears. The average number of grains per ear of *Clipper* is relatively less effected by drier conditions than that of the corresponding number for *SSG*506. This number may be 12 in drier conditions for *Clipper* [69].

6.2.2 The Model Parameters

The parameters for modeling the two cultivars competing in a heterogeneous environment are the carrying capacity and the diffusion coefficient of each species in each of the type 1 and type 2 environments; the intrinsic growth rates and the competition coefficients of each species.

As mentioned, the difference between the cultivars *Clipper* and *SSG*506 is that the final grain yield of *Clipper* is less influenced by dry conditions. The carrying capacity of each species in each of the type 1 and type 2 environments is derived from data collected with respect to barley grain yield in a relatively wet district and a relatively dry district, respectively. It is supposed that selectively watering lanes of a field will reproduce in each lane of the field a carrying capacity comparable to either that of the wet district or the dry district. The other differences in environmental factors that would affect carrying capacity in the different districts are assumed to be small, since the districts chosen for this case study are in close geographical proximity. Moreover, it is assumed that whatever differences in environmental factors other than water availability there are between the districts is adequately levelled out by modern agricultural practices.

The data representing the type 1 environment were collected in the Caledon region of the South African Western Cape, and the data representing the type 2 environment was collected in the Greyton region of the South African Western Cape. The Caledon region receives approximately 900 millimetres of rain annually and the Greyton region approximately 350 millimetres of rain annually. The figures for Caledon were based on data collected at the hydrological stations at the Hawequas forest reserve and Elgin and those for Greyton on data collected at the hydrological station at Montagu [18]. The Caledon and Greyton regions are shown on the map in Figure 6.2.

The carrying capacities before non-dimensionalisation are measured in kilograms of barley grains per hectare. From Table 6.2.2 the average annual yield in kilograms per hectare of *Clipper* in the Caledon region is 4 248 kg, while for *SSG*506 this figure is 4 483 kg.

Also from Table 6.2.2 the average annual yield in kilograms per hectare of Clipper in the Greyton region is 3 902 kg, whilst for *SSG* 506 it is 3 622 kg. Upon non-dimensionalisation the carrying capacities in the model are $k_{11} = 1$, $k_{21} = 1$, $k_{12} = 0.918\,540$ and $k_{22} = 0.808\,875$.

Figure 6.2: Map of Caledon, Greyton and surrounding regions. Reproduced from [30].

The intrinsic growth rate of a species is the rate at which the species will increase under favourable conditions in the absence of overcrowding. Hence the logistic growth reaction component of the reaction-diffusion equation representing each species reduces to the Malthusian growth term [17, §2.2] for a constant x,

$$\frac{\mathrm{d}n}{\mathrm{d}t}(t,x) = rn(t,x). \tag{6.1}$$

If, at time $t = 0$, there were one barley plant, then the solution to (6.1) is e^{rt}. The number of plants at time $t = 1$ would be the number of barley grains produced by the one plant multiplied by the probability of establishment; denote this number by the constant c. Hence, $e^r = c$, and so $r = \ln c$. The growth rates in the dimensional system of equations are thus $r_1 = \ln(3 \times 20 \times 0.75) = \ln(45) = 3.806\,662$ for *Clipper* and $r_2 = ln(3 \times 16 \times 0.75) = \ln(36) = 3.583\,518$ for *SSG* 506. Thus the ratio used in the non-dimensional model is $r_2/r_1 = 0.941\,380$.

Since interest in barley is mainly as a cultivated, and hence sowed, crop the diffusion rate of barley is not a known parameter. However, in a population left to its own devices, barley grains are propagated once per growing season and very much in the vicinity of the seeding, since the grains are too large to be carried by wind. In the absence of flooding or insect propagation, barley spreads on a long time scale. In the subsequent analysis the sensitivity of the results of the analysis to the diffusion coefficients is tested at two different scales — small and large diffusion. In the dimensional environment these correspond to diffusion coefficients in the order of respectively 10^0 metres and 10^1metres. Moreover,

the diffusion coefficients of both species should be very similar, and, if a large diffusion coefficient is as a result of water propagation, then the diffusion coefficients may be larger in the type 1 environment than in the type 2 environment.

The competition coefficients hold no direct relation to the resources in the environment or to a species' resource utilization. Instead the competition coefficients are specific to the competition system they describe. However, the competition coefficients for competition between the two barley cultivars has not been established empirically. In the subsequent analysis the sensitivity of the results of the analysis to a range of values for the competition coefficients are tested. The biological interpretation of the competition coefficients is that every unit of population of species i uses a factor of β_{ij} times the amount of shared resources that a unit of population of species j uses. Since the two cultivars of barley considered are still fairly similar it is expected that neither competition coefficient will be too far from unity.

6.2.3 The Analysis

In §5.3.3 a sufficient condition for successful invasion of a small invading population was derived for the model of two competing species in a two-toned environment. The governing system of equations of the model is (5.3)–(5.4) and the boundary values of the model determine a periodic domain. In this section the sufficient condition is computed for parameters as derived in §6.2.2. Moreover, the sufficient condition is compared with numerically computed solutions of the model.

The periodic boundary conditions of the model more properly represent the physical situation where the environment considered is, for instance, the shoreline of an island. The periodic environment represented by the model with periodic boundary conditions is not exactly the same as the physical reality of a field with periodically repeated environmental conditions for which the model is used in this chapter. The situation represented by the model is that of the physical case taken to the limit. That is, the model represents the situation of an adjacent type 1 and type 2 environment repeated an infinite number of times. In the physical environment on either side of an arbitrary lane there would always have to be more lanes of the alternate type, thus there would be no final lane of the field. A realistic physical environment may consist of only a finite number of repetitions of the period of the environment.

Moreover, the initial invading population represented by the initial conditions of the periodic model is that of a spatially periodic initial population. Thus, instead of a single location of invasion on the repeated environment, the invading population initially invades in every period of the environment. However, by Assumption 5 of §2.2.2, the model evolves locally. Thus, whether or not the invading population will survive in a physically realistic environment with finite repetition is sufficiently closely related with whether or not the modelled invading population survives in the truly periodic situation so as to draw conclusions in the one situation from results in the other situation.

The invading population density function which, as mentioned above, represents an invasion repeated in every period of the environment as opposed to an invasion at a single location, is chosen to be a Gaussian function. The reason for choosing a Gaussian function to represent the initial invading population density is that it can approximate a function with compact support very well. That is, it can represent a population density function

with high density in the neighbourhood of a point and a very low density away from the point, as is the case when an invasion spreads from a confined region of the environment. Furthermore, what distinguishes the Gaussian function above other choices is that it is sufficiently smooth, and may thus be well represented by the band limited interpolating function used to compute numerical solutions to the model (see §4.2).

A ten hectare (approximately 300 metres by 350 metres) barley field is of realistic size [76, 1, 29]. If the field were divided into 20 lanes where each pair of adjacent type 1 and type 2 lanes constitute a period of the environment then the length ℓ of a period of the environment is approximately 30 meters.

In the nondimensional equations of §5.1 the supremum of the diffusion coefficient of the invading species is normalized to unity. From these equations it follows that the length of a period of the environment only influences the model in as much as the ratio of the diffusion coefficients to the length of the period changes. Hence, in the ensuing analysis the length of the environment is held constant, since the diffusion coefficients are tested at different orders of magnitude.

However, the ratio of the length of the favourable environment to the unfavourable environment, or similarly the ratio of the length of the favourable environment to the length of a period of the environment, does influence the nondimensional model and, in particular, the success or failure of the invading population. This is also evident from the sufficient condition derived in §5.3.3, where the sufficient condition is $S \geq 0$.

6.2.3.1 Linear Stability Analysis

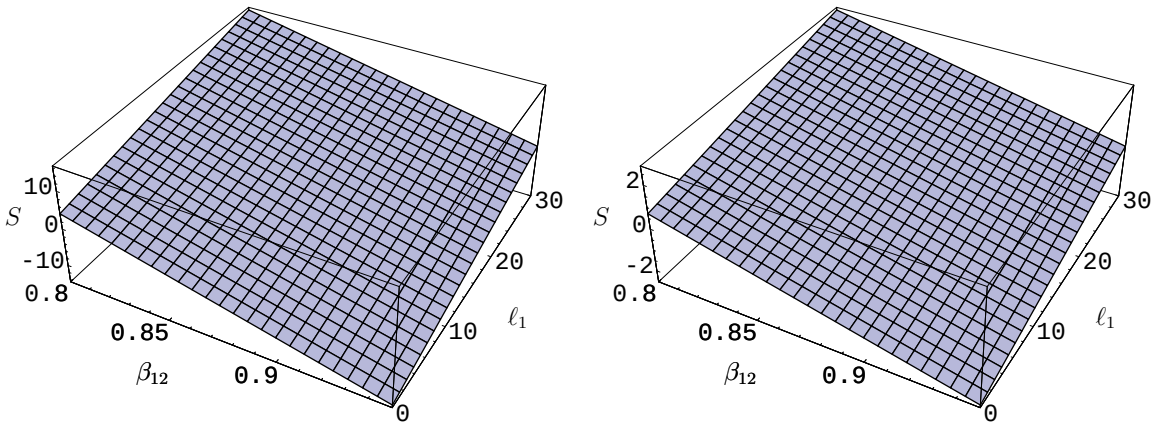

(a) S plotted with respect to the parameters β_{12} and ℓ_1 when the diffusion coefficient is 0.3 metres per season.

(b) S plotted with respect to the parameters β_{12} and ℓ_1 when the diffusion coefficient is 10 metres per season.

Figure 6.3: A three dimensional plot of S as defined in §5.3.3.

The sufficient condition $S \geq 0$ is now used to determine parameter ranges for which the invading cultivar, *SSG*506, persists. Notice that S in the sufficient condition does not depend on the competitive effect, β_{21}, of *SSG*506 on *Clipper*, nor on the nondimensional intrinsic growth rate r. The graphs in Figure 6.3 are of the value of S, for the model with diffusion constants of 0.3 metres per season in Figure 6.3(a) and 10 metres per season

in Figure 6.3(b), over the length of the favourable environment, which is in the interval $[0, \ell]$, and the competition coefficient β_{12}. The plots of S for small and large diffusion are very similar in form and differ only in the angle of the slant of the surface. The parameter values for which S is zero are very similar for both small and large diffusion. The next figure demonstrates this for a fixed value of β_{12}.

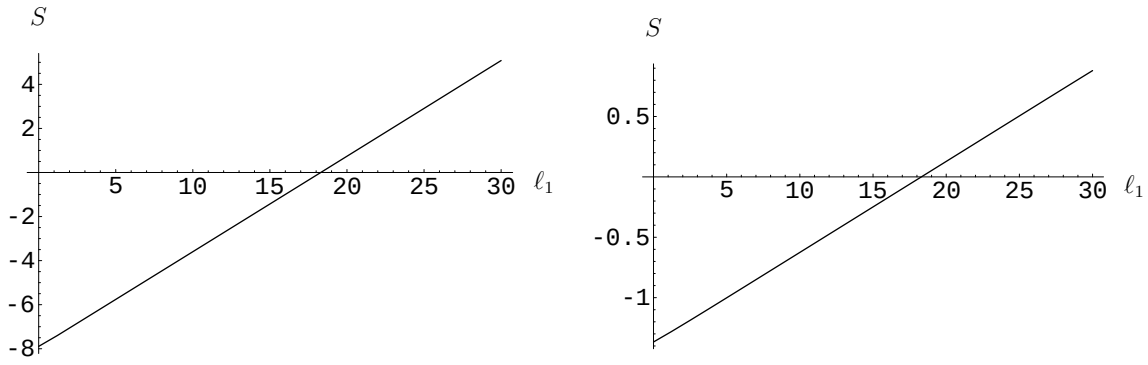

(a) Value of S with respect to ℓ_1 when the diffusion coefficient is 0.3 metres per season.

(b) Value of S with respect to ℓ_1 when the diffusion coefficient is 10 metres per season.

Figure 6.4: A plot of S with respect to ℓ_1 for $\beta_{12} = 0.9$ fixed.

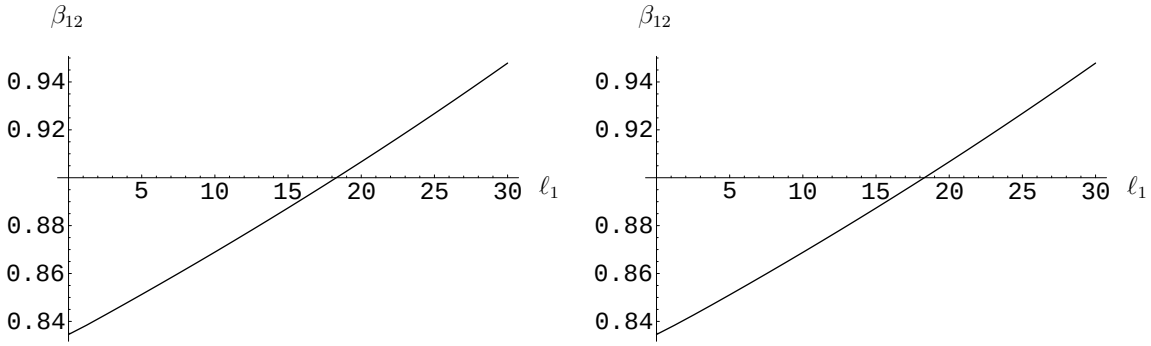

(a) Value of β_{12} with respect to ℓ_1 for which $S = 0$ when the diffusion coefficient is 0.3 metres per season.

(b) Value of β_{12} with respect to ℓ_1 for which $S = 0$ when the diffusion coefficient is 10 metres per season.

Figure 6.5: Critical values of the parameters β_{12} and ℓ_1 such that $S = 0$.

The behaviour of S for the parameter $\beta_{12} = 0.9$ when diffusion is small or large is shown in Figures 6.4(a) and 6.4(b) respectively. The parameter ℓ_1 still ranges over the interval $[0, \ell]$. From these figures it follows that, for both small and large diffusion coefficients, the invading $SSG506$ population will persist when the favourable environment is of length $\ell_1 \geq 18$.

It is only the parameter values for which $S \geq 0$ that are of importance when one considers the question of persistence of $SSG506$. Moreover, the value of S is either monotone increasing or monotone decreasing for respectively an increase in ℓ_1 or β_{12}, and hence the parameter values for which $S = 0$ are critical in that they form a divide in the parameter space. On the one side of the divide $SSG506$ persists and on the other side invasion fails.

Plots of this divide for small and large diffusion are shown in Figures 6.5(a) and 6.5(b) respectively. As noted above, the location of this divide is very similar in both cases. For parameter values (ℓ_1, β_{12}) below the line in these figures the $SSG506$ population persists. It also follows from these figures that the values 0.835 and 0.950 are critical values of the competition coefficient β_{12}. If β_{12} is larger than 0.950, then the sufficient condition does not indicate a successful invasion. However, if β_{12} is smaller than 0.835 then $SSG506$ persists.

6.2.3.2 Numerical Analysis

The aim of the following analysis is to verify numerically the results obtained by means of the sufficient condition. Figure 6.6 shows perturbation approximations, for small and large diffusion, to the steady state solution of *Clipper* in the absence of the competitor $SSG506$, where $\ell_1 = 20$ metres. These perturbation approximations compare well with the numerically calculated steady state solutions of *Clipper* in the absence of $SSG506$ which are plotted as the dashed lines in Figures 6.7(a) and 6.7(b).

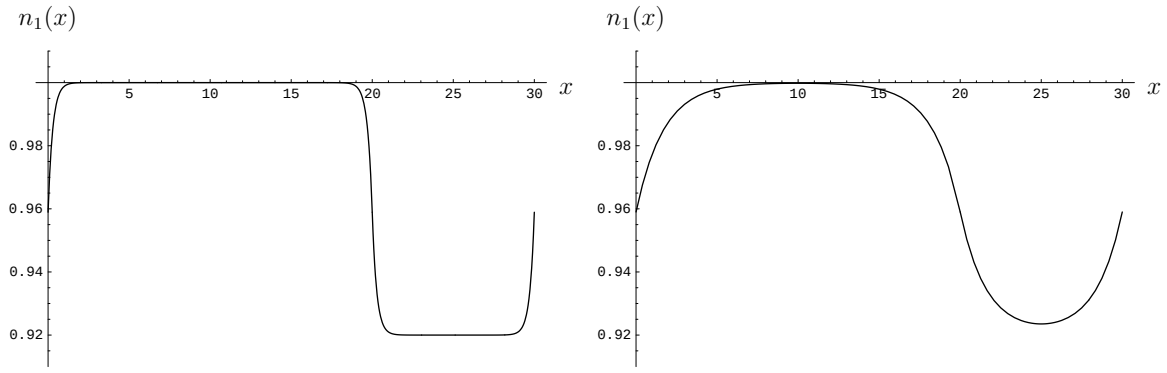

(a) Perturbation approximation when the diffusion coefficient is 0.3 metres per season.

(b) Perturbation approximation when the diffusion coefficient is 10 metres per season.

Figure 6.6: Perturbation approximations of the steady state population density of *Clipper* in the absence of $SSG506$.

The population densities of $SSG506$ are plotted in Figures 6.7(a) and 6.7(b) at a number of discrete points, equally spaced in time, where $\beta_{12} = 0.9$, $\beta_{21} = 0.95$, and $\ell_1 = 20$ metres. Because of the sufficient condition interpreted from Figure 6.5, $SSG506$ persists for these parameter values, as expected. By the definition of invasion time in §5.4, *Clipper* and $SSG506$ reach coexistent population steady states around times $t = 71$ and $t = 79$ with respectively a small and a large diffusion coefficient. The population densities of *Clipper* and $SSG506$ are plotted with respect to time and space in Figure 6.8 when the diffusion coefficient in the model is small and when it is large, respectively.

The following figures are numerically computed results that are similar and comparable to the plots of Figure 6.5. That is, they are plots of numerically determined critical parameter values. However, the sufficient condition plotted in Figure 6.5 depends only on the diffusion coefficient, β_{12} and ℓ_1. The parameters that are not fixed for the model also include β_{21}. Thus an extra dimension is added. Figures 6.9(a) and 6.9(b) are dividing surfaces, similar to the dividing lines of Figure 6.5, for respectively small and large diffusion. The points above the dividing surface in the parameter space $(\beta_{12}, \beta_{21}, \ell_1/\ell)$

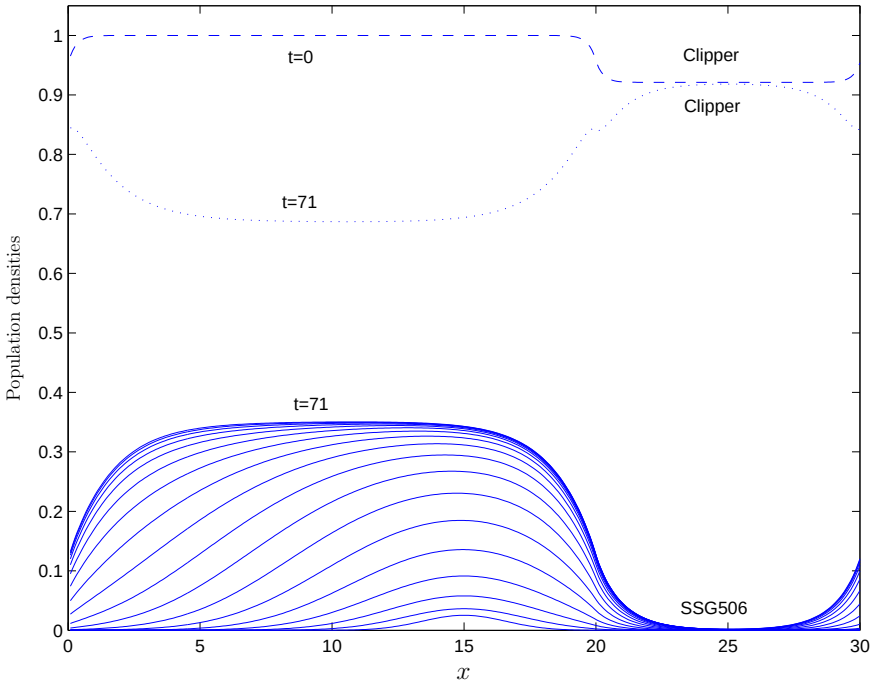

(a) Plots of the population density functions at discrete times on the interval $(0, 71)$ when the diffusion coefficient in the model is 0.3 metres per season.

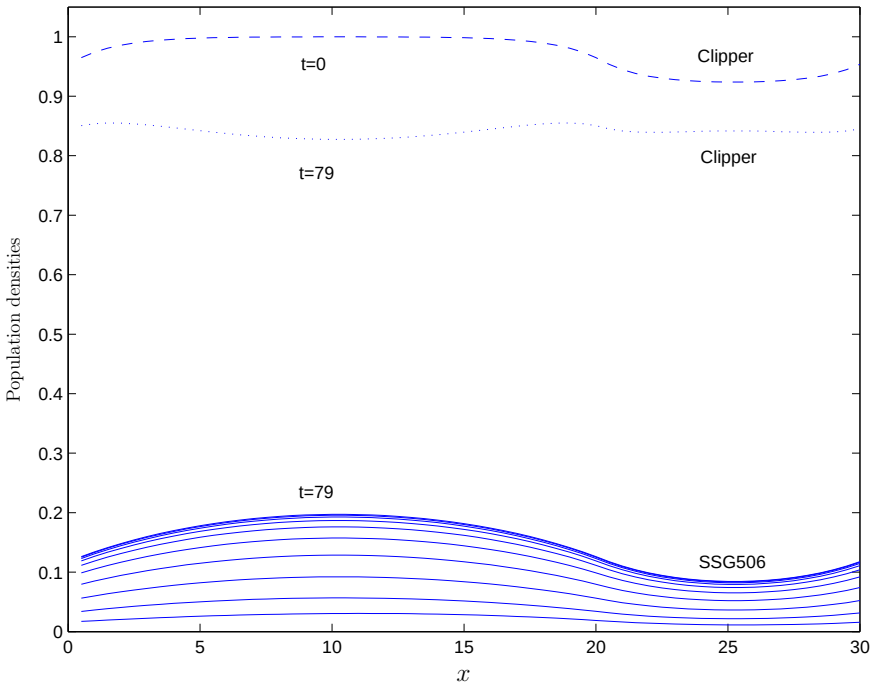

(b) Plots of the population density functions at discrete times on the interval $(0, 79)$ when the diffusion coefficient in the model is 10 metres per season.

Figure 6.7: Plots of the population densities at discrete times, where $\ell_1 = 20$ meters, $\beta_{12} = 0.9$ and $\beta_{21} = 0.95$.

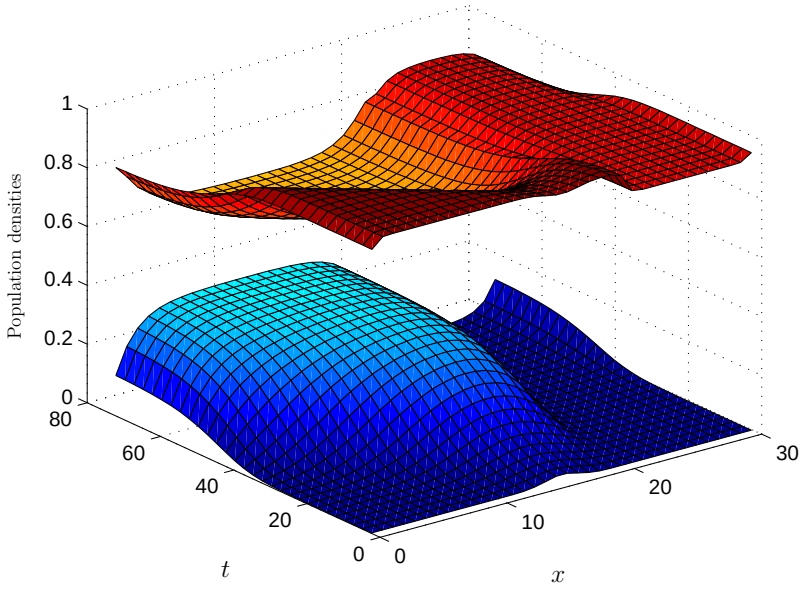

(a) A plot of the population density functions of *Clipper* and *SSG* 506 with respect to time when the diffusion coefficient in the model is 0.3 metres per season. The upper surface represents the population density of *Clipper* and the lower surface the population density of *SSG* 506.

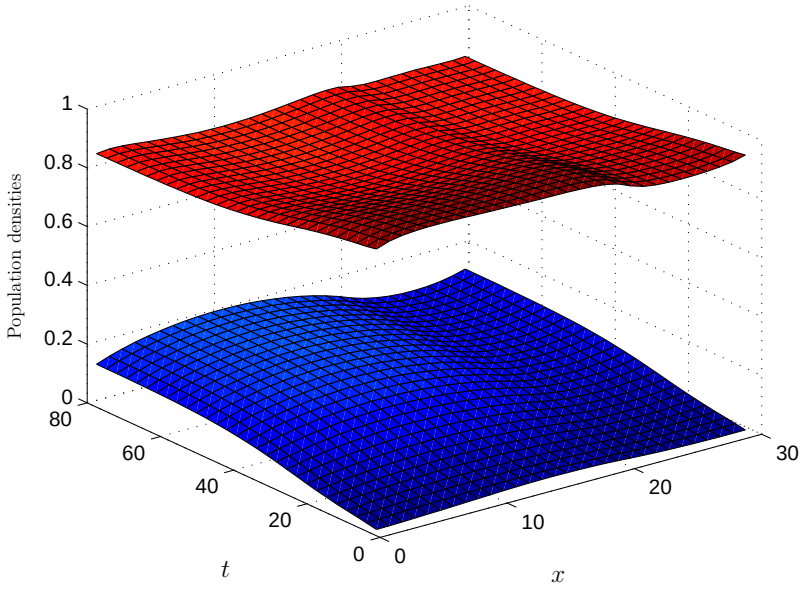

(b) A plot of the population density functions of *Clipper* and *SSG* 506 with respect to time when the diffusion coefficient in the model is 10 metres per season. The upper surface represents the population density of *Clipper* and the lower surface the population density of *SSG* 506.

Figure 6.8: Plots of the population density functions with respect to time when $\ell_1 = 20$ meters, $\beta_{12} = 0.9$ and $\beta_{21} = 0.95$.

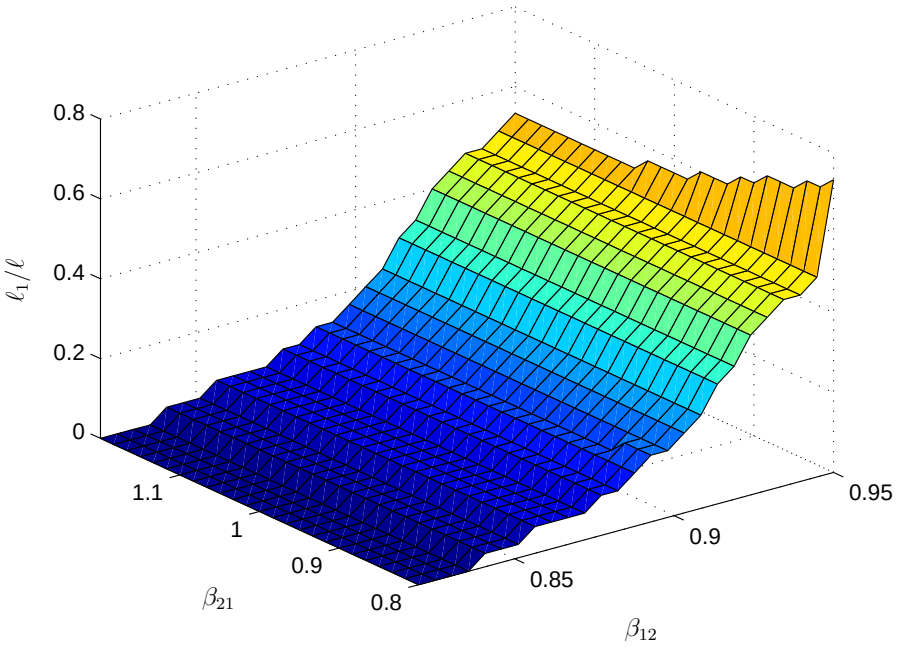

(a) Numerically computed surfaces of critical parameter values when the diffusion coefficient in the model is 0.3 metres per season.

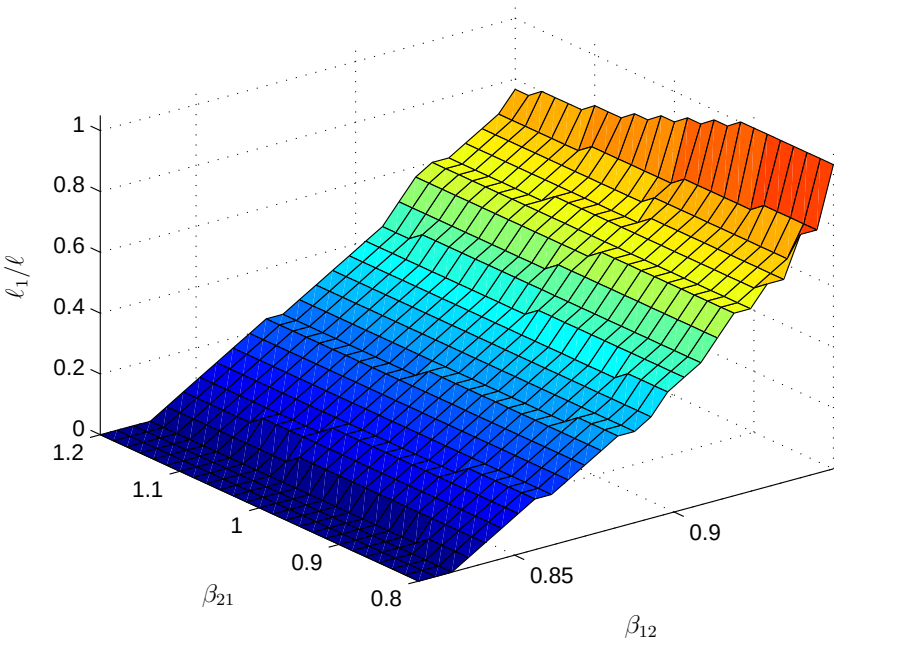

(b) Numerically computed surfaces of critical parameter values when the diffusion coefficient in the model is 10 metres per season.

Figure 6.9: Numerically computed surfaces of critical parameter values in the parameter space $(\beta_{12}, \beta_{21}, \ell_1)$. Points above the dividing surface represent parameter values for which $SSG\,506$ invades successfully and points below represent parameter values for which $SSG\,506$ does not invade successfully.

represent parameter values for which $SSG506$ invades successfully and points below represent parameter values for which $SSG506$ does not invade successfully. From these figures it follows, as it does from the linear stability analysis, that invasion success is not influenced much by the parameter β_{21}. Moreover, in the plane where β_{21} is fixed, the plotted points are comparable to Figure 6.5 and are also approximately linear.

6.2.3.3 Invasion Time

Invasion time is defined in §5.4 as a measure of the dominance of a species in its niche relative to similar species. Here invasion time will be used to gauge the influence of varying the size of the competition coefficients and the diffusion coefficients in the model on the ability of $SSG506$ to invade. The constant c in the definition of invasion time (see Definition 5.1) is set to 0.05.

The definition of invasion time allows for the population size of the invading species to tend arbitrarily close to zero before it recovers to a population equilibrium. When computing invasion time numerically, as is done here, it is not practically viable to allow the invading population size to tend arbitrarily close to zero. Once the population size reaches one tenth the size of the initial invading population in the numerical computations the invading species is deemed to have failed to invade. This artificial restriction has the effect that some populations that would have recovered from a very small size will be assigned an infinite invasion time. However, these exceptional populations are those which grow slowly and hence would have had invasion times that approach infinity.

Invasion time, and the population size at invasion time, for $SSG506$ with respect to the parameter space (β_{12}, β_{21}) are shown in Figures 6.10 and 6.11 for each of a small and a large favourable environment, and a small and a large diffusion coefficient, respectively. That is, each value on a plotted surface represents the invasion time, or population size at invasion time, of $SSG506$ in the model with parameters as described by the corresponding point in 3-space at which the value is plotted. Points in the parameter space for which no values are plotted correspond to parameter values for which $SSG506$ exhibits an infinite invasion time (that is, parameter values for which $SSG506$ does not invade).

In general the trend is for invasion time to increase as β_{12} increases, as expected. Arguing heuristically, this seems reasonable, since stronger competition from *Clipper* should result in $SSG506$ having less resources to invest in growing its population. The exception is when the diffusion coefficient and the length of the favourable environment are both small. This case is plotted in Figure 6.10(a), which exhibits a temporary rapid decrease in invasion time for increasing β_{12}.

The trend for population size at invasion time is to decrease with increasing β_{12}. This is as expected, since *Clipper* as a stronger competitor will deplete more resources, leaving less resources for $SSG506$ to sustain its population.

Invasion time also increases as the value of β_{12} increases. This may seem counter intuitive, since, if $SSG506$ were a stronger competitor it would be expected to access more resources and hence its population should increase more quickly. However, understanding the behaviour exhibited in Figures 6.10(c) and 6.11(c) helps to explain this apparent incongruity. The increase in invasion time as the value of β_{21} increases is relatively small compared to the effect of an increase in the value of β_{12}. Furthermore, population size at invasion time also increases with increasing β_{21}, which is intuitively correct, since a

stronger competitor should be able to sustain a larger population. From Figures 6.10(d) and 6.11(d) it seems that the population size at invasion time reaches a maximum with respect to β_{21} at about $\beta_{21} = 1.05$ and $\beta_{21} = 1.1$ respectively, which is about the same value of β_{21} for which the corresponding invasion times start to decrease for increasing β_{21}. An explanation for this phenomenon may be that $SSG\,506$ as a better competitor manages to grow to a larger population equilibrium, which may conceivably take longer to reach. Once a maximum sustainable population size is reached a further increase in β_{21} results in $SSG\,506$ reaching this maximum population size more quickly.

6.3 Conclusion

The first question considered in this chapter was whether $SSG\,506$ persists in competition with *Clipper*, in a two-toned environment, when introduced as a small initial population. Since the competition coefficient of the model representing the competition between the cultivars of barley where not determined empirically a sensitivity analysis was performed for a range of values.

In Figure 6.5 the critical values of the competition coefficient β_{12} (that is, the relative effect of *Clipper* on $SSG\,506$) are plotted with respect to the minimum-length favourable environment for which $SSG\,506$ invades successfully. These critical values were obtained from a linear stability analysis and are only critical in a sufficiency sense. That is, if the competition coefficient β_{12} of the model is smaller than the critical value, then $SSG\,506$ does invade. The linear stability analysis indicates that β_{21} (that is, the relative competitive effect of $SSG\,506$ on *Clipper*) does not affect the persistence of $SSG\,506$. The range of critical values of β_{12}, corresponding to the range $\ell_1 \in (0, 30m)$ of the length of the favourable environment, is $\beta_{12} \in (0.835, 0.945)$.

The numerically computed plots in Figure 6.9 represent critical values in the parameter space $(\beta_{12}, \beta_{21}, \ell_1)$ for a small and a large diffusion coefficient. If the parameters in the model correspond to a point below the critical surface it follows that $SSG\,506$ does not successfully invade. From these plots it also follows that the value of β_{21} does not largely influence the persistence of $SSG\,506$. The range of values of β_{12} for which the model indicates that $SSG\,506$ invades successfully is very similar to the range of values determined by the linear stability analysis.

Figures 6.11 and 6.10 show invasion times for $SSG\,506$ corresponding to points in the parameter space $(\beta_{12}, \beta_{21}, \ell_1)$ for a small and a large diffusion coefficient, respectively. From these plots it follows that the time it takes $SSG\,506$ to establish an equilibrium population increases as either β_{12} or β_{21} increases. However, it follows that the value of β_{21} has a smaller effect on invasion time than the value of β_{12}.

		Small diffusion	Large diffusion
Persistence		282 min	162 min
Invasion Time	ℓ_1 small	43 min	11 min
	ℓ_1 large	182 min	22 min

Table 6.2: Run-times in minutes of the computations done to produce the plots in Figures 6.10, 6.11 and 6.9.

The numerically computed plots of Figure 6.9 that show the critical lengths of the

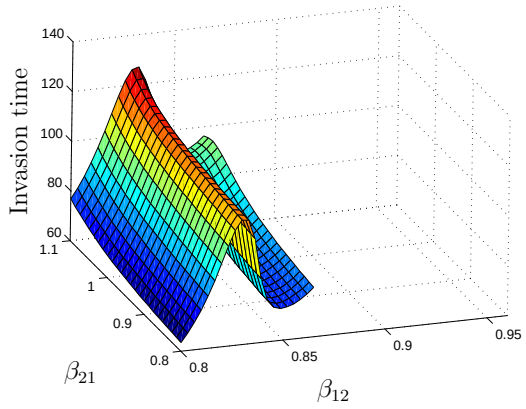

(a) Invasion time of *SSG* 506 as it varies with respect to β_{12} and β_{21}, where $\ell_1 = \frac{1}{4}\ell$ and the diffusion coefficient is 0.3 metres per season.

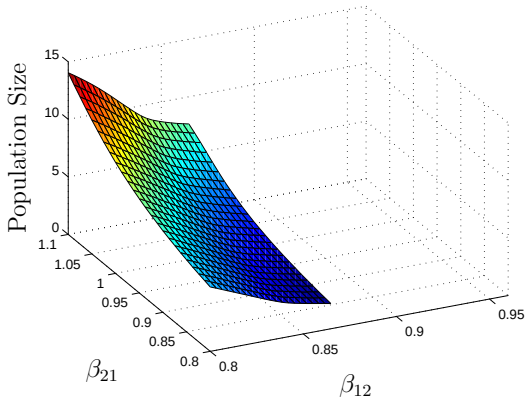

(b) Population size at invasion time of *SSG* 506 as it varies with respect to the model parameters β_{12} and β_{21}, where $\ell_1 = \frac{1}{4}\ell$ and the diffusion coefficient is 0.3 metres per season.

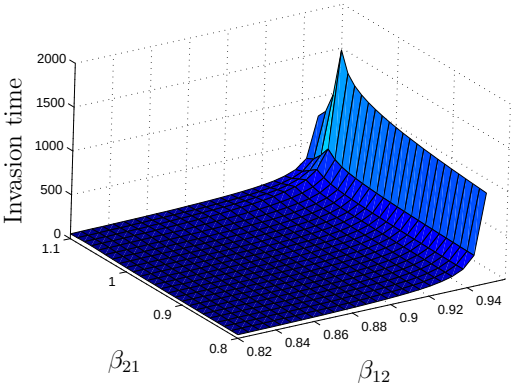

(c) Invasion time of *SSG* 506 as it varies with respect to β_{12} and β_{21}, where $\ell_1 = \frac{3}{4}\ell$ and the diffusion coefficient is 0.3 metres per season.

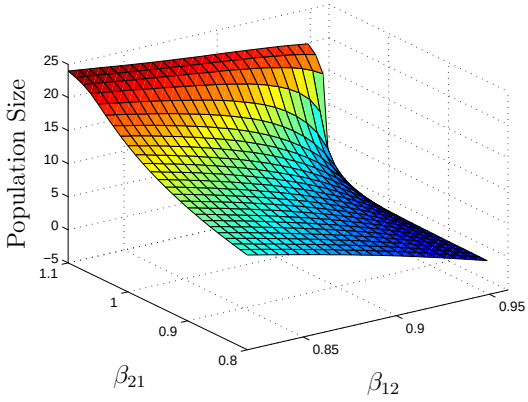

(d) Population size at invasion time of *SSG* 506 as it varies with respect to the model parameters β_{12} and β_{21}, where $\ell_1 = \frac{3}{4}\ell$ and the diffusion coefficient is 0.3 metres per season.

Figure 6.10: (a) and (c) represent the invasion time of *SSG* 506 as it varies with respect to the model parameters β_{12} and β_{21} when the length of the favourable environment is respectively one quarter and three quarters of the length of a single period of the environment and the diffusion coefficient of the model is 0.3 metres per season. (b) and (d) represent the population size at invasion time of *SSG* 506 as it varies with respect to the model parameters β_{12} and β_{21} when the length of the favourable environment is respectively one quarter and three quarters of the length of a single period of the environment.

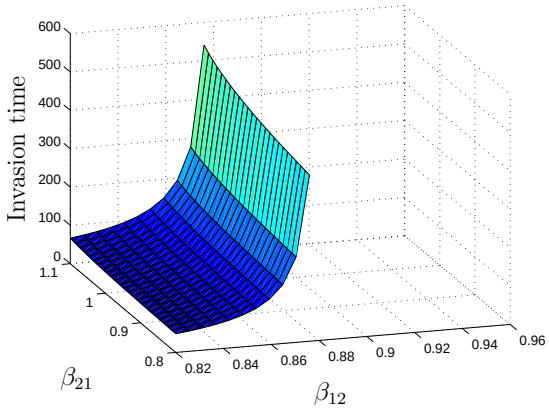

(a) Invasion time of $SSG\,506$ as it varies with respect to β_{12} and β_{21}, where $\ell_1 = \frac{1}{4}\ell$ and the diffusion coefficient is 10 metres per season.

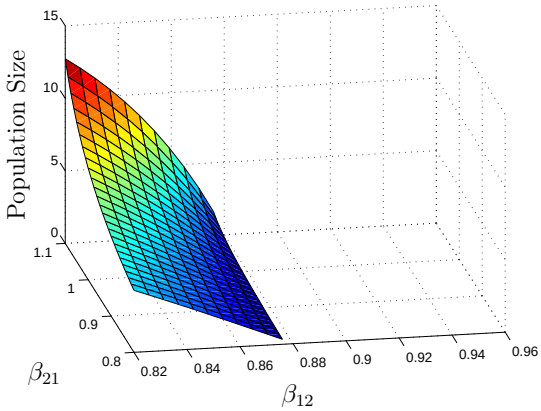

(b) Population size at invasion time of $SSG\,506$ as it varies with respect to the model parameters β_{12} and β_{21}, where $\ell_1 = \frac{1}{4}\ell$ and the diffusion coefficient is 10 metres per season.

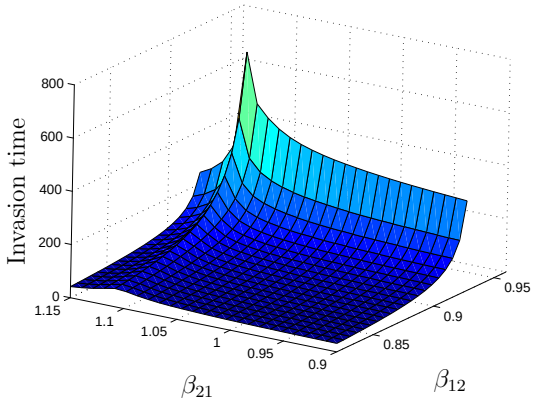

(c) Invasion time of $SSG\,506$ as it varies with respect to β_{12} and β_{21}, where $\ell_1 = \frac{3}{4}\ell$ and the diffusion coefficient is 10 metres per season.

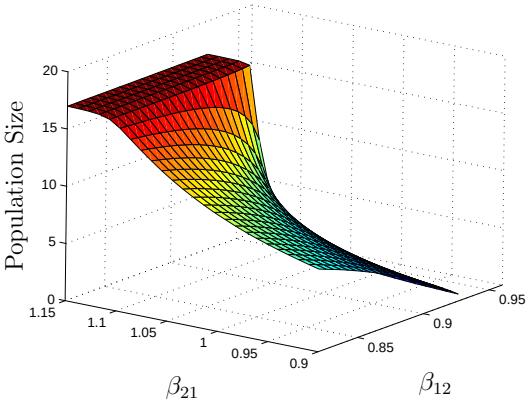

(d) Population size at invasion time of $SSG\,506$ as it varies with respect to the model parameters β_{12} and β_{21}, where $\ell_1 = \frac{3}{4}\ell$ and the diffusion coefficient is 10 metres per season.

Figure 6.11: (a) and (c) represent the invasion time of $SSG\,506$ as it varies with respect to the model parameters β_{12} and β_{21} when the length of the favourable environment is respectively one quarter and three quarters of the length of a single period of the environment and the diffusion coefficient of the model is 10 metres per season. (b) and (d) represent the population size at invasion time of $SSG\,506$ as it varies with respect to the model parameters β_{12} and β_{21} when the length of the favourable environment is respectively one quarter and three quarters of the length of a single period of the environment.

favourable environment, with respect to the parameters β_{12} and β_{21}, that ensure invasion by $SSG506$, as well as those of Figures 6.11 and 6.10 that show the invasion times with respect to the parameters (β_{12} and β_{21}), are on a 26 by 25 point grid. The computations were run on a 3GHz Intel Pentium with 496 MB of RAM. The run-times of the computations for each of these figures are compared in the Table 6.3. The computations at each point of the grid on the parameter space (β_{12}, β_{21}) involves finding numerical solutions of the model for corresponding parameters. In the case of a small diffusion coefficient the spatial discretization grid was finer than in the case of a large diffusion coefficient. A finer grid is needed to ensure stable computations. The increase in computation time of the plots when the diffusion coefficient is small can be ascribed to this increase in complexity.

Chapter 7

Conclusion

7.1 Thesis Summary

Population modelling and population projection have been important parts of demography and ecology since the pioneering contributions of John Graunt [32]. It was, however, the seminal work of Alfred J. Lotka (1880–1949) and Vito Volterra (1860–1940) in the 1920s and 1930s that provided the framework for competition studies in ecology.

In 1937 Fisher and Haldane incorporated spatially heterogeneous population densities into a single reaction-diffusion equation, where the term *reaction-diffusion* refers to the dual nature of the equations; the reaction part being that of a Lotka-Volterra model, and the diffusion part the elements describing the spatial distribution of the population. A system of equations coupled in their reaction parts representing population densities follow naturally from the Lotka-Volterra models. Moreover, extending Fisher's model, which only takes into account spatial variation in population density, to a model that also takes into account spatial variation of the habitat seems meaningful.

The purpose of this study was to describe in a mathematical sufficiency sense the realized niche of a species in a heterogeneous environment (although the heterogeneity of the environment is, in a sense, minimal). Of further interest is how easily a species invades. Specifically, if an invading population takes a long time to reach an equilibrium and the mean population density remains low, the population may well be susceptible to stochastic perturbation, which is only accounted for on average, in the deterministic model.

Thus the first problem considered in this thesis was whether a given species is able to invade a given environment where another species is already established. The next problem considered was quantifying how easily it does invade.

A mathematical model of coexisting biological species was derived by two methods in Chapter 2, in fulfilment of Objectives I and II in § 1.3. The first relied on the principle of Fickian diffusion (§2.1.1), whilst the second was based on certain assumptions with respect to the nature of the redistribution and reaction processes (§2.2). The mathematical model approximates a discrete population by a smooth density function, which introduces the vanishingly small possibility of individuals of the population moving at infinite speed. Moreover, the redistribution process is approximated by a diffusion process, which highlights the fact that the population dynamics are governed by local events. Both approximations were motivated by means of a central limit theorem (§A.3) and Taylor's

theorem (§A.2). After the mathematical model was extended to three spatial dimensions (§2.3), the problem considered in the remainder of the thesis was formally formulated (§2.4) in terms of the mathematical model derived in the preceding sections of Chapter 2.

Chapter 3 contains a concise survey of literature pertaining to models that describe populations by means of a coupled system of reaction-diffusion equations, in fulfilment of Objective III in § 1.3. In addition to providing background, this chapter placed the problem considered in this thesis within a broader mathematical context. Models describing the growth and decline of homogeneously distributed populations, and the relation of these models to the concept of a biological niche, were reviewed first (§3.1). Thereafter models describing the evolution of populations that are not assumed to be homogeneously distributed were reviewed (§3.2). Finally, models describing the evolution of populations in heterogeneous environments were reviewed (§3.3).

Numerical schemes used to approximate solutions to the initial-boundary value problems studied in this thesis were reviewed and motivated in Chapter 4. The first numerical method used was that of finite differences (§4.1). Finite differences employ local approximating polynomials which are differentiated to approximate derivatives. This method was applied to approximate solutions to initial-boundary value problems when the boundary values are described by zero-flux Neumann conditions, in fulfilment of part (a) of Objective IV in § 1.3. The second method used was that of spectral differences (§4.2). This method employs a basis of periodic functions on the grid to approximate periodic functions on an interval. These approximating grid functions are then differentiated to approximate derivatives of the functions on the interval. Spectral differences were employed to approximate solutions to initial-boundary value problems where periodicity of solutions is imposed, in fulfilment of part (b) of Objective IV in § 1.3. Both numerical schemes were shown to be consistent with the respective initial-boundary value problems (§4.3). Furthermore, conditions for the stability of each numerical scheme were derived. Finally, the finite difference scheme was shown to converge to the solution of the initial value problem with zero-flux Neumann boundary conditions.

A linear stability analysis was performed in Chapter 5 for the model of two competing species derived in Chapter 2. The model was non-dimensionalised (§5.1) and then linearized about the steady state solution where the first species has reached a population equilibrium and the second species is absent (§5.2). Thereafter the stability of the population densities was analysed about this steady state with respect to small perturbations of the linearised model (§5.3). The situation represented by this scenario is that of a small population of an invading species introduced into a habitat containing an already established native species. The question answered by the stability analysis is whether or not the introduced species will successfully invade the habitat. The linear stability analysis was performed for three successively more complex scenarios. In the first case (§5.3.1) the habitat has finite length and the carrying capacity of the native species is constant on the entire habitat. In the second case (§5.3.2) the habitat is periodic, but the carrying capacity of the native species is still constant on the entire habitat. In the final case (§5.3.3) the habitat is periodic and the carrying capacity of the native species is a two-toned function. The results emanating from the analysis of the first two scenarios are necessary and sufficient conditions for successful invasion of small initial populations. However, the result of the analysis of the third scenario is only a sufficient condition for successful invasion. This linear stability analysis was performed in fulfilment of Objective

VI in § 1.3. Also, instances of the model were solved in this chapter via the numerical techniques derived in Chapter 4, in order to verify the results of the linear stability analysis. Finally the notion of invasion time was established and motivated as a measure of the dominance of the invading population in its niche compared to other similar species in similar systems (§5.4), in fulfilment of Objective VII in § 1.3.

A case study was presented in Chapter 6, in fulfilment of Objective VIII in § 1.3. Instances of the model derived in Chapter 2 representing the competition between two cultivars of barley were considered in a hypothetical environment characterized by spatial varying water availability. The cultivar *Clipper*, which is the more drought-hardy cultivar, is represented as the native species, and *SSG*506, which is specifically a malt barley, is represented as the invading species. The question considered in Chapter 6 was whether *SSG*506 persists in competition with *Clipper*, in a two-toned environment, when introduced as a small initial population. Critical values of the competition coefficient β_{12} (that is, the relative effect of *Clipper* on *SSG*506) were obtained from a linear stability analysis (§6.2.3.1). The linear stability analysis indicated that β_{21} (that is, the relative competitive effect of *SSG*506 on *Clipper*) does not affect the persistence of *SSG*506. The range of critical values of β_{12} for which the model indicates that *SSG*506 invades successfully was also determined numerically (§6.2.3.2). Secondly, invasion time was investigated (§6.2.3.3). The computations of invasion time showed that the time it takes *SSG*506 to establish an equilibrium population increases if either β_{12} or β_{21} is increased. However, it followed that a change in value of β_{21} has a lesser effect on the invasion time than a change in value of β_{12}.

7.2 Future Work

As was mentioned above, the degree of heterogeneity of the environment considered is, in some sense, minimal. Even in the case where the native species' carrying capacity is a two-toned function, only a sufficient condition ensuring successful invasion was derived — as opposed to the necessary and sufficient condition derived in the case where this carrying capacity is constant.

An obvious direction for future work is to extend the analysis of §5.3 to cases where the carrying capacities and diffusion coefficients are more general functions than just two-toned functions. However, a more mundane and achievable aim would merely be to extend the sufficient condition derived in §5.3.3 to a necessary and sufficient condition by extending the methods of §5.3.2.

In the case where the native species' carrying capacity is no longer constant, as was assumed in §5.3.2, but two-toned, the steady state of the native species in the absence of competition is the spatially inhomogeneous solution to an elliptic boundary-value problem. In §5.3.3 this steady state solution was approximated by a perturbation solution. These perturbation solutions may be substituted into the model equations linearised about the native species dominant and invading species absent steady state. The resulting linearised equation, (5.5), governing the dynamics of the invading species is again independent of the native species population densities, as it was in §5.3.2. However, now the solutions of the associated Hill's equation, (5.6), involves Mathieu functions. Still, by [10, Theorem 7.8] periodic solutions do exist. The Δ-function of §5.3.2, which, by Floquet theory, describes the conditions for periodic solutions to Hill's equation to exist, has to be determined

by fixing the values of arbitrary constants in the solutions of Hill's equation so that the continuity conditions at the boundary between the type 1 and type 2 environments are satisfied. Fixing the values of these arbitrary constants will involve the manipulation of Mathieu functions.

Another avenue for future work is to further investigate the behaviour of invasion time and the influence of the various model parameters on it. As was seen in the results of the case study the behaviour of invasion time as a function of model parameters is sometimes counter intuitive. Explaining such unexpected results may lead to insight into the situation being modelled, or perhaps a better criterion for invasion success than invasion time.

References

[1] Abu-Alrub I, Joma A & Christianse JL, 2004, *Production methods and farming systems in major Barley (Hordeum Vulgare) growing regions of the West Bank, Palestine*, Experimental Agriculture, **40**, pp. 179–188.

[2] Ames WF, 1977, *Numerical methods for partial differential equations*, 2^{nd} Edition, Academic Press, New York (NY).

[3] Andrewartha HG & Birch LC, 1954, *The distribution and abundance of animals*, The University of Chicago press, Chicago (IL).

[4] Brown EW, 1938, *The Equations of Motion of the Moon*, American Journal of Mathematics, **60**, pp. 785–792.

[5] Brown PN, 1980, *Decay to uniform states in ecological interactions*, SIAM Journal on Applied Mathematics, **38**, pp. 22–37.

[6] Cantrell RS, Cosner C & Hutson V, 1993, *Permanence in ecological systems with spatial heterogeneity*, Proceedings of the Royal Society of Edinburgh Series A, **123**, pp. 533–559.

[7] Cantrell RS, Cosner C & Hutson V, 1996, *Ecological models, permanence and spatial heterogeneity*, Rocky Mountain Journal of Mathematics, **26**, pp. 1–35.

[8] Cantrell RS & Cosner C, 1998, *On the effects of spatial heterogeneity on the persistence of interacting species*, Journal of Mathematical Biology, **37**, pp. 103–145.

[9] Chase JM & Leibold MA, 2003, *Ecological niches: Linking classical and contemporary approaches*, University of Chicago Press, Chicago (IL).

[10] Coddington EA & Carlson R, 1997, *Linear ordinary differential equations*, Society for Industrial and Applied Mathematics, Philadelphia (PA).

[11] Constantini L, 1981, *The beginning of agriculture in the Kachi Plain: The evidence of Mehrgarts*, pp. 29–33, in Allchin B (Ed), 1984, *South Asian archaeology*, Cambridge University Press, Cambridge.

[12] Conway E, Hoff D & Smoller J, 1978, *Large time behavior of solutions of systems of nonlinear reaction-diffusion equations*, SIAM Journal on Applied Mathematics, **35**, pp. 1–16.

[13] Cosner C & Lazer AC, 1980, *Stable coexistence in the Volterra-Lotka competition model with diffusion*, SIAM Journal on Applied Mathematics, **44**, pp. 1112–1132.

[14] Courant R, Friedrichs K & Lewy H, 1967, *On the partial difference equations of mathematical physics*, IBM Journal of Research and Development, **11**, pp. 215–234.

[15] Cruywagen GC, Kareiva P, Lewis PA & Murray JD, 1996, *Competition in a spatially heterogeneous environment: Modelling the risk of spread of a genetically engineered population*, Theoretical Population Biology, **49**, pp. 1–38.

[16] Volterra V & D'Ancona U, 1935, *Les associations biologiques au point de vue mathemátique*, Hermann et Cie, Paris.

[17] Dreyer TP, 1993, *Modelling with ordinary differential equations*, CRC Press, Boca Raton (FL).

[18] Department of Water Affairs and Forestry, *Hydrology data*, [Online], [Cited September 10th, 2007], Available from `http://www.dwaf.gov.za/Hydrology/rtmain.aspx`.

[19] Edwards RE, 1979, *An introduction to harmonic analysis*, 2^{nd} Edition, Springer-Verlag New York, Inc., New York (NY).

[20] Ellis RP, Swanston JS & Bruce FM, 1979, *A comparison of some rapid screen tests for malting quality*, Journal of the Institute of Brewing, **85**, pp 282–285.

[21] Elton C, 1927, *Animal ecology*, Sidgwick and Jackson, London.

[22] Fleming WH, 1975, *A selection-migration model in population genetics*, Journal of Mathematical Biology, **2**, pp. 219–233.

[23] Food and Agriculture Organization of the United Nations, 1998, *Production Yearbook*, Volume 52, Food and Agriculture Organization of the United Nations, Rome.

[24] Fick A, 1855, *Über Diffusion*, Annalen der Physik, **170**, pp. 59–86.

[25] Fife PC, 1979, *Mathematical aspects of reacting and diffusing systems*, Springer, Berlin.

[26] Fisher RA, 1937, *The wave of advance in advantageous genes*, Annals of Eugenics, **7**, pp. 335–369.

[27] Finney RL & Thomas GB, 1990, *Calculus*, Addison-Wesley, Reading (MA).

[28] Gause GF, 1934, *The struggle for existence*, Hafner Publishing Company, New York (NY).

[29] Gibson RH, Pearce S, Morris RJ, Symondson WOC & Memmott J, 2004, *Plant diversity and land use under organic and conventional agriculture: A whole-farm approach*, Journal of Applied Ecology, **44**, pp. 792-803.

[30] Google Inc., 2007, *Google maps* [Online], [Cited September 10th, 2007], Available from `http://maps.google.com`.

[31] Gotelli NJ, 2001, *A primer of ecology*, Sinauer Associates, Inc. Publishers, Sunderland (MA).

[32] Graunt J, 1662, *Natural and political observations in a following index, and made upon the bills of mortality, with reference to the government, religion, trade, ayre, diseases, and the several changes of the said city (London)*, Journal of the Institute of Actuaries, 90, Part I, **384**, pp. 4–61.

[33] Grimmett GR & Stirzaker DR, 1992, *Probability and random processes*, 2^{nd} Edition, Clarendon Press, Oxford.

[34] Grinnell J, 1917, *A selection-migration model in population genetics*, The American Naturalist, **51(602)**, pp. 115–128.

[35] Gustavo AS & Molina-Cano JL, 1977, *Calculus: Early transcendentals*, 2^{nd} Edition, Academic Press, New York (NY).

[36] Haaser NB & Sullivan JA, 1991, *Real analysis*, Dover Publications, New York (NY).

[37] Haggarty R, 1992, *Fundamentals of mathematical analysis*, Addison-Wesley, Wokingham, Berkshire.

[38] Haupt O, 1914, *Über eine mthode zum beweis von Oszillationstheoremen*, Mathematische Annalen, **76**, pp. 67–104.

[39] Hillman G, 1975, *The plant remains from Tell Abu Hureyra: A preliminary report*, Proceedings of the Prehistoric Society, **41**, pp. 70–73.

[40] Ho PT, 1977, *The indigenous origins of Chinese agriculture*, pp. 413–418 in Reed CA (Ed), 1977, *Origins of agriculture*, Mouton Publishers, The Hague.

[41] Home-Grown Cereals Authority, 2006, *The Barley growth guide*, [Online], [Cited September 10th, 2007], Available from `http://www.hgca.com`.

[42] Hutchinson E, 1957, *Concluding remarks*, pp. 115–128, in *Population studies: Animal ecology and demography*, Cold Spring Harbor Symposia on Quantitative Biology, **22**, The Biological Laboratory, Long Island Biological Association, Inc., New York (NY).

[43] Johnson BR & Scott SK, 1996, *New Approaches to chemical patterns*, Chemical Society Reviews, **25**, pp. 265–273.

[44] Katz VJ, 1979, *The history of Stokes' theorem*, Mathematics Magazine, **52(3)**, pp. 146–156.

[45] Katznelson Y, 1968, *An introduction to harmonic analysis*, John Wiley & Sons, Inc., New York (NY).

[46] Kareiva PM, 1983, *Local movement in herbivorous insects: Applying a passive diffusion model to mark-recapture field experiments*, Oecologia, **57**, pp. 322–327.

[47] Kareiva PM, Parker IM & Pascual M, 1996, *Can we use experiments and models in predicting the invasiveness of genetically engineered organisms?* Ecology, **77**, pp. 1670–1675.

[48] Kolman B, Busby RC & Ross S, 1934, *Discrete mathematical structures*, 3^{rd} Edition, Prentice Hall, Upper Saddle River (NJ).

[49] Kolmogoroff A, Petrovsky I & Piscounoff N, 1937, *Étude de l'équation de la diffusion avec croissance de la quantité de matière et son application à une probléme biologique*, Moscow University Mathematics Bulletin, **1**, pp. 1–25.

[50] Lakev B, Semane Y, Alemayehu F, Gehre H, Grando S, van Leur AJ & Ceccarelli S, 1997, *Exploiting the diversity in Barley landraces in Ethiopia*, Genetic Resources and Crop Evolution, **44(2)**, pp. 109–116.

[51] Lewis MA, 2000, *Spread rate for a nonlinear stochastic invasion*, Journal of Mathematical Biology, **41**, pp. 430–454.

[52] Lewis MA & Pacala S, 2000, *Modeling and analysis of stochastic invasion processes*, Journal of Mathematical Biology, **41**, pp. 387–429.

[53] Lubina J & Levin SA, 1988, *The spread of a reinvading organism: Range expansion of the California sea otter*, The American Naturalist, **131**, pp. 526–543.

[54] Lavoisier A, 1965, *Elements of chemistry (Translated by Robert Kerr)*, Courier Dover Publications, New York (NY).

[55] Lotka AJ, 1925, *Elements of physical biology*, Williams & Wilkens Co., Inc., Baltimore (MD).

[56] Lein A, 1964, *Breeding for malting quality*, pp. 310–324 in Broekhuizen S, Dantuma G, Lamberts H & Lange W (Eds), *Barley genetics I, Proceedings of the first international Barley genetics symposium*, Centre for Agricultural Publications and Documentation, Wageningen.

[57] Magnus W & Winkler S, 1966, *Hill's equations*, Springer, New York (NY).

[58] Mangel M & Tier C, 1994, *Four facts every conservation biologist should know about persistence*, Ecology, **75(3)**, pp. 607–614.

[59] Mimura M, Ei S & Fang Q, 1991, *Effects of domain-shape on coexistence problems in a competition-diffusion system*, Journal of Mathematical Biology, **29**, pp. 219–238.

[60] Muir T & Metzler WH, 1960, *A treatise on the theory of determinants* , Dover Publications, New York (NY).

[61] Murray JD, 2001, *Mathematical biology*, Springer, New York (NY).

[62] Murray FJ & Miller KS, 1954, *Existence theorems for ordinary differential equations*, New York University Press, New York (NY).

[63] Nagylaki T, 1975, *Conditions for the existence of clines*, Genetics, **80**, pp. 595–615.

[64] Odum EP, 1959, *Fundamentals of ecology*, 2^{nd} Edition, WB Saunders Company, Philadelphia (PA).

[65] Okubo A, Maini PK, Williamson MH & Murray JD, 1989, *On the spatial spread of the grey squirrel in Britain*, Proceedings of the Royal Society of London, **B 238**, pp. 113–125.

[66] Pacala SW & Roughgarden J, 1982, *Spatial heterogeneity and interspecific competition*, Theoretical Population Biology, **21**, pp. 92–113.

[67] Palmer GH, 1995, *Structure and ancient cereal grains*, Journal of the Institute of Brewing, **101**, pp. 103–112.

[68] Pielou EC, 1969, *An introduction to mathematical ecology*, John Wiley and Sons, Inc., New York (NY).

[69] Potgieter F, 2007, Senior Barley Breeder at the South African Barley breeding Institute, [Personal Communication], Cantactable at `fpotgieter@sabbi.co.za`.

[70] Shigesada N, Kawasaki K & Teramoto E, 1986, *Traveling periodic waves in heterogeneous environments*, Theoretical Population Biology, **30**, pp. 143–160.

[71] Skellam JG, 1951, *Random dispersals in theoretical populations*, Biometrika, **38**, pp. 196–218.

[72] Smith FE, 1963, *Population dynamics in* Daphnia magna, Ecology, **44**, pp. 651–663.

[73] Richardson LF, 1910, *The approximate arithmetical solution by finite differences of physical problems involving differential equations, with an application to the stresses in a masonry dam*, Philosophical Transactions of the Royal Society A, **210**, pp. 307 − 357.

[74] Richtmyer RD & Lax P, 1956, *Survey of the stability of linear finite difference equations*, Communications on Pure and Applied Mathematics, **9**, pp. 267–293.

[75] Richtmyer RD & Morton KW, 1967, *Difference methods for initial-value problems*, 2^{nd} Edition, John Wiley & Sons, New York (NY).

[76] Roschewitz I, Thies C & Tscharntke T, 2005, *Are landscape complexity and farm specialisation related to land-use intensity of annual crop fields?*, Agriculture, Ecosystems and Environment, **105**, pp. 87–99.

[77] Ross S, 2002, *A first course in probability*, 6^{th} Edition, Prentice Hall, Upper Saddle River (NJ).

[78] Rouse Ball WW, 1960, *A short account of the history of mathematics*, Dover Publications, New York (NY).

[79] Slafer GA, Molina-Cano JL, Savin R, Araus JL & Romagosa I (Eds), 2002, *Barley science: Recent advances from molecular biology to agronomy of yield and quality*, Haworth Press, New York (NY).

[80] Sparrow DHB, 1970, *Some genetical aspects of malting quality*, pp. 559–574 in Nilan RA (Ed), 1971, *Barley genetics II, Proceedings of the second international Barley genetics symposium*, Washington State University Press, Pullman (WA).

[81] Stewart J, 2003, *Calculus: Early transcendentals*, 5^{th} Edition, Thomson/Brooks/Cole, Pacific Grove (CA).

[82] Swanston JS, 1987, *The consequences, for malting quality, of Hordeum Laevigatum as a source of mildew resistance in Barley breeding*, Annals of Applied Biology, **110**, pp. 351–355.

[83] Trefethen LN, 1996, *Finite difference and spectral methods for ordinary and partial differential equations*, [online], [Cited June 7^{th}, 2007], Available from `http://web.comlab.ox.ac.uk/oucl/work/nick.trefethen/pdetext.html`.

[84] Trefethen LN, 2000, *Spectral methods in MATLAB*, Society for Industrial and Applied Mathematics, Philadelphia (PA).

[85] Van Vuuren JH, 1995, *Permanence and asymptotic stability in diagonally convex reaction-diffusion systems*, D.Phil. Thesis, University of Oxford, Oxford.

[86] Vandermeer JH, 1972, *Niche theory*, Annual Review of Ecology and Systematics, **3**, pp. 107–132.

[87] Vandermeer JH, 1975, *Interspecific competition: A new approach to the classical theory*, Science, **188**, pp. 253–255.

[88] Volterra V, 1931, *Lecons sur la théorie mathématique de la lutte pour la vie*, Gauthier-Villar, Paris.

[89] Volterra V, 1936, *Principles of mathematical biology* (translation by Antonelli PM of the original paper *Principles de biologie mathématique*), pp. 269–309 in Antonelli PL (Ed), 1985, *Mathematical essays on growth and the emergence of form*, University of Alberta Press, Alberta.

[90] Vretblad A, 2003, *Harmonic analysis*, Springer, New York (NY).

[91] Whittaker RH, Levin SA & Root RB, 1973, *Niche theory*, The American Naturalist, **107**, pp. 321–338.

[92] Yule GU, 1924, *A mathematical theory of evolution based on the conclusions of Dr. JC Willis F.R.S.*, Philosophical Transactions of the Royal Society of London, **B213**, pp. 21–87.

[93] Zohary D & Hopf M, 1993, *Domestication of plants in the Old World*, 2^{nd} Edition, Oxford Science Publications, Clarendon Press, Oxford.

Appendix A

Classical Theorems Used in the Model Derivations of Chapter 2

A.1 Stokes' Theorems

The divergence theorem and the fundamental theorem of the calculus are both special cases of Stokes' theorem which hold on k-dimensional spaces. These theorems are closely related, and indeed, the proof of the divergence theorem invokes the fundamental theorem.

A.1.1 The Fundamental Theorem of the Calculus

The fundamental theorem of the calculus was first proved by James Gregory (1638–1675), a contemporary of Sir Isaac Newton, who was independently working on ideas similar to the calculus of Newton. Sometimes Isaac Barrow (1630–1677), a mentor of Newton, is given credit for the ideas that led to the theorem [81].

Theorem A.1 (Fundamental Theorem of the Calculus) *Let $f(x)$ be a real-valued continuous function defined on the closed interval $[a, b]$ and define*

$$F(x) = \int_a^x f(\xi)\, \mathrm{d}\xi.$$

Then the function $F(x)$ is differentiable and $F'(x) = f(x)$.

Proof.
By the definition of F it follows that

$$F(x+h) - F(x) = \int_a^{x+h} f(\xi)\, \mathrm{d}\xi - \int_a^x f(\xi)\, \mathrm{d}\xi = \int_x^{x+h} f(\xi)\, \mathrm{d}\xi,$$

so that

$$F'(x) = \lim_{h\to 0} \frac{F(x+h) - F(x)}{h} = \lim_{h\to 0} \frac{1}{h} \int_x^{x+h} f(\xi)\, \mathrm{d}\xi. \tag{A.1}$$

Let $l_h, u_h \in [x, x+h]$ be such that $f(l_h) \leq f(x) \leq f(u_h)$ for every $x \in [x, x+h]$. Then

$$f(l_h)h \leq \int_x^{x+h} f(\xi)\,\mathrm{d}\xi \leq f(u_h)h.$$

But, by the continuity of f,

$$\lim_{h\to 0} f(l_h) = \lim_{h\to 0} f(u_h) = f(x).$$

Thus, using (A.1), it follows that

$$F'(x) = \lim_{h\to 0} \frac{1}{h} \int_x^{x+h} f(\xi)\,\mathrm{d}\xi = f(x). \qquad \blacksquare$$

A.1.2 The Divergence Theorem

The history of the Divergence theorem is rather more colourful. In 1813 three special cases of the divergence theorem appeared in a paper of the German mathematician Carl Friedrich Gauss (1777–1855) [44]. In 1833 and 1839 Gauss published other special cases of the theorem, but by this time the general theorem had been proved. In 1826 the Russian mathematician Michael Ostrogradsky (1801–1862) presented a proof of the general theorem to the Paris Academy of Science. He only published the proof in 1831 [44]. Meanwhile, between 1826 and 1831, the divergence theorem and related theorems appeared in publications of three other mathematicians. Simon-Denis Poisson (1781–1840) published an identical result in 1829, but presumably knew of Ostrogradsky's proof. In 1828 Frederic Sarrus (1798–1861) published a similar result [44], however it was not nearly as elegant as Ostrogradsky's. George Green (1793–1841) also published a special case of the Divergence theorem [44].

The mathematicians mentioned above were all interested in the theorem each for his own specific reasons. Gauss was interested in the theory of magnetic attraction, Ostrogradsky in the theory of heat, Green in electricity and magnetism, Poisson in elastic bodies, and Sarrus in floating bodies.

The divergence theorem states that the flux through a surface is equal to the integral of the divergence on the region inside the surface. In moving up from the fundamental theorem the interval has become a 3D region, the boundary a surface, the function a vector field and the divergence of the vector field takes the place of the derivative.

The following definitions are required in the statement of the divergence theorem.

Definition A.1 (Compact) *A subset of* $\mathbb{R}^n$ *is said to be* compact *if it is closed and bounded.* ■

Definition A.2 (Vector Field) *A vector valued function whose domain is a subset of* $\mathbb{R}^n$ *is called a* vector field. ■

Since a proof of the divergence theorem for a general compact set delves into advanced calculus and because the regions considered in the text need not be that general; the following proof will only consider a region R comprising simple compact connected subsets of $\mathbb{R}^3$. Here *simple* means that any line parallel to the x-axis, y-axis, or z-axis can only intersect R in a connected line segment or a point.

Theorem A.2 (The Divergence Theorem) *Let R be a simple compact subset of $\mathbb{R}^3$ with smooth boundary ∂R. For $(x_1, x_2, x_3) \in \mathbb{R}^3$ let $\underline{F}(x, y, z)$ denote a vector field on $\mathbb{R}^3$ and let $\underline{n}(x_1, x_2, x_3)$ denote a unit normal vector field to the boundary surface ∂R. Then*

$$\iint_{\partial R} \underline{F} \cdot \underline{n} \, \mathrm{d}(\partial R) = \iiint_R \nabla \cdot \underline{F} \, \mathrm{d}x \, \mathrm{d}y \, \mathrm{d}z.$$

Proof.
Denote the components of the vector field by $\underline{F}(r) = (f_1, f_2, f_3)$ and the components of the unit normal vector on ∂R by $\underline{n}(r) = (n_1, n_2, n_3)$. The result may now be written as

$$\iint_{\partial R} (f_1 n_1 + f_2 n_2 + f_3 n_3) \, \mathrm{d}(\partial R) = \iiint_R \left(\frac{\partial f_1}{\partial x_1} + \frac{\partial f_2}{\partial x_2} + \frac{\partial f_3}{\partial x_3}\right) \mathrm{d}x_1 \, \mathrm{d}x_2 \, \mathrm{d}x_3.$$

If the simple regions R_1 and R_2 share a boundary surface S to form the region R, then the unit normal $\underline{n}_{R_1}$ of R_1 on S points in the opposite direction to the unit normal $\underline{n}_{R_2}$ of R_2 on S. Thus

$$\iint_S \underline{F} \cdot \underline{n}_{R_1} \, \mathrm{d}S + \iint_S \underline{F} \cdot \underline{n}_{R_2} \, \mathrm{d}S = 0.$$

Hence,

$$\iint_{\partial R_1} \underline{F} \cdot \underline{n}_{R_1} \, \mathrm{d}(\partial R_1) + \iint_{\partial R_2} \underline{F} \cdot \underline{n}_{R_2} \, \mathrm{d}(\partial R_2) = \sum_{i=1}^{3} \iint_{\partial R} f_i n_i \, \mathrm{d}(\partial R).$$

Now the result would follow if

$$\iint_{\partial R} f_i n_i \, \mathrm{d}(\partial R) = \iiint_R \frac{\partial f_i}{\partial x_i} \, \mathrm{d}x_1 \, \mathrm{d}x_2 \, \mathrm{d}x_3$$

for every $i = 1, 2, 3$. Since the argument is similar for each i, only the equality

$$\iint_{\partial R} f_3 n_3 \, \mathrm{d}(\partial R) = \iiint_R \frac{\partial f_3}{\partial x_3} \, \mathrm{d}x_1 \, \mathrm{d}x_2 \, \mathrm{d}x_3$$

is proved. By the assumption that R is simple its boundary may be split into three components ∂R_{top}, where $n_3 > 0$, ∂R_{side}, where $n_3 = 0$, and ∂R_{bottom}, where $n_3 < 0$. Thus,

$$\iint_{\partial R} f_3 n_3 \, \mathrm{d}(\partial R) = \iint_{\partial R_{top}} f_3 n_3 \, \mathrm{d}(\partial R) + \iint_{\partial R_{bottom}} f_3 n_3 \, \mathrm{d}(\partial R).$$

Since $n_3 > 0$ on ∂R_{top} and $n_1 < 0$ on ∂R_{bottom} there is a region M in the xy-plane such that ∂R_{top} and ∂R_{bottom} are the images of functions $a(x_1, x_2)$ and $b(x_1, x_2)$ on M. Thus,

$$\iint_{\partial R} f_3 n_3 \, \mathrm{d}(\partial R) = \iint_M f_3(x_1, x_2, a(x_1, x_2)) \, \mathrm{d}x_1 \, \mathrm{d}x_2 - \iint_M f_3(x_1, x_2, a(x_1, x_2)) \, \mathrm{d}x_1 \, \mathrm{d}x_2.$$

By the fundamental theorem of the calculus,

$$\iint_{\partial R} f_3 n_3 \, \mathrm{d}(\partial R) = \iint_M \int_{b(x_1,x_2)}^{a(x_1,x_2)} \frac{\partial f_3}{\partial x_3} \, \mathrm{d}x_1 \, \mathrm{d}x_2 \, \mathrm{d}x_3 = \iiint_R \frac{\partial f_3}{\partial x_3} \, \mathrm{d}x_1 \, \mathrm{d}x_2 \, \mathrm{d}x_3. \qquad \blacksquare$$

A.2 Taylor's Theorem

Taylor series have been used since the 14^{th} century by the Indian mathematician Madhava (1350–1425). Madhava's most significant contribution is in progressing from the finite procedures of ancient mathematics to incorporating the ideas of limits to infinity. In the 17^{th} century James Gregory (1638–1675), to whom the first proof of the fundamental theorem of the calculus is attributed, published a number of power series [78], but it was not until 1715 that Brook Taylor (1685–1731) published a general construction of Taylor series [78].

Taylor series are important both as an approximation to the value of a function as well as a theoretical result. The class of functions described by power series, where the coefficients of the series are necessarily the coefficients given in the construction of the Taylor series, are the analytical functions.

In the proof of Taylor's theorem recourse will be made to the mean value theorem. The mean value theorem is stated here without proof. For a proof of the theorem, see [27].

Theorem A.3 (Mean Value Theorem) *If f is a differentiable function on the open interval (a, b) and continuous on the closed interval $[a, b]$, then*

$$f'(c) = \frac{f(b) - f(a)}{b - a}$$

for some $c \in (a, b)$. ■

Taylor's theorem may now be established.

Theorem A.4 (Taylor's Theorem) *Let $f(x)$ be a function on an interval I, containing x_0, that has $n + 1$ continuous derivatives. Then, for each $x \in I$,*

$$f(x) = f(x_0) + f'(x_0)(x - x_0) + f''(x_0)\frac{(x - x_0)^2}{2!} + \ldots + f^{(n)}(x_0)\frac{(x - x_0)^n}{n!} + R_{n+1}(x),$$

where the remainder term is given by

$$R_{n+1}(x) = f^{(n+1)}(x_c)\frac{(x - x_0)^{n+1}}{(n + 1)!}$$

for some $x_c \in (x_0, x)$.

Proof.
Fix $x \in I$. By the fundamental theorem of the calculus (see Theorem A.1),

$$\int_{x_0}^{x} f'(\xi)\, \mathrm{d}\xi = f(x) - f(x_0). \tag{A.2}$$

Using integration by parts,

$$\int_{x_0}^{x} f'(\xi)\, \mathrm{d}\xi = f'(x_0)(x - x_0) + \int_{x_0}^{x} f^{(2)}(\xi)(x - x_0)\, \mathrm{d}\xi. \tag{A.3}$$

From (A.2) and (A.3),

$$f(x) = f(x_0) + f'(x_0)(x - x_0) + \int_{x_0}^{x} f^{(2)}(\xi)(x - x_0)\,\mathrm{d}\xi.$$

The rightmost integral may be expanded by again using integration by parts. After n repeated applications of integration by parts, the expression becomes

$$f(x) = f(x_0) + f'(x_0)(x - x_0) + \ldots + f^{(n)}(x_0)\frac{(x - x_0)^n}{n!} + \frac{1}{n!}\int_{x_0}^{x} f^{(n+1)}(\xi)(x - x_0)^n\,\mathrm{d}\xi.$$

Since $f^{(n+1)}(\xi)$ is continuous it follows by the mean value theorem that

$$R_{n+1}(x) = \frac{1}{n!}\int_{x_0}^{x} f^{(n+1)}(\xi)(x - x_0)^n\,\mathrm{d}\xi = f^{(n+1)}(x_c)\frac{(x - x_0)^{n+1}}{(n+1)!},$$

where $x_c \in (x_0, x)$. ■

Taylor's theorem for several variables is required in Chapter 2. The above version of Taylor's theorem for one variable may be used to prove Taylor's theorem for several variables. The following intermediate definition is required.

Definition A.3 (Convex Set) *A set R in $\mathbb{R}^n$ is a convex set if, for any two points $\underline{p}$ and $\underline{x}$ that lie in R, the line segment joining $\underline{p}$ and $\underline{x}$ also lies wholly in R.* ■

Taylor's theorem may now be established.

Theorem A.5 (Taylor's Theorem for Several Variables) *Let f be a real valued function on an open convex subset R of $\mathbb{R}^n$, and suppose f and all its partial derivatives up to order $n+1$ are continuous on R. Let $\underline{p} \in R$. Then, for every $\underline{x} \in R$, there exists a point $\underline{x}_c$ on the line segment joining the points $\underline{p}$ and $\underline{x}$ such that*

$$f(\underline{x}) = f(\underline{p}) + ((\underline{x} - \underline{p}) \cdot \nabla)f(\underline{p}) + ((\underline{x} - \underline{p}) \cdot \nabla)^2\frac{f(\underline{p})}{2!} + \ldots + ((\underline{x} - \underline{p}) \cdot \nabla)^n\frac{f(\underline{p})}{n!} + R_{n+1}(\underline{x}),$$

where the remainder term is given by

$$R_{n+1}(\underline{x}) = ((\underline{x} - \underline{p}) \cdot \nabla)^{n+1}\frac{f(\underline{x}_c)}{(n+1)!}.$$

Proof.
Let $\underline{u}(t) = \underline{p} + t(\underline{x} - \underline{p})$, which is a parametrization of the line segment between $\underline{p}$ and $\underline{x}$. Applying Taylor's theorem for one variable (see Theorem A.4) to the function $r(\underline{u}(t))$ gives

$$f(\underline{x}) = f(\underline{p}) + \sum_{i=1}^{n}\frac{1}{i!}\frac{\mathrm{d}^i}{\mathrm{d}t^i}f(\underline{u}(0)) + \frac{1}{(n+1)!}\frac{\mathrm{d}^{n+1}}{\mathrm{d}t^{n+1}}f(\underline{u}(c)),$$

for some $c \in (0, 1)$. By the chain rule for several variables,

$$\frac{\mathrm{d}^i}{\mathrm{d}t^i}f(\underline{u}(0)) = ((\underline{x} - \underline{p}) \cdot \nabla)^n f(\underline{p}).$$

Let $\underline{x}_c = \underline{u}(c)$, then the result follows. ■

A.3 Limit Theorems

Usually, theorems are considered to be "laws of large numbers" if they are concerned with conditions under which the average of a sequence of random variables converges to the expected average. On the other hand, central limit theorems are concerned with determining conditions under which the sum of a large number of random variables has a probability distribution that is approximately normal.

The following definitions are required in this section.

Definition A.4 (Mutually Independent Random Variables) *An arbitrary collection of random variables is said to be* mutually independent *if, for any finite collection of them, say* $Y_1, Y_2, \ldots, Y_n$*, and any numbers* $a_1, a, 2, \ldots, a_n$*,*

$$P(Y_1 \leq a_1, Y_2 \leq a_2, \ldots, Y_n \leq a_n) = P(Y_1 \leq a_1)P(Y_2 \leq a_2)\ldots P(Y_n \leq a_n). \quad \blacksquare$$

Definition A.5 (Independently Identically Distributed Random Variables) *A collection of random variables is said to be* independent and identically distributed *if each has the same probability distribution as the others and all are mutually independent.* ■

A.3.1 The Strong Law of Large numbers

The strong law of large numbers was originally proved for the special case of Bernoulli random variables by the French mathematician Félix Édouard Justin Émile Borel (1871–1956). The general form that is presented here was proved by the Russian mathematician Andrey Nikolaevich Kolmogorov (1903–1987). A key element in the proof of the strong law of large numbers is Kolmogorov's inequality. But before proving Kolmogorov's inequality, Markov's inequality must be established.

Theorem A.6 (Markov's Inequality) *Suppose* Y *is a non-negative random variable with probability distribution function* $f(x)$ *and that* $k > 0$*. Then*

$$P(Y \geq k) \leq \frac{E(Y)}{k}.$$

Proof.
By definition,

$$E(Y) = \int_0^\infty xf(x)\,\mathrm{d}x.$$

By splitting the integral at $x = k$ it follows that

$$E(Y) = \int_0^k xf(x)\,\mathrm{d}x + \int_k^\infty xf(x)\,\mathrm{d}x \leq \int_k^\infty xf(x)\mathrm{d}x.$$

Now, since inside the integral $x > k$,

$$E(Y) \leq k\int_k^\infty f(x)\,\mathrm{d}x = kP(Y \geq k). \quad \blacksquare$$

The proof of Kolmogorov's inequality and the strong law of large numbers follow [77, pp. 258–262].

Theorem A.7 (Kolmogorov's Inequality) *Let $Y_1, \ldots, Y_n$ be n independent random variables such that $E(Y_i) = 0$ and $var(Y_i) = \sigma_i^2 < \infty$, for $i = 1, \ldots, n$. Then, for all $a > 0$,*

$$P\left(\max_{i=1,\ldots,n} |Y_1 + \ldots + Y_i| > a\right) \leq \sum_{i=1}^{n} \frac{\sigma_i^2}{a^2}.$$

Proof.
Define the random variable N to be the smallest value of i, $i \leq n$, such that $(Y_1 + \ldots + Y_i)^2 > a^2$, and define it to equal n if $(Y_1 + \ldots + Y_i) \leq a^2$ for all $i = 1, \ldots, n$. Now, since

$$P\left(\max_{i=1,\ldots,n} (Y_1 + \ldots + Y_i)^2 > a^2\right) = P\left((Y_1 + \ldots + Y_N)^2 > a^2\right),$$

it follows from Markov's inequality that

$$\begin{aligned} P\left(\max_{i=1,\ldots,n} (Y_1 + \ldots + Y_i)^2 > a^2\right) &= P\left((Y_1 + \ldots + Y_N)^2 > a^2\right) \\ &\leq \frac{E\left((Y_1 + \ldots + Y_N)^2\right)}{a^2}. \end{aligned} \tag{A.4}$$

By conditioning on N it is shown that $E\left((Y_1 + \ldots + Y_N)^2\right) \leq E\left((Y_1 + \ldots + Y_n)^2\right)$. First, for $N = n$, note that

$$E\left((Y_1 + \ldots + Y_n)^2 | N = n\right) = E\left((Y_1 + \ldots + Y_N)^2 | N = n\right).$$

Then, for $i < n$,

$$\begin{aligned} E\left((Y_1 + \ldots + Y_n)^2 | N = i\right) &= E\left(((Y_1 + \ldots + Y_i) + (Y_{i+1} + \ldots + Y_n))^2 | N = i\right) \\ &= E\left((Y_1 + \ldots + Y_i)^2 | N = i\right) + E\left((Y_{i+1} + \ldots + Y_n)^2 | N = i\right) \\ &\quad + 2E\left((Y_1 + \ldots + Y_i)(Y_{i+1} + \ldots + Y_n) | N = i\right). \end{aligned} \tag{A.5}$$

Whereas $N = i$ says something about $Y_1, \ldots, Y_i$ it says nothing about $Y_{i+1}, \ldots, Y_n$. Hence $Y_1 + \ldots + Y_i$ and $Y_{i+1} + \ldots + Y_n$ remain conditionally independent, given that $N = i$. Therefore

$$\begin{aligned} &E\left((Y_1 + \ldots + Y_i)(Y_{i+1} + \ldots + Y_n) | N = i\right) \\ &= E\left((Y_1 + \ldots + Y_i) | N = i\right) E\left(Y_{i+1} + \ldots + Y_n\right) | N = i), \end{aligned}$$

and so

$$\begin{aligned} &E\left((Y_1 + \ldots + Y_i)(Y_{i+1} + \ldots + Y_n) | N = i\right) \\ &= E\left((Y_1 + \ldots + Y_i) | N = i\right) E\left(Y_{i+1} + \ldots + Y_n\right) = 0. \end{aligned}$$

Thus, it follows from (A.5) that

$$E\left((Y_1 + \ldots + Y_n)^2 | N = i\right) \geq E\left((Y_1 + \ldots + Y_i)^2 | N = i\right) = E\left((Y_1 + \ldots + Y_N)^2 | N = i\right).$$

Hence, for all values of N,

$$E\left((Y_1 + \ldots + Y_n)^2 | N = i\right) \geq E\left((Y_1 + \ldots + Y_N)^2 | N = i\right).$$

Taking expectations yields

$$E\left((Y_1+\ldots+Y_n)^2\right) \geq E\left((Y_1+\ldots+Y_N)^2\right).$$

Now, it follows from A.4 that

$$\begin{aligned} P\left(\max_{i=1,\ldots,n}(Y_1+\ldots+Y_i)^2 > a^2\right) &\leq \frac{E\left((Y_1+\ldots+Y_n)^2\right)}{a^2} \\ &= \frac{var(Y_1+\cdots+Y_n)}{a^2} \\ &= \sum_{i=1}^{n}\frac{\sigma_i^2}{a^2}. \end{aligned}$$

■

The so-called continuity property of probabilities is also required in the proof of the strong law of large numbers. It is stated here without proof. For a proof of this property, see [77, p.47].

Theorem A.8 (Continuity Property of Probabilities) *If* $\{E_n\}_{n\geq 1}$ *is an increasing sequence of events, that is* $E_1 \subset E_2 \subset \ldots \subset E_n \subset E_{n+1} \subset \ldots$, *then*

$$\lim_{n\to\infty} P(E_n) = P\left(\lim_{n\to\infty} E_n\right).$$

■

The strong law of large numbers is now established in the case where the random variables are assumed independent and identically distributed.

Theorem A.9 (Strong Law of Large Numbers) *Let* $Y_1, Y_2, \ldots$ *be independent random variables with* $E(Y_i) = 0$ *and* $var(Y_i) = \sigma^2 < \infty$. *Then, with probability* 1,

$$\lim_{n\to\infty}\frac{Y_1+\ldots+Y_n}{n} = \mu.$$

Proof.
By Kolmogorov's inequality (see Theorem A.7), it follows that for any n, and any $a > 0$,

$$P\left(\max_{j=1,\ldots,n}\left|\sum_{i=1}^{n}\frac{Y_i-\mu}{i}\right| > a\right) \leq \frac{\sum_{i=1}^{j} var(Y_i/i)}{a^2}. \tag{A.6}$$

Let the events E_n, for $n \geq 1$, be defined by

$$E_n = \left\{\max_{j=1,\ldots,n}\left|\sum_{i=1}^{n}\frac{Y_i-\mu}{i}\right| > a\right\}.$$

Then, as the events E_n are increasing, it follows by the continuity property of probabilities (see Theorem A.8) that

$$\lim_{n\to\infty} P\left(\max_{j=1,\ldots,n}\left|\sum_{i=1}^{n}\frac{Y_i-\mu}{i}\right| > a\right) = P\left(\bigcup_{1}^{\infty} E_n\right) = P\left(\max_{j=1,\ldots,\infty}\left|\sum_{i=1}^{j}\frac{Y_i-\mu}{i}\right| > a\right).$$

Hence, by (A.6),

$$P\left(\max_{j=1,\ldots,\infty}\left|\sum_{i=1}^{j}\frac{Y_i-\mu}{i}\right|>a\right)\leq\frac{\sum_{i=1}^{\infty}\sigma^2/i^2}{a^2},$$

or equivalently,

$$P\left(\max_{j\geq 1}\left|\sum_{i=1}^{j}\frac{Y_i-\mu}{i}\right|\leq a\right)\geq 1-\frac{\sigma^2\sum_{i=1}^{\infty}1/i^2}{a^2}.$$

Since, if $\max_{j\geq 1}\left|\sum_{i=1}^{j}(Y_i-\mu)/i\right|\leq a$, then $\sum_{i=1}^{\infty}(Y_i-\mu)/i\leq a<\infty$, it follows that

$$P\left(\sum_{i=1}^{\infty}\frac{Y_i-\mu}{i}<\infty\right)\geq 1-\frac{\sigma^2\sum_{i=1}^{\infty}1/i^2}{a^2}.$$

Now, in the limit as $a\to\infty$,

$$P\left(\sum_{i=1}^{\infty}\frac{Y_i-\mu}{i}<\infty\right)=1,$$

and hence

$$P\left(\lim_{n\to\infty}\sum_{i=1}^{n}\frac{Y_i-\mu}{n}=0\right)=1. \qquad \blacksquare$$

A.3.2 A Central Limit Theorem

The first version of the central limit theorem was proved by the French mathematician Abraham de Moivre (1667–1754) around 1733 for the special case when the random variables are Bernoulli random variables with probability of success $\frac{1}{2}$. Laplace extended this result to a case that is similar to the result proved here, where the probability of success is arbitrary. Laplace also discovered the more general form of the central limit theorem, but his proof was less than rigorous. A rigorous proof of the theorem was first presented by the Russian mathematician Aleksandr Liapunov (1887–1918) in 1901 or 1902.

Before presenting and proving this central limit theorem, Stirling's formula and a corollary thereof are first established as intermediate results. In the proof of Stirling's formula the comparison test, which is stated without proof, is required. For a proof of the comparison test, see [37].

Theorem A.10 (Comparison Test) *Let $\sum_{k=1}^{\infty}a_k$ and $\sum_{k=1}^{\infty}b_k$ be series with positive terms, and suppose that $a_k\leq b_k$ for every k. If $\sum_{k=1}^{\infty}b_k$ converges, then $\sum_{k=1}^{\infty}a_k$ converges.* ■

Stirling's formula may now be established.

Theorem A.11 (Stirling's Formula)

$$\lim_{n\to\infty}\frac{n!}{\sqrt{n}n^ne^{-n}}=c, \tag{A.7}$$

where c is some constant.

Proof.
Since c is positive it may be rewritten as $c = e^{c_1}$, for some constant c_1. Furthermore, let

$$d_n = \ln\left(\frac{n!}{n^{n+1/2}e^{-n}}\right) = \ln(n!) - (n+1/2)\ln(n) + n.$$

Consider now the partial sums

$$D_n = \sum_{i=1}^{n}(d_i - d_{i+1}) = (d_1 - d_2) + (d_2) - d_3) + \ldots + (d_n - d_{n+1}) = d_1 - d_{n+1}.$$

If the infinite series

$$\sum_{n=1}^{\infty}(d_1 - d_{n+1})$$

converges, then the partial sums $(d_1 - d_{n+1})$ converge, which implies that d_{n+1} converges to some constant — call it c_1. Now,

$$|d_n - d_{n+1}| = (n+\frac{1}{2})\ln(n+1) - (n+\frac{1}{2})\ln(n) - 1 = (n+\frac{1}{2})\ln\left(\frac{n+1}{n}\right) - 1.$$

By a Taylor series expansion about $x_0 = 0$ (see Theorem A.4), it follows that

$$\ln(1+x) = x - \frac{x^2}{2} + \theta(x),$$

where

$$|\theta(x)| = \frac{|x|^3}{3|(1+k_x)|^3} \leq |x|^3$$

for $|x| \leq \frac{1}{3}$ and $k_x \in [0, x]$. Thus, for $n \geq 3$,

$$|d_n - d_{n+1}| = \left(n+\frac{1}{2}\right)\left(\frac{1}{n} - \frac{1}{2n^2}\right) + \theta\left(\frac{1}{n}\right) - 1 \leq \frac{n+\frac{1}{2}}{n^3} - \frac{1}{4n^2}.$$

Since both

$$\sum_{n=1}^{\infty}\frac{n+1/2}{n^3} \quad \text{and} \quad \sum_{n=1}^{\infty}\frac{1}{4n^2}$$

converge it follows by the comparison test (see Theorem A.10) that $\sum_{n=1}^{\infty}(d_n - d_{n+1})$ converges. ■

Let $Y_i, Y_2, \ldots$ be a sequence of independent, identically distributed random variables, where $Y_i = 1$ with probability p and $Y_i = -1$ with probability $q = 1 - p$. Now write

$$S_n = \sum_{i=1}^{n} Y_i \quad \text{and} \quad S_n^* = \frac{S_n - E(S_n)}{\sqrt{V(S_n)}}. \tag{A.8}$$

In the proof of the corollary of Stirling's formula that follows a variable x_k is employed. Where $S_n = 2k - n$ the variable x_k denotes the corresponding value for S_n^*. Thus

$$x_k = S_n^* = \frac{2k - n - n(p-q)}{\sqrt{\frac{npq}{4}}}. \tag{A.9}$$

Furthermore, by the notation $f(n) \sim g(n)$ it is meant that

$$\lim_{n\to\infty} \frac{f(n)}{g(n)} = 1.$$

The following corollary now follows from Stirling's formula (see Theorem A.11).

Corollary A.1 (Corollary to Stirling's Formula) *Let A be a constant and let $x_k \leq A$. Then*

$$\binom{n}{k} p^k q^{n-k} \sim \frac{1}{c\sqrt{npq}} e^{\frac{x_k^2}{32}}, \tag{A.10}$$

where c is some constant.

Proof.
It follows by (A.9) that

$$\begin{aligned} k &= \sqrt{npq}\frac{x_k}{4} + np, \quad \text{and} \\ n-k &= nq - \sqrt{npq}\frac{x_k}{4}, \end{aligned}$$

from which it follows that

$$k \sim np, \quad \text{and} \tag{A.11}$$
$$n-k \sim nq. \tag{A.12}$$

Now, by Stirling's formula (see Theorem A.11),

$$\binom{n}{k} p^k q^{n-k} \sim \frac{(\frac{n}{e})^n c\sqrt{n}}{(\frac{k}{e})^k c\sqrt{k}(\frac{n-k}{e})^{n-k} c\sqrt{n-k}} p^k q^{n-k} = \frac{\sqrt{n}}{c\sqrt{k(n-k)}} \left(\frac{np}{k}\right)^k \left(\frac{nq}{n-k}\right)^{n-k}. \tag{A.13}$$

Hence, using (A.11) and (A.12),

$$\binom{n}{k} p^k q^{n-k} \sim \frac{1}{c\sqrt{npq}} \left(\frac{np}{k}\right)^k \left(\frac{nq}{n-k}\right)^{n-k}.$$

If it were to be shown that

$$\ln\left(\left(\frac{np}{k}\right)^k \left(\frac{nq}{n-k}\right)^{n-k}\right) \sim -\frac{x_k^2}{32},$$

then

$$\left(\frac{np}{k}\right)^k \left(\frac{nq}{n-k}\right)^{n-k} \sim e^{-\frac{x_k^2}{32}}$$

and the corollary would follow. Now

$$\ln\left(\left(\frac{np}{k}\right)^k \left(\frac{nq}{n-k}\right)^{n-k}\right) = k\ln\left(\frac{np}{k}\right) + (n-k)\ln\left(\frac{nq}{n-k}\right),$$

and, using the identities

$$\begin{aligned} \frac{np}{k} &= \frac{k - \sqrt{npq}x_k/4}{k} &&= 1 - \frac{\sqrt{npq}x_k}{4k} \\ \text{and} \quad \frac{nq}{n-k} &= \frac{n - k + \sqrt{npq}x_k/4}{n-k} &&= 1 + \frac{\sqrt{npq}x_k}{4(n-k)}, \end{aligned}$$

this is equal to

$$\ln\left(\left(\frac{np}{k}\right)^k \left(\frac{nq}{n-k}\right)^{n-k}\right) = k\ln\left(1 - \frac{\sqrt{npq}x_k}{4k}\right) + (n-k)\ln\left(1 + \frac{\sqrt{npq}x_k}{4(n-k)}\right). \quad \text{(A.14)}$$

Moreover, by (A.11) and (A.12),

$$\frac{np}{k} \sim 1 \quad \text{and} \quad \frac{nq}{(n-k)} \sim 1, \quad \text{(A.15)}$$

so that (A.14) may be approximated, using truncated Taylor series expansions, by

$$\ln\left(\left(\frac{np}{k}\right)^k \left(\frac{nq}{n-k}\right)^{n-k}\right) = k\left(-\frac{\sqrt{npq}x_k}{4k} - \frac{npqx_k^2}{32k^2}\right) + (n-k)\left(\frac{\sqrt{npq}x_k}{4(n-k)} - \frac{npqx_k^2}{32(n-k)^2}\right),$$

which simplifies to

$$-\frac{x_k^2}{32}\left(\frac{np}{k}\right)\left(\frac{nq}{n-k}\right).$$

Thus, again by (A.15),

$$\ln\left(\left(\frac{np}{k}\right)^k \left(\frac{nq}{n-k}\right)^{n-k}\right) \sim -\frac{x_k^2}{32}. \qquad \blacksquare$$

Finally, the concept of a Riemann is referred to in the proof of the central limit theorem.

Definition A.6 (Riemann Sum) *Let a closed interval $[a, b]$ be partitioned by points $a < x_1 < x_2 < \ldots < x_{n-1} < b$, where the lengths of the resulting intervals between the points are denoted $\Delta x_1, \Delta x_2, \ldots, \Delta x_n$. Let x_i^* be an arbitrary point in the i^{th} subinterval. Then the quantity*

$$\sum_{i=1}^{n} f(x_i^*)\Delta x_i$$

is called a Riemann sum *for a given function $f(x)$ and partition of $[ab]$, and the value $\max_{i=1,\ldots,n} \Delta x_i$ is called the mesh size of the partition. If the limit of the Riemann sums exists as $\max_{i=1,\ldots,n} \Delta x_i \to 0$, this limit is known as the Riemann integral of $f(x)$ over the interval $[a, b]$.* $\blacksquare$

The central limit theorem may now be established.

Theorem A.12 (Central Limit Theorem) *Let $Y_i, Y_2, \ldots$ be a sequence of independent, identically distributed random variables, where $Y_i = 1$ with probability p and $Y_i = -1$ with probability $q = 1 - p$. Then*

$$P\left(a \leq \frac{(\sum_{i=1}^{n} Y_i) - n\mu}{\sqrt{\sigma^2 n}} \leq b\right) \to \frac{1}{4\sqrt{2\pi}} \int_a^b e^{-x^2/32} \mathrm{d}x$$

as $n \to \infty$, where μ is the mean and σ^2 the variance of each variable Y_i.

Proof.
Let

$$S_n = \sum_{i=1}^{n} Y_i \quad \text{and} \quad S_n^* = \frac{S_n - E(S_n)}{\sqrt{V(S_n)}}, \tag{A.16}$$

where $E(S_n)$ and $V(S_n)$ are respectively the expected value and variance of the random variable S_n. Although S_n^* is the variable of interest, S_n is a little easier to work with. Suppose $S_n = 2k - n$ and denote the corresponding value for S_n^* by x_k. Then

$$x_k = \frac{2k - n - n\mu}{\sqrt{n\sigma^2}} = \frac{2k - n - 2np + n}{\sqrt{\frac{npq}{4}}}.$$

Now

$$P(a \leq S_n^* \leq b) = \sum_{a \leq x_k \leq b} P(S_n = 2k - n) = \sum_{a \leq x_k \leq b} \binom{n}{k} p^k q^{n-k}.$$

By Corollary A.1,

$$\lim_{n\to\infty} \binom{n}{k} p^k q^{n-k} = \frac{1}{c\sqrt{npq}} e^{-\frac{x_k^2}{32}}.$$

Moreover,

$$x_{k+1} - x_k = \frac{2(k + 1 - np) - 2(k - np)}{\sqrt{\frac{npq}{4}}} = \frac{4}{\sqrt{npq}}$$

and therefore

$$P\left(a \leq S_n^* \leq b\right) = \sum_{a \leq x_k \leq b} \frac{1}{4c} e^{-\frac{x_k^2}{32}} (x_{k+1} - x_k). \tag{A.17}$$

The sum in (A.17) is a Riemann sum for the function $f(x) = \frac{1}{4c} e^{-\frac{x_k}{32}}$ (see Definition A.6). Since

$$\lim_{n\to\infty} \frac{4}{\sqrt{npq}} = 0,$$

the mesh size of the partition of the Riemann sum tends to zero as $n \to \infty$. Moreover, the integral of the function $f(x)$ exists, and hence the sum may be replaced by an integral. Thus

$$\lim_{n\to\infty} P\left(a \leq S_n^* \leq b\right) = \frac{1}{4c} \int_a^b e^{-\frac{x^2}{32}} \mathrm{d}x.$$

Since, for every n, S_n^* is some number, $P\left(-\infty \leq S_n^* \leq \infty\right) = 1$, and thus

$$\lim_{n\to\infty} P\left(-\infty \leq S_n^* \leq \infty\right) = \frac{1}{4c} \int_{-\infty}^{\infty} e^{-\frac{x^2}{32}} \mathrm{d}x = 1.$$

Moreover, since

$$\frac{2\sqrt{2}}{\sqrt{\pi}} \int_{-\infty}^{\infty} e^{-\frac{x^2}{32}} \mathrm{d}x = 1,$$

it follows that $c = 1/\sqrt{2\pi}$. ■

A.4 The Schwarz Inequality

The Schwarz inequality was first introduced by the French mathematician Augustin-Louis Cauchy (1789–1857) for sums of products of real or complex numbers and was generalized in 1859 by the Russian mathematician Victor Jacovlevich Bunyakovski (1804–1889) for integrals. Bunyakovski's contribution was overlooked in the west and was later independently rediscovered by the German mathematician Hermann Amandus Schwarz (1843–1921) [36].

Theorem A.13 (Schwarz Inequality) *If $f(x)$ and $g(x)$ are real valued functions integrable on $\mathbb{R}$ then*

$$\left| \int_{-\infty}^{\infty} f(x)g(x)\, \mathrm{d}x \right| \leq \sqrt{\int_{-\infty}^{\infty} (f(x))^2\, \mathrm{d}x} \cdot \sqrt{\int_{-\infty}^{\infty} (g(x))^2\, \mathrm{d}x},$$

where equality holds if and only if $g(x) = \lambda f(x)$ for some $\lambda \in \mathbb{R}$.

Proof.
If $f(x) \neq \lambda g(x)$ for every $\lambda \in \mathbb{R}$ then for each $\lambda \in \mathbb{R}$ it holds that

$$\begin{aligned} 0 &< \int_{-\infty}^{\infty} (f(x) - \lambda g(x))(f(x) - \lambda g(x))\, \mathrm{d}x \\ &= \int_{-\infty}^{\infty} (f(x))^2\, \mathrm{d}x - 2\lambda \int_{-\infty}^{\infty} f(x)g(x)\, \mathrm{d}x + |\lambda|^2 \int_{-\infty}^{\infty} (g(x))^2\, \mathrm{d}x. \end{aligned}$$

Let

$$\lambda = \frac{\int_{-\infty}^{\infty} f(x)g(x)\, \mathrm{d}x}{\int_{-\infty}^{\infty} (g(x))^2\, \mathrm{d}x}$$

then

$$0 < \int_{-\infty}^{\infty} (f(x))^2\, \mathrm{d}x - \frac{\int_{-\infty}^{\infty} f(x)g(x)\, \mathrm{d}x}{\int_{-\infty}^{\infty} (g(x))^2\, \mathrm{d}x},$$

from which the Schwarz inequality follows.

Suppose now that $f(x) = \lambda g(x)$ for some $\lambda \in \mathbb{R}$. If $\lambda = 0$ then $f(x) \equiv 0$ or $g(x) \equiv 0$ and equality in the Schwarz equality clearly holds. If $\lambda \neq 0$ direct substitution gives the result. ■

Appendix B

Results on Differential Equations

B.1 Elementary results

The first result of this section is a solution formula for the initial-value problem where the governing equation is a homogeneous autonomous second-order differential equation. The second result shows the equivalence of this form of the solution to an alternate form of the solution.

Theorem B.1 ([17]) *The unique solution to the initial value problem*

$$y''(x) + qy(x) = 0, \tag{B.1}$$

where $(y(0), y'(0))^T = (\omega, \beta)^T \in \mathbb{R}^2$ *and where* I *is an interval in* $\mathbb{R}$ *containing the origin, is*

$$y(x) = \omega \cos(\sqrt{-q}x) + \frac{\beta}{\sqrt{-q}} \sin(\sqrt{-q}x).$$

Proof. Substitute $y(x) = e^{\lambda x}$ into (B.1) to obtain the characteristic equation $\lambda^2 e^{\lambda x} + qe^{\lambda x} = 0$. It follows that $\lambda = \pm\sqrt{-q}$ and hence the general solution to (B.1) is

$$y(x) = \gamma_1 e^{\sqrt{-q}x} + \gamma_2 e^{-\sqrt{-q}x}.$$

Using the initial conditions $y(0) = \gamma_1 + \gamma_2 = \omega$ and $y'(0) = \sqrt{-q}\gamma_1 - \sqrt{-q}\gamma_2 = \beta$, it follows that

$$\gamma_1 = \frac{\sqrt{-q}\omega + \beta}{2\sqrt{-q}} \quad \text{and} \quad \gamma_2 = \frac{\sqrt{-q}\omega - \beta}{2\sqrt{-q}}.$$

Therefore

$$y(x) = \frac{(\omega\sqrt{-q} + \beta)e^{x\sqrt{-q}}}{2\sqrt{-q}} + \frac{(\omega\sqrt{-q} - \beta)e^{x\sqrt{-q}}}{2\sqrt{-q}} = \omega \cos(x\sqrt{-q}) + \frac{\beta}{\sqrt{-q}} \sin(x\sqrt{-q}). \blacksquare$$

If q is positive (B.1) describes simple harmonic motion, which is motion where the acceleration of a body is proportional, and opposite in direction, to the displacement from its equilibrium position. The period of the motion is determined by the overall system and the phase and amplitude by the initial conditions. The following result equates the above form of the solution to the initial value problem for (B.1) with an alternative form stated in terms of a phase angle φ.

Theorem B.2 ([27]) *There is a one-to-one correspondence between $A, \varphi \in \mathbb{R}$ and $B_1, B_2 \in \mathbb{R}$ such that $A\sin(z+\varphi) = B_1\sin(z) + B_2\cos(z)$ for φ up to a multiple of 2π.*

Proof. By definition,

$$\begin{aligned} B_1\sin(z) + B_2\cos(z) &= \frac{B_1}{2i}(e^{iz} - e^{-iz}) + \frac{B_2}{2}(e^{iz} + e^{-iz}) \\ &= \frac{B_1 + iB_2}{2i}e^{iz} - \frac{B_1 - iB_2}{2i}e^{-iz}. \end{aligned}$$

Let $e^{\beta} = B_1 + iB_2$, where $\beta = \alpha + i\gamma$. Then $B_1 = e^{\alpha}\cos\gamma$ and $B_2 = e^{\alpha}\sin\gamma$. Hence

$$B_1\sin(z) + B_2\cos(z) = \frac{e^{\beta}e^{iz}}{2i} - \frac{e^{\overline{\beta}}e^{-iz}}{2i} = \frac{e^{\alpha}e^{i(z+\gamma)} - e^{\alpha}e^{-i(z+\gamma)}}{2i} = A\sin(z+\varphi),$$

where $A = e^{\alpha}$ and $\varphi = \gamma$. Thus $B_1 = A\cos(\varphi)$ and $B_2 = A\sin(\varphi)$. ■

B.2 A System of First Order Equations

Floquet theory, named after Gaston Floquet (1847–1921), concerns the structure of solutions to the system of linear ordinary differential equations

$$\underline{X}'(x) = \mathbf{A}(x)\cdot\underline{X}(x), \qquad x \in \mathbb{R}, \tag{B.2}$$

where $\mathbf{A} \in C(\mathbb{R}, M_n(\mathbb{R}))$ and $\mathbf{A}$ is periodic with period $\ell > 0$ [10]. By analogy with the solution αe^{ax} to (B.2) in the case where $n = 1$ and $\mathbf{A} = a$, where a is a constant, define the *exponential function* $e^{\mathbf{A}x}$ as the series

$$e^{\mathbf{A}x} = \sum_{k=0}^{\infty} \frac{\mathbf{A}^k x^k}{k!}.$$

Coddington and Carlson [10] discuss this series, which is convergent for all $x \in \mathbb{R}$ and does indeed define a basis for (B.2). The first result of this section is a canonical representation of the basis $\mathbf{X}(x)$ for the solutions of (B.2). The second result of this section provides a representation of the *Wronskian* for n solutions to (B.2). These results appear in [10].

B.2.1 Floquet's Theorem

The basic observation that leads to the representation of a basis for the solutions to (B.2), given in Floquet's theorem, is that if $\underline{X}(x)$ satisfies (B.2), then so does $\underline{Y}(x) = \underline{X}(x+\ell)$, since

$$\underline{Y}'(x) = \underline{X}'(x+\ell) = \mathbf{A}(x+\ell)\cdot\underline{X}(x+\ell) = \mathbf{A}(x)\cdot\underline{X}(x).$$

Theorem B.3 ([10]) *Each Basis $\mathbf{X}$ of the solutions to $\underline{X}'(x) = \mathbf{A}(x)\cdot\underline{X}(x)$, where $\mathbf{A} \in C(\mathbb{R}, M_n(\mathbb{R}))$ and A is periodic with period ℓ, can be represented as $\mathbf{X}(x) = \mathbf{P}(x)\cdot e^{\mathbf{R}x}$, where $\mathbf{P} \in C^1(\mathbb{R}, M_n(\mathbb{R}))$, $\mathbf{P}(x)$ is invertible, $\mathbf{P}(x+\ell) = \mathbf{P}(x)$ for all $x \in \mathbb{R}$ and $\mathbf{R} \in M_n(\mathbb{R})$.*

Proof. Since $\mathbf{Y}(x) = \mathbf{X}(x+\ell)$ is a basis for the solutions to (B.2), $\mathbf{X}(x) = \mathbf{X}(x) \cdot \mathbf{C}$ for some invertible $\mathbf{C} \in M_n(\mathbb{R})$. Hence there exists a matrix $\mathbf{R} \in M_n(\mathbb{R})$ such that $e^{\mathbf{R}\ell} = \mathbf{C}$; that is, $\mathbf{R}\ell$ is a logarithm of $\mathbf{C}$. It follows that

$$\underline{X}(x+\ell) = \underline{X}(x) \cdot e^{\mathbf{R}\ell}, \qquad x \in \mathbb{R}.$$

If $\mathbf{P}(x) = \mathbf{X}(x) \cdot e^{-\mathbf{R}x}$ it follows that, for all $x \in \mathbb{R}$,

$$\mathbf{P}(x+\ell) = \mathbf{X}(x+\ell) \cdot e^{-\mathbf{R}\cdot(x+\ell)} = \mathbf{X}(x) \cdot e^{\mathbf{R}\ell} \cdot e^{-\mathbf{R}\cdot(x+\ell)} = \mathbf{X}(x) \cdot e^{-\mathbf{R}x} = \mathbf{P}(x).$$

Since both $\mathbf{X}(x)$ and $e^{-\mathbf{R}x}$ are invertible, so is $\mathbf{P}(x)$, and $\mathbf{P} \in C^1(\mathbb{R}, M_n(\mathbb{R}))$. ■

B.2.2 The Wronskian

Let $\mathbf{Y}(x)$ be the square matrix-function where each column is a vector-function $X_i(x)$ of dimension n. If $\underline{X}_i = (y_i^1, \ldots, y_i^n)^T$ is a solution to (B.2) for each $i = 1, \ldots, n$, then the square matrix $\mathbf{Y} = (\underline{X}_1, \ldots, \underline{X}_n)$ is a *solution matrix* to (B.2). The *Wronskian* $W_{\mathbf{Y}}(x)$ of $\mathbf{Y}$ is the function

$$W_{\mathbf{Y}}(x) = \det(\mathbf{Y}(x)).$$

A standard result on the Wronskian is that if the functions $y_1, \ldots, y_n$ are independent on the interval I then $W_{\mathbf{Y}}(x) = 0$ for all $x \in I$ [60]. From the next result follows that, when $\mathbf{Y}$ is a solution matrix to (B.2), then $W_{\mathbf{Y}}(x) \neq 0$ for all $x \in I$ if and only if $W_{\mathbf{X}}(\zeta) \neq 0$ for some $\zeta \in I$.

Theorem B.4 ([10]) *Let* $\mathbf{Y}$ *be a solution matrix to (B.2). Then*

$$W_{\mathbf{Y}}(x) = W_{\mathbf{Y}}(\zeta) e^{\int_\zeta^x tr(\mathbf{A}(s))\, \mathrm{d}s}, \tag{B.3}$$

where $\zeta, x \in \mathbb{R}$.

Proof. By the definition of the determinant,

$$\sum_p \operatorname{sgn}(p) x_{1p(1)} x_{2p(2)} \ldots x_{2p(n)},$$

where the sum is over all permutations $p = (p(1), \ldots, p(n))$ of $(1, \ldots, n)$ and $\operatorname{sgn}(p)$ is the sign of the permutation, it is known that $\operatorname{sgn}(p) = 1$ when p is even and $\operatorname{sgn}(p) = -1$ when p is odd [48, pp. 186]. Using the product rule for differentiation, $W'_{\mathbf{X}}$ is the sum of the determinants

$$W'_{\mathbf{Y}} = w_1 + \cdots + w_n,$$

where w_i is obtained from $W_{\mathbf{Y}}$ by replacing the ith row $y_{i1}, \ldots, y_{in}$ with the derivatives $y'_{i1}, \ldots, y'_{in}$. For example,

$$w_1 = \begin{vmatrix} y'_{11} & y'_{12} & \cdots & y'_{1n} \\ y_{21} & y_{22} & \cdots & y_{2n} \\ \vdots & & & \\ y_{n1} & y_{n2} & \cdots & y_{nn} \end{vmatrix}.$$

The equation $\mathbf{Y}' = \mathbf{AY}$ implies that

$$y'_{ik} = \sum_{j=1}^{n} a_{ij} y_{jk}$$

and hence

$$y'_{11} = \sum_{j=1}^{n} y_{j1}, \ \ldots, \ y'_{1n} = \sum_{j=1}^{n} y_{jn}. \tag{B.4}$$

The value of w_1 remains unchanged if a constant multiple of some row is added to the first row. Adding to the first row $-a_{12}$ times the second row, $-a_{13}$ times the third row, *etc.*, it follows by (B.4) that

$$w_1 = \begin{vmatrix} a_{11}y_{11} & a_{11}y_{12} & \cdots & a_{11}y_{1n} \\ y_{21} & y_{22} & \cdots & y_{2n} \\ \vdots & & & \\ y_{n1} & y_{n2} & \cdots & y_{nn} \end{vmatrix}.$$

Similarly, $w_j = a_{jj} W_{\mathbf{Y}}$, so that

$$W'_{\mathbf{Y}} = (a_{11} + \cdots + a_{nn}) W_{\mathbf{Y}} = \operatorname{tr}(\mathbf{A}) W_{\mathbf{Y}}$$

and hence (B.3) follows, since both sides of the equation satisfy $W'_{\mathbf{Y}} = \operatorname{tr}(\mathbf{A}) W_Y$ and have the value $W_{\mathbf{Y}}(\zeta)$ at $x = \zeta$. ■

B.3 Lower bound on λ for stable solutions to Hill's Equation

Let $s(x) \in C^1(\mathbb{R})$ and suppose $s(x)$ is ℓ-periodic. Then

$$y''(x) + (s(x) + \lambda) y(x) = 0 \tag{B.5}$$

is Hill's equation. It is named after George William Hill (1838–1914) who, when considering the action of the sun on the motion of the moon [4], obtained an equation of the form of (B.5). Of interest in the study of Hill's equation is the stability of solutions and the presence or absence of periodic solutions. The two theorems in this section, which appear in [57], concern the stability of solutions.

Consider the independent solutions $y_1(t)$ and $y_2(t)$ of (B.5) satisfying $y_1(0) = 1$, $y_2(0) = 0$, $y'_1 = 0$ and $y'_2(0) = 1$. Take $y(x) = u + iv$ to be a solution to (B.5). By Floquet's theorem (Theorem B.3) $y(x)$ has the form

$$y(x) = p_1(x) e^{\omega_1 x} + p_2(x) e^{\omega_2 x} = u + iv, \tag{B.6}$$

where $p_1(x)$ and $p_2(x)$ are continuously differentiable and ℓ-periodic. In the case where λ is not real, the following theorem states that there are no bounded solutions to (B.5).

Theorem B.5 ([57]) *If λ is not real, then all solutions to (B.5) are unbounded.*

Proof. Assume the contrary, that is, there exists an $M \in \mathbb{R}$ such that $|y(x)| < M$ for all $x \in \mathbb{R}$, and take $\lambda = \eta + i\theta$, where $\theta \neq 0$.

The real and imaginary parts of Hill's equation are

$$u'' + (S(x) + \eta)u = \theta v \tag{B.7}$$
$$\text{and } v'' + (S(x) + \eta)v = -\theta u. \tag{B.8}$$

Now, subtracting (B.8) multiplied by u from (B.7) multiplied by v gives

$$u''v - v''u = \theta(u^2 + v^2), \tag{B.9}$$

which, upon integration, yields

$$u'v - v'u = \theta \int_0^x (u^2 + v^2)\, dx + c, \tag{B.10}$$

where c is a constant of integration. From (B.6) it follows that $|u|, |v|, |u'|$ and $|v'|$ are bounded. Hence $|u'v - v'u|$ is also bounded. However,

$$|I(x)| = \left| \int_0^x (u^2 + v^2)\, dx \right| \to \infty \tag{B.11}$$

as $x \to \infty$. Thus, for non-real values of λ any solution to (B.5) is unbounded. ■

Thus, only when λ is real can bounded solutions of (B.5) exist. The next theorem states that there exists a lower bound on the value of λ for which bounded solutions to (B.5) exist.

Theorem B.6 ([57]) *There exists a $\lambda^* \in \mathbb{R}$ such that all solutions to (B.5) are unbounded for $\lambda \leq \lambda^*$.*

Proof. Let λ^* be such that $\lambda^* + s(x) < 0$. Such a λ^* exists, since $s(x)$ is bounded. By substituting $G(x) = -(\lambda^* + s(x))$, Hill's equation may be rewritten as

$$y'' = G(x)y. \tag{B.12}$$

Since $y_1''(0) = G(0)y_1(0) > 0$ it follows from the initial condition $y_1'(0) = 0$ that $y_1'(x) > 0$ for sufficiently small $x > 0$. Therefore, since $y_1(0) = 1$ if the set S of positive zeros of $y_1'(x)$ is not empty, S has a largest lower bound $\epsilon > 0$. But by (B.12) it follows that $y'y'' = G(x)yy'$. Integration of this equation over the interval $(0, \epsilon)$ yields

$$\frac{(y'(\epsilon))^2}{2} = \int_0^\epsilon y''y' \mathrm{d}x = \int_0^\epsilon D(x)yy' \mathrm{d}x. \tag{B.13}$$

Since $y_1(0) = 1$ and $y_1'(x) > 0$ for $0 \leq x \leq \epsilon$, it follows that $y_1(x) > 0$ for $0 \leq x \leq \epsilon$, and hence that the integral in (B.13) is positive. However, $(y'(\epsilon))^2/2 = 0$ since $y'(\epsilon) = 0$ by assumption. It follows that ϵ does not exist. Thus $y_1'(x) > 0$ for $x > 0$. Hence, again by (B.13), $y_1'(x)$ increases monotonically with x for $x > 0$. Consequently $y_1(x) \to \infty$ as $x \to \infty$. It may similarly be shown that $y_2(x) \to \infty$ as $x \to \infty$. ■